T-PM-Sym1 STATISTICAL PROPERTIES OF THE GATING OF SINGLE SODIUM CHANNELS. Richard Horn, Dept. of Physiol., UCLA School of Medicine, Los Angeles, CA 90024.

When activated by depolarization single Na channels fluctuate between two conductance levels, open and closed. "Silent transitions" can also occur among kinetically distinct states, e.g. from one closed state to another, or between open states. These transitions can be inferred from a detailed analysis of single channel fluctuations in a series of voltage pulses using the patch clamp method. Such an analysis was applied to single channel currents of membrane patches of neuroblastoma and rat myotubes. The number of open states was determined by a comparison of the open time histogram with maximum likelihood estimates of the dwell time in open states under the usual conditions, where a membrane patch contained several channels. In general the shape of the histogram depended on the probability of overlapping openings, which could be varied by controlling the amount of slow or fast inactivation during a pulse. The transitions between closed states was studied by a comparison of the probability of a channel being open as a function of time during a voltage step and the histogram of latency between the onset of an activating pulse and the opening of the first channel. For proper scaling both of these measurements required an accurate determination of the number of channels in a patch. This was feasible when the probability of overlapping openings was reasonably high.

T-PM-Sym2 KINETIC BEHAVIOR OF SINGLE SODIUM CHANNELS. R.W. Aldrich, D.P. Corey, C.F. Stevens, Dept. of Physiology, Yale Univ. School of Medicine, New Haven, CT.

We have been investigating the properties of sodium channels with the single channel recording method, mostly in a neuroblastoma clonal cell line (N1E115). Our experiments have used the cell-attached, inside-out and outside-out configurations. Observations have been made on over 50 patches containing from one to half a dozen or more channels each. We find a single channel conductance of 15 to 20 pS and a mean channel open time of less than 1 ms at room temperature. Average currents reveal kinetic behavior characteristic of Na channels in a variety of preparations. Cell-attached patches have an activation curve that reaches half maximum for depolarizations of about 15 mV from resting potential and a steady-state inactivation curve with about half of the channels inactivated at the resting potential. Significant inactivation occurs in channels that have never opened, but appears to proceed more rapidly from the open state. We have studied the distribution of latency until first channel opening and various statistical properties of channel behavior to elucidate activation and inactivation kinetics.

T-PM-Sym3 PHARMACOLOGY OF SINGLE SODIUM CHANNELS. F.N. Quandt, Dept. of Pharmacology, Northwestern Univ. Med. School, Chicago, Ill. 60611; and Dept. of Med. Physiol., Univ. of Calgary, Calgary, Alberta T2N 1N4.

One approach toward the goal of a molecular description of the behavior of membrane ion channels is to examine the interactions of active sites of these channels with a drug or toxin. Single channel analysis can give direct information concerning the conductance, lifetime, and probability of occurrence of states of the channel for both the normal and modified conditions. It is also possible to determine whether the modification is in a uniform manner; and whether it is dependent on any state of the channel. The actions of Na channel modifiers or blockers have therefore been evaluated using single channel analysis applied to excised membrane patches of neuroblastoma cells. In contrast to the normal situation, after exposure to batrachotoxin, the observed open states of Na channels are best described by two homogeneous populations. One class corresponds to the toxin-modified open state which exhibits both a reduction in conductance and an increase in lifetime. BTX also eliminates the decline in the probability of opening during maintained depolarization normally caused by inactivation. For tetrodotoxin, the frequency of closed-to-open state transitions for a series of depolarizations was found to be reduced in a dose-dependent manner (K_i=2nM) while the remaining conducting states have normal lifetime and current amplitude. TTX likely reduces the probability of a closed state normally leading to the open state, by inducing a closed-blocked state. In contrast, the block by 9-aminoacridine is best interpreted to be due to an interaction with the open state since 9-AA causes a transient and periodic reduction in conductance during the time the channel is gated open.

T-PM-Sym4 SINGLE CHANNEL KINETICS OF ANOMALOUS RECTIFICATION. Yasuo Fukushima, Department of Physiology and Jerry Lewis Neuromuscular Research Center, UCLA, Los Angeles, CA 90024.

It has been known that the tunicate egg cell membrane shows the anomalous K current when the cell membrane is hyperpolarized. The anomalous K current is activated almost instantaneously and is blocked time-dependently in solutions containing several impermeant cations. The blocking kinetics of these cations in the anomalous K rectifier channel are dependent on the membrane potential, on the blocking cations and their concentration, and also on the external K concentration. The blocking kinetics of Na, Cs and Sr were analyzed by single channel recording. The tunicate egg was conventionally voltage-clamped with two microelectrodes. A third electrode was pushed against the egg cell and the patch current was measured with a current-voltage converter when a hyperpolarizing command pulse was applied to the whole egg cell membrane.

The open-close kinetics in a single channel with a blocking cation present were consistent with the blocking kinetics of the total anomalous K current. The open-close kinetics in a single channel could be regarded as a first order transition between the open and closed states. The closing rate constant of the single channel for the first order transition increased almost linearly on a semi-logarithmic scale as the membrane potential became more negative, while the opening rate constant decreased and then increased, showing the minimum. The latter indicated that the channel was released from the blocking by excessive hyperpolarization. When there were two kinds of blocking cations such as Na and Cs, the kinetic properties in a single channel indicated that the two kinds of cations blocked in the single channel independently. The single channel conductance in 200mM Na and 200mM K solution was 1.5 times larger than in Na-free 200mM-K solution.

T-PM-Sym5 INTERPRETATION OF THE DISTRIBUTIONS OF THE OPEN AND SHUT INTERVALS OF THE CALCIUM-ACTIVATED POTASSIUM CHANNEL IN TERMS OF MOLECULAR MECHANISM. K. L. Magleby and B. S. Pallotta, Dept. of Physiology and Biophysics, University of Miami School of Medicine, Miami, Florida 33101.

Information about the underlying molecular mechanism of an ionic channel is contained in the distributions of all open and shut intervals for that channel (Colquhoun & Hawkes, 1981). To illustrate this point, the distributions of all open and shut intervals of the Ca-activated K channel in excised patches of membrane from cultured rat muscle will be presented and interpreted in terms of possible underlying molecular mechanisms. The distribution of all open intervals is found to be described by two exponentials suggesting a minimum of two open channel states. The distribution of all shut intervals is described by three exponentials, suggesting a minimum of three readily occurring closed channel states. In addition, there are also a few longer shut intervals not accounted for by the three exponential distributions of shut intervals suggesting an additional closed channel state. To illustrate how possible relationships between the various open and shut states can be determined, the effect of $[Ca]_i$ on the distributions of the open and shut intervals will be presented and the results used to develop models of possible mechanisms. The data suggest that openings to the long open state require the binding of more Ca ions than openings to the short open state. Mathematical descriptions and stochastic simulations of the proposed models are then used to test the models by comparison of theoretical results to the experimental data. Supported by NIH grants NS 10277, NS 12207, and the Muscular Dystrophy Association.

T-PM-Sym6 MULTIPLE CONDUCTING STATES OF THE ACETYLCHOLINE-CHANNEL. F. Sachs, Dept. of Biophysical Sciences, SUNY, Buffalo, NY 14214.

The nicotinic acetylcholine activated channel (AchR) has more than one conducting state, contrary to what has been assumed in the analysis of macroscopic currents, and contrary to what was assumed in early single channel patch clamp experiments. Aside from a variety of independent ion channel populations, a given AchR may show two (or more) discrete conducting states, two kinetic components of apparently equal conductance and a variety of other states which appear as excess noise in the conducting states. The discrete states have a probability of occurrence (and/or lifetime) which is agonist dependent, although the dependency has not been well characterized.

Several experiments (1,2) have shown that the subconducting states may not be in kinetic equilibrium since they preferentially occur at the end of bursts rather than at the beginning of bursts. The energy source for this lack of equilibrium has not been determined, but could conceivably arise from current flow through the channel.

The significance of multiple components to the open time distribution is unclear. It is known, however, that bursts of activity from a single channel contain two time constants (2). The excess low frequency open channel noise, which appears non-stationary in many experiments, is not clearly understood. Four state models of flickering kinetics are not enough to explain the distinguishable discrete conducting states and the equal amplitude but kinetically distinguishable discrete conducting states, let alone excess noise of the open channels.

1) Hamill & Sakmann (1981), Nature, 294:462
2) Auerbach & Sachs (1982), (in preparation)

T-PM-A1 SIMULTANEOUS OBSERVATION OF SEVERAL DISCRETE POSITIONS IN A SINGLE ACYL CHAIN USING ^{2}H-NMR OF SINGLE CHAIN PERDEUTERATED PHOSPHOLIPIDS Michael R. Paddy, Alan J. Deese, and F.W. Dahlquist Institute of Molecular Biology, U. of Oregon (MRP and FWD) and Division of Natural Sciences, U. of California, Santa Cruz (AJD).

Model membranes made from phospholipids which have perdeuterated palmitic acid esterified at the sn-1 position give rise to ^{2}H-NMR spectra which contain five or six well resolved splittings. These splittings are quite sensitive to relatively small changes in the acyl chain motions of the phospholipid, such as those that occur when different fatty acyl chains are esterified at the sn-2 position. Oriented spectra computed from the powder spectra (using the "dePaking" procedure developed by Davis and Bloom) contain five or six non-overlapping sets of doublets. When such oriented spectra are calculated from a T_1 series of powder spectra, it is possible to obtain the T_1 relaxation time of several positions on the acyl chain simultaneously. This possibility for simultaneous observation of the NMR properties of several positions along a single, easily synthesized acyl chain makes these molecules attractive for detailed studies of acyl chain dynamics in bilayers. Applications of these labelled molecules to the study of lipid-protein interactions in bilayers will be presented.

T-PM-A2 BIAXIAL ORDERING OF THE WATER IN THE RIPPLE (P_β) PHASE OF PHOSPHATIDYLCHOLINE BILAYERS. L. Strenk[+], N. Vaz[+], P. Westerman[+*] and J. W. Doane[+*], [+]Department of Physics and Liquid Crystal Institute, Kent State University, Kent, Ohio 44242 and *Molecular Pathology Program, Northeastern Ohio Universities College of Medicine, Rootstown, Ohio 44272.

^{2}H NMR methods have been used to study dipalmitoylphosphatidylcholine (DPPC) and dimyristoylphosphatidylcholine (DMPC) bilayers, hydrated with D_2O in the P_β phase. Like other workers we observe unusual spectral patterns in this phase. In a detailed study using D_2O/lipid molar ratios, n, in the range $7 \leq n \leq 12$, we find the spectra can be analysed in terms of a large asymmetry in the time-averaged quadrupole interaction, indicative of biaxial ordering. This observed asymmetry is attributed to a modulation of the quadrupole interaction resulting from rapid translational diffusion of the oriented water molecules over the surface of the rippled structure during the time scale of the ^{2}H NMR measurement (10^{-3}s). The degree of asymmetry reflects the shape of the ripple as well as its dimensions. Measured values of the asymmetry parameter, η, in DPPC and DMPC bilayers in the ripple phase, at several D_2O/lipid molar ratios and temperatures are compared with values of η calculated for the sinusoidal and sawtooth models that have been proposed for the ripple phase.

(Supported by the NIGMS with Grant No. GM 27127 and by the NSF with magnet facilities Grant No. DMR 78-09046).

T-PM-A3 THE CONFORMATION OF THE GLYCEROL MOEITY IN PHOSPHATIDYLCHOLINE BILAYERS AND A SUGGESTED MODEL FOR THE P_β PHASE. P. W. Westerman, L. M. Strenk and J. W. Doane, Northeastern Ohio Universities College of Medicine, Rootstown, Ohio 44272 and Liquid Crystal Institute and Department of Physics, Kent State University, Kent, Ohio 44242.

An analysis, in the L_α phase of ^{2}H quadrupole splittings from multiple sites in the glycerol group of dimyristoylphosphatidylcholine (DMPC), indicates that this moeity adopts a conformation similar to that of conformer B as observed in the crystal structure of DMPC.$2H_2O$[1]. Other conformers or combinations of conformers do not produce a self-consistent set of quadrupole splittings in the ^{2}H NMR spectrum. This conformational analysis and the observation of two components in the ^{2}H NMR spectra of DMPC-H_2O mixtures in the P_β phase is suggestive that this phase is a mixture of two populations of DMPC molecules, each with a distinct conformation about its glycerol moeity. Possible structures for these two conformers will be described. A sawtooth structure, which will be shown to be consistent with ^{13}C NMR, ^{2}H NMR and freeze-facture electron microscopic data, is proposed for DMPC multibilayers in the P_β phase.

(Supported by NIGMS with Grant No. GM 27127).

1.R. H. Pearson and I. Pascher, Nature, 281, 499 (1979).

T-PM-A4 FREQUENCY DEPENDENT ^{13}C-NMR RELAXATION STUDIES OF RHODOPSIN-LIPID INTERACTIONS IN ROD DISK MEMBRANE VESICLES. A.J. Deese*, E.A. Dratz*, G.D. Williams†, and M.F. Brown† *Dept. of Chemistry, Univ. of Calif., Santa Cruz, CA 95064 and †Dept. of Chemistry, Univ. of Virginia, Charlottesville, VA 22901.

At present, natural abundance ^{13}C T_1 relaxation time measurements have been made for retinal rod outer segment (ROS) disk membrane vesicles, as well as vesicles of total extracted ROS phospholipids, at the following magnetic field strengths: 1.4T (15MHz); 2.3T (25MHz); 4.2T (45MHz); 4.7T (50MHz); and 8.4T (90MHz). To date, the following results have been obtained: First, in contrast to earlier work (1), we have not observed any large differential broadening of the saturated vs. polyunsaturated acyl chain resonances of the ROS phospholipids due to specific rhodopsin-lipid interactions, suggesting that these earlier conclusions should be viewed with some caution. Second, the present ^{13}C T_1 measurements have been made over a wider frequency range than reported at last year's meeting (2); we now find a significant frequency dependence for both the ROS membrane and total ROS phospholipid vesicles. At all magnetic field strengths (frequencies), rhodopsin produces a decrease in the T_1's of the resolved phospholipid resonances, with the greatest effects appearing at the lower frequencies. This suggests that rhodopsin may exert its greatest effects on the lower frequency motions of the ROS phospholipids, either by enhancing cooperative modes (3) (viewed as unlikely), or by inducing a new type of slowly relaxing structure in the immediate vicinity of the protein.

1) N. Zumbulyadis and D.F. O'Brien, Biochemistry 18, 5427 (1979); 2) A.J. Deese et al., Biophys. J. 37, 277a (1982); M.F. Brown, J.Chem. Phys. 77, 1576 (1982).

Work supported by NIH fellowship 1F32EY05607 (A.J.D.), NIH grants EY00175 (E.A.D.) and EY03754 (M.F.B.), and by the Monsanto Company (M.F.B.).

T-PM-A5 HIGH-RESOLUTION SOLID-STATE CARBON-13 NMR STUDIES OF UNSONICATED MEMBRANE DISPERSIONS. M.D. Sefcik*, J. Schaefer*, E.O. Stejskal*, R.A. McKay*, J.F. Ellena†, S.W. Dodd†, and M.F. Brown†. *Monsanto Company, St. Louis, MO 63166 and †Department of Chemistry, University of Virginia, Charlottesville, VA 22901.

Using solid-state NMR techniques, we have recently obtained high-resolution, natural abundance ^{13}C-NMR spectra of unsonicated multilamellar dispersions of 1,2-dilauryl-sn-glycero-3-phosphocholine (DLPC), in the liquid crystalline phase, as well as unsonicated retinal rod outer segment (ROS) disk membranes containing rhodopsin as their major integral membrane protein component. The spectra were obtained using cross polarization/magic-angle spinning together with high-power ^{1}H decoupling, and in each case are superior in resolution to ^{13}C-NMR spectra of suspensions of the corresponding sonicated vesicles. The ^{13}C-NMR spectra of the ROS disk membranes contain distinct resonances attributable to the saturated and polyunsaturated acyl chains and choline methyl head groups of the ROS membrane phospholipids; in addition we have for the first time resolved distinct resonances from the visual pigment rhodopsin. For both the multilamellar DLPC dispersions and the ROS disk membranes, rotating-frame relaxation time measurements have been made as a function of spin-locking field strength, thereby providing information on molecular motions in the kHz frequency regime. These results suggest that the application of solid-state ^{13}C-NMR techniques to the study of lipid bilayers and biomembranes offers a promising new avenue for structure/function investigations.

Work supported by NIH fellowship 1F32EY05635 (to J.F.E.), NIH grant R01 EY03754 (to M.F.B.), and by the Monsanto Company.

T-PM-A6 PERTURBATIONS OF PHOSPHOLIPID HEADGROUP BY MEMBRANE PROTEINS IN BIOLOGICAL MEMBRANES AND RECOMBINANTS. P.L. Yeagle, B.S. Selinsky, and A.D. Albert, Dept. of Biochemistry, SUNY Buffalo, School of Medicine, Buffalo, NY 14214

^{31}P Nuclear magnetic resonance (NMR) spin-lattice relaxation times (T_1) have been used to probe the behavior of phospholipid headgroups in the presence of membrane proteins. Measurements have been made on rabbit muscle sarcoplasmic reticulum and recombinants of the Ca^{2+}-Mg^{2+} ATPase, rod outer segment disk membranes and recombinants of rhodopsin, and human erythrocyte ghosts and recombinants of human erythrocyte glycophorin. T_1 studies on pure phosphatidylcholine as a function of frequency and temperature support a predominantly dipolar mechanism for spin-lattice relaxation for the phosphorus. These measurements and nuclear Overhauser effects indicate that the effective correlation time is about a nanosecond. Frequency-dependent measurements for the biological membranes indicate similar behavior for the phospholipid headgroups. Recombinant membranes with lipid/protein ratios greater than or equal to that found in biological membranes showed T_1 behavior similar to the biological membranes and pure phosphatidylcholine. However, recombinants with a low lipid/protein ratio exhibited a T_1 that was dramatically shorter than any of the other systems. Analysis of the relaxation mechanism and the factors contributing to it implicate a phospholipid headgroup conformation change at high protein content. It is suggested that this is due to trapping of phospholipids between proteins and is not the same phenomenon as motional restriction at the lipid-protein interface at higher lipid contents.

T-PM-A7 HEXANE IN DMPC AND DOPC BILAYERS: AN NMR AND CALORIMETRIC STUDY
R. E. Jacobs & S. H. White, Dept. Physiology & Biophysics, UC Irvine, Irvine, CA 92717
This work represents an attempt to characterize a simple two component lipid bilayer system in which the minor component is similar in structure to the hydrophobic portion of the membrane. Deuterium and phorphorous nuclear magnetic resonance (NMR) and differential scanning calorimetry (DSC) have been used to examine the behavior of dimyristoyl and dioleoyl phosphatidylcholine bilayers to which hexane has been added. DSC thermograms indicate that a phase separation occurs in the DMPC/hexane mixture between approximately 0 °C and 23 °C and that even small amounts of hexane significantly change the thermal properties of the bilayer. The DOPC phase transition braodens and shifts to lower temperatures as hexane is added. Phosphorous NMR spectra show no change upon the addition of hexane. Deuterium NMR spectra of perdeuterated hexane dissolved in either bilayer above its phase transition show three overlapping powder patterns indicating that hexane is moving rapidly between the opposing monolayers with its long axis parallel to the lipid acyl chains. In both lipid systems the temperature dependence of the hexane deuterium quadrupole splittings exhibits a maximum at about the lipid phase transition temperature. Below 5 °C the hexane powder patterns in the DMPC bilayer coalesce into a single wide line regardless of hexane concentration. In the DOPC bilayer this behavior is seen at about -15 °C at high hexane concentrations. All temperature dependent spectral changes were reversible. Deuterium NMR spectra of acyl chain perdeuterated DMPC plus hexane indicate that the acyl chain motion is disordered only slightly by the presence of the alkane. These results indicate that the thermal and dynamical properties of the membrane interior in this mixture are significantly different from those found in the pure lipid system. Supported by NSF grant PCM-8104518 and NIH grant GM 26246.

T-PM-A8 ^{39}K, ^{23}Na, and ^{31}P NMR STUDIES OF ION TRANSPORT AND INTRACELLULAR pH IN YEAST.
Takashi Ogino, Jan A. den Hollander and Robert G. Shulman, Dept. of Molecular Biophysics and Biochemistry, Yale University, P.O. Box 6666, New Haven, CT 06511.
It has been reported that yeast cells, when energized, can rapidly excrete H^+ and simultaneously take up K^+ from the medium. The exact relation between K^+, H^+ and Na^+ transport has been a subject of considerable interest, although many questions still remain. To test this stoichiometry and to investigate its mechanism, we studied the relationship between efflux and uptake of Na^+, K^+ and intracellular pH (pH^{in}) upon energizing yeast cells by oxygenation, using the non-invasive technique of NMR spectroscopy. With the aid of our home built solenoid coil probe and an anionic paramagnetic shift reagent, Dy(III) $(P_3O_{10})_2$ (Gupta, R.K. J.M.R., 47, 344, 1982), we can now follow time courses of Na^+ and K^+ ion transport as well as pH^{in} with a time resolution of 1 minute in yeast cell suspensions. A concentration of shift reagent of 2 mM was used and external Na^+ and K^+ concentrations were 20 and 7 mM respectively at the beginning of the experiment. The internal and external Na^+ and K^+ peaks were separated by 8-10 ppm. The K^+ line-width is 10 ppm, and deconvolution is required to separate the signals. Na^+ line-width was $\sim$ 1 ppm. The ^{23}Na and ^{31}P resonances were observed in a double tuned probe by switching back and forth every 1 min. Upon oxygenation of the yeast cells, pH^{in} was observed to increase rapidly from pH 6.5 to pH 7.2 and K^+ was taken up rapidly to a new steady state value. Na^+ was slowly taken up before energizing the cells. These experiments show that ^{23}Na and ^{39}K NMR can be applied to study Na^+ and K^+ ion transport in intact cells and tissues, supplementing the information obtained by ^{31}P NMR.

T-PM-A9 CHARGE INTERACTIONS IN THE LIPID-PROTEIN COMPLEX OF PANCREATIC PHOSPHOLIPASE A_2 AND ORGANIZED SUBSTRATE.
Johannes J. Volwerk & Patricia C. Jost, Institute of Molecular Biology, University of Oregon, Eugene, Oregon 97403.

The lipolytic enzyme phospholipase A_2 (EC 3.1.1.4) specifically catalyzes the hydrolysis of the 2-acyl ester bonds of 3-sn phosphoglycerides. When the substrate is present in an organized lipid-water interface the enzyme shows greatly enhanced catalytic efficiency. So far most studies on the lipid binding properties of the protein have employed neutral (zwitterionic) substrates or substrate analogs and the results suggest that hydrophobic interaction is the main stabilizing force in these lipid protein complexes.

We have found that introduction of a negative surface charge in the lipid-water interface, either by using a negatively charged substrate or by using a negatively charged detergent, greatly increases the susceptibility of long chain phospholipids towards enzymatic hydrolysis by porcine pancreatic phospholipase A_2. Furthermore, the presence of a negatively charged spinlabeled substrate analog in an otherwise neutral lipid system produces a motion restricted component in the ESR-spectrum upon addition of phospholipase A_2. This motion restricted component is observed to a much lesser degree when a spinlabeled molecule carrying a net positive charge is used. The data suggest strong and selective binding of the negatively charged substrate analog to the protein in the lipid-protein interface and indicate a possible role for charge interactions in formation of the complex between pancreatic phospholipase and its organized substrate and/or interfacial activation of the enzyme. Supported by NIH Grant GM 25698.

T-PM-A10 REAL-TIME X-RAY DIFFRACTION USING SYNCHROTRON RADIATION: APPLICATION TO THE STUDY OF MEMBRANE LIPID PHASE TRANSITION DYNAMICS. Martin Caffrey, (Intr. by George P. Hess) Section of Biochemistry, Molecular and Cell Biology, Clark Hall and CHESS (Cornell High Energy Synchrotron Source), Wilson Laboratory, Cornell University, Ithaca, New York 14853.

Herein, I report the first real-time observation and recording of the x-ray diffraction pattern of an unoriented hydrated membrane lipid, dipalmitoylphosphatidylcholine (DPPC), through its thermotropic gel/liquid crystal phase transition. Synchrotron radiation from the Cornell High Energy Synchrotron Source was used as an x-ray source of extremely high brilliance and the dynamic display of the diffraction image was effected using a 4-stage image intensifier tube coupled to an external fluorescent screen. The image on the output phosphor was sufficiently intense to be recorded cinematographically and to be displayed on a television monitor using a vidicon camera at 30 frames/sec. These measurements have allowed me to put an upper limit of 2 seconds on the $L_{\beta'} \rightarrow L_{\alpha}$ transition of DPPC. A video presentation of these dramatic real-time changes in the diffraction behavior of DPPC will be made at the Meetings. This real-time method provides information on detailed structural changes in membranes as they occur. The method does not require an exogenous probe, is relatively nonperturbing and can be used with membranes in a variety of physical states.

Characterization of the present real-time system with regard to sensitivity, dynamic range, image quality, temporal response and spatial resolution will be reported on. Image processing of the video recorded material to obtain quantitative diffracted intensity information will be described.

T-PM-A11 MOLECULAR ORGANIZATION IN CHOLESTEROL-LECITHIN BILAYERS BY X-RAY AND ELECTRON DIFFRACTION MEASUREMENT. S.W. Hui and Neng-Bo He, Biophysics Department, Roswell Park Memorial Institute, Buffalo, N.Y. 14263.

The molecular organization in multilamellar vesicles and in free-standing bilayers of cholesterol-dimyristoylphosphatidylcholine (DMPC) were studied by x-ray and electron diffraction respectively. When 5% of cholesterol was added to DMPC, the lamellar repeat spacings measured at $T<23°$ increased significantly, while those measured at $T>23°$ remained unchanged. This difference diminished at 20 mole percent or higher portions of cholesterol. A sharp wide angle reflection observed from low cholesterol samples was broadened when the temperature was raised above 23°. With increasing cholesterol contents, the sharp diffraction became gradually broadened and the peak spacings increased continuously. No co-existence of gel and fluid phases was observed. At 20 mole percent or more cholesterol, abrupt thermotropic changes in the peak width and peak spacing were no longer observed. The loses of diffraction asymmetry and the increase in repeat spacing in samples containing 5% or more cholesterol suggest that the acyl chains are no longer tilted. The gradual broadening and shifting of the wide angle reflection with increasing cholesterol suggest that lecthin and cholesterol molecules are microscopically evenly distributed, and that 20% cholesterol marks the limit of cooperation between DMPC molecules. A two-fold asymmetry in broad band electron diffraction patterns indicates some degree of unidirectional orientation of molecules. We therefore favor a molecular arrangement model wherein lecithin and cholesterol molecules are freely miscible, but the cholesterol molecules are partically aligned thereby forming unidirectionally ordered stripes.

T-PM-A12 REACTIVITY OF MALONDIALDEHYDE IN ISOTOPE EXCHANGE REACTIONS AND WITH SUPEROXIDE ANION. Claudio A. Chuaqui, Noemi Chuaqui-Offermanns and John Merritt, Medical Biophysics Branch, Atomic Energy of Canada Research Company, Whiteshell Nuclear Research Establishment, Pinawa, Manitoba, Canada, ROE 1LO.

Malondialdehyde (MDA) is produced in vivo principally during the peroxidation of phospholipids. It has mutagenic properties and it can react with proteins, enzymes and nucleic acids. The acidity of MDA is relatively high (pKa = 4.46), so that at physiological conditions, it exists mainly in the anionic form, which is less reactive than its conjugate acid. NMR studies have shown the enolic nature of MDA, its conformational dependence on the solvent and that deuterium exchange occurs in D_2O (Bacon, N., George W.O. and Stinger, B.H. (1965), Chemistry and Industry 31, 1377-1378; Bothner-By, A.A. and Harris, R.K. (1965), J. Org. Chem. 30, 254-257; Osman, M.M. (1972) Helv. Chim. Acta 55, 239-244; Chuaqui C.A. and Chuaqui-Offermanns N. (1982) submitted paper). The isotope exchange reaction occurs even at pH values well above the pKa of MDA, and the solvent composition influences the rate of the process. For example, the rate shows a six-fold increase when the solvent changes from water to a 90% DMSO-10% water mixture. Also, experiments with superoxide anion, generated in DMSO-H_2O, demonstrate that MDA catalyses the dismutation of O_2^-. Furthermore, when diphenylisobenzofuran (DPBF) is present in the solution, o-dibenzoylbenzene (o-DBB) is formed. These results indicate that MDA facilitates the dismutation of O_2^- by providing the necessary proton at a faster rate than water. The formation of o-DBB strongly suggests that, under these conditions, the oxygen generated during the dismutation of O_2^- is singlet oxygen.

T-PM-A13 X-RAY DIFFRACTION STUDY OF THE CORNEA. H. Inouye*and C. R. Worthington,Department of Biological Sciences, Carnegie-Mellon University, Pittsburgh, PA.

The corneal transparency has been discussed using the electron microscopic data, although the agreement of the collagen fibril size and volume fraction by different authorities is poor.For the fish cornea the fibril size was evaluated by x-ray diffraction (Inouye and Worthington,1981). We report here the diffraction patterns of rabbit, beef and frog corneas. Samples were sealed in thin wall capillary tube with vitreous,aqueous humour,Ringer's soln. or distilled water. Setting the sample parallel to the slit all hydrated specimen showed intense primary peak at Bragg spacing,55-74nm and maxima 22-26nm,13-15nm.After dehydration similar bands were not detected. The rabbit cornea with Ringer's soln. gave maxima,62.2nm,24.4nm,14.5nm. On partial dehydration the same cornea showed 50.9nm,23.6nm,14.3nm and subsidiary maxima up to 8nm spacing. On rehydration the maxima 70.0 nm,25.7nm,15.7nm and broad reflections up to 8nm spacing were observed. Setting the sample perpendicular the sharp reflections of 3-9th orders of 66.4nm collagen axial period were recorded from hydrated rabbit cornea.After air drying 3-20th orders of 65.8nm period were observed.The fiber diagram suggests that the collagen fibrils are approximately running parallel in the present system. Assuming 1.the fibrils are solid cylinders with 36.4nm and 41.1nm in diameter for rabbit partially dehydrated and rehydrated cornea,2.the arrangement of the fibrils is shown in EM image, the equatorial intensity was calculated and found agree with the observed intensity.Fibril diameter of the hydrated cornea,40nm for rabbit,39nm for beef,38nm for frog,was obtained.If the bound water is 0.25 gr/gr the volume fraction of the fibrils is 0.3, which agrees with the estimate from the hard cylinder liquid model.(*at:Children's Hospital Medical Center and Harvard Medical School,Boston,MA.)

T-PM-A14 DETERMINATION OF IN VIVO RATES OF REACTION BY TWO DIMENSIONAL ^{31}P NMR. R.S. Balaban, H.L. Kantor and J.A. Ferretti*. NHLBI, LKEM, LC*, NIH, Bethesda, MD 20205

We report the application of two dimensional FTNMR spectroscopy to the measurement of reaction rates in vivo. The study was carried out on the upper hind limb of an anesthetized rat. The rat was placed in a specifically designed probe equipped with an animal cradle. A Helmholtz coil 2 cm in width was carefully positioned around the region of interest to optimize the homogeneity of the applied rf field. A pulse width of 90 μsec was then required to produce a 90° pulse. Optimization of the static magnetic field homogeneity yielded water proton linewidths which were less than 50 Hz at 360 mHz. All experiments were carried out on a Nicolet NT-360 spectrometer with an Oxford 89 mm bore magnet.

The usual one-dimensional ^{31}P NMR spectrum of the hind limb of the rat showed the presence of creatine phosphate and adenosine triphosphate (ATP) in the expected proportions as well as a small amount of inorganic phosphate, P_i. An important advantage of the two dimensional method is that separate peaks appear in the "2D" matrix, called crosspeaks, which represent all molecules that have undergone exchange under steady state conditions in a prescribed time interval. In this study we were able to monitor the reaction of creatine with the terminal phosphate of ATP to form creatine phosphate and adenosine diphosphate. The reaction is catalyzed by the enzyme creatine phosphokinase. Equal crosspeaks in the 2D matrix were observed for both the forward and reverse reactions. Crosspeaks were not observed between the terminal phosphorus of ATP and P_i indicating that the rate of ATP hydrolysis was low. These results demonstrate the technical and interpretive value provided by 2D FTNMR for studies of in vivo phosphate metabolism.

T-PM-B1 DNA BINDING KINETICS OF BIS-INTERCALATORS. Richard H. Shafer and Donald L. Wade, Department of Pharmaceutical Chemistry, School of Pharmacy, University of California, San Francisco, CA. 94143.

Stopped-flow and hand-mixing experiments have been carried out to determine the association and dissociation rate contants for the binding of bis-methidium spermine (gift of Dr. P. B. Dervan) to poly (dG-dC) and poly (dA-dT) in low salt conditions (0.075 M Na^+) at 20°C. Results for the association experiments yielded bimolecular rate constants of 1.4×10^7 M^{-1} s^{-1} and 0.8×10^7 $M^{-1}s^{-1}$ for poly (dA-dT) and poly (dG-dC), respectively. Dissociation rates were measured by competition with calf thymus DNA, based on differences in the visible absorption properties of the different bound complexes. The measured off rates were dependent on the concentration of competing DNA, both the sonicated and unsonicated forms. In the case of poly (dG-dC), in the limit of vanishing competitive DNA concentration, the unimolecular rate constant was found to be 7.6×10^{-5} S^{-1} and, for poly (dA-dT) was 3×10^{-4} S^{-1}. These rate constants yield an affinity constant of 1×10^{11} M^{-1} for poly (dG-dC) and 5×10^{10} M^{-1} for poly (dA-dT). Similar measurements have been carried out at higher salt, resulting in smaller association rate constants and large dissociation rate constants, consistent with lower affinities under these conditions. Experiments on a second bis-methidium compound with a methylene chain instead of spermine will be described. Results will be discussed in terms of the direct transfer model for ligand binding and the importance of the nature of the chain linking the chromophores as well as the mode of binding, i.e. mono- or bis-intercalation. This work was supported by PHS Grant CA 27343 awarded by the National Cancer Institute, DHHS.

T-PM-B2 BINDING OF NETROPSIN TO DNA. Luis A. Marky, Kenneth Blumenfeld, and Kenneth J. Breslauer, Department of Chemistry, Rutgers University, New Brunswick, NJ 08903.

Netropsin is a basic oligopeptide which exhibits antibacterial, antifungal and antiviral activities. It is known that the drug has an absolute requirement for the "B" conformation of DNA. Because it binds to poly d(AT) and poly d(IC) but not to poly d(GC), it was suggested that the 2-NH_2 group of guanine sterically hinders binding at the dG•dC site (Zimmer et al. (1971) J. Mol. Biol. 58, 329-348; Wartell et al. (1974) J. Biol. Chem. 249, 6719-6731). We have confirmed the above observation by studying the binding of netropsin to $d(TA)_3$ and to $d(T\text{-}2aminoA)_3$ by C.D. titrations of the deoxyoligomer with the drug at low temperatures.

In addition, we have characterized the binding of netropsin to poly dAT and oligomeric systems by a combination of spectroscopic and calorimetric techniques. In 10mM phosphate buffer pH = 7.0, U.V. melting curves of poly dAT-netropsin solutions at different phosphate to drug ratios display biphasic behavior with the bound drug stabilizing the helix by 35°C. Increasing the ionic strength does not affect the binding of the drug as seen by C.D. titration. This indicates that the binding is governed primarily by specific and not electrostatic interactions.

The enthalpy change associated with the binding process was measured by differential scanning and batch calorimetry. We find that the enthalpy is exothermic by 9-10 kcal/mole of drug. The results will be discussed in terms of specific molecular interaction.

This work was supported by NIH Grant GM-23509.

T-PM-B3 SPECIFICITY OF THE DAUNOMYCIN-DNA INTERACTION, J. B. Chaires, Department of Biochemistry, The University of Mississippi Medical Center, Jackson, MS 39216

Daunomycin (DM) is an anthracycline antibiotic widely used in cancer chemotherapy. Interaction of DM with DNA is thought to be an important aspect of its mode of action. In a previous study (Chaires, et al. (1982) Biochemistry 21, 3933) competition dialysis experiments demonstrated that daunomycin prefers G-C base pairs as a binding site, although the drug will bind to A-T base pairs. The interaction of daunomycin with poly dG-polydC, poly d(G-C), poly dA-poly dT and poly d(A-T) has been examined to further explore the specificity of the daunomycin-DNA interaction. Absorbance and fluorescence titration measurements and equilibrium dialysis were used to obtain binding data. The binding of DM to poly dG-poly dC, poly d(G-C) and poly d(A-T) may be described by the standard neighbor exclusion model. The primary difference between these polynucleotides is in the value of the exclusion parameter required to fit the data. Poly dA-poly dT, in contrast, showed pronounced positive cooperativity at low binding ratios. DM stabilized, to varying degrees, all four polynucleotides in thermal denaturation experiments. Biphasic melting curves were evident for all of the polynucleotides. Supported by grants awarded by the BRSG Program, NIH (5 SO7 RR05386) and by the Division of Research Resources, NIH, for the PROPHET Computer Network.

T-PM-B4 LOCATING POSSIBLE HIGH AFFINITY CARCINOGEN BINDING SITES ON ϕX174RF DNA AND ON THE PLASMID PBR322. Stephen A. Winkle, Michael Mallamaci and David P. Reed, Department of Chemistry, Rutgers - The State University of New Jersey, New Brunswick, New Jersey 08903.

Recent studies (e.g., Winkle and Krugh [1981] Nucleic Acids Res. 9, 3175-3186) of the equilibrium binding of the carcinogens N-hydroxy-N-acetyl-2-aminofluorene (N-hydroxyAAF) and 4-nitroquinoline-1-oxide (NQO) to various DNAs, including ϕX174RF and pBR322, suggest that these carcinogens may bind in a highly selective manner to a small number of sites on ϕX174RF DNA. We have examined the covalent binding of N-acetoxyAAF to the sequenced DNAs ϕX174RF and pBR322 for site selectivity using 3H-N-acetoxyAAF (circa 1 Ci/mmole) and the restriction endonucleases Alu I, Hae III, Hha I, Hinf I and Hpa II. Restriction fragments containing bound ^{3}H-labeled carcinogen were separated by gel electrophoresis and the amount of radioactivity in each fragment determined by liquid scintillation counting. In these experiments, there were 100-300 base pairs per bound carcinogen and experiments were conducted in both sequences, i.e. 1) enzyme digestion then 2) carcinogen reaction and the reverse. On both DNAs, there are small numbers of high affinity reaction sites for N-acetoxyAAF binding. On each DNA similar locations of these high affinity sites were obtained with the different enzymes. Results of experiments on the effects of the presence of equilibrium bound NQO on the binding of N-acetoxyAAF to pBR322 are also presented.

T-PM-B5 LARGE TRIPLET STATE PERTURBATIONS OF THE 9,10-EPOXY-7,8,9,10-TETRAHYDROBENZO(A)PYRENE CHROMOPHORE UPON IN VITRO BINDING TO DNA. S. M. Lefkowitz*, V. Kolubayev, and H. C. Brenner, Department of Chemistry, New York University, New York, NY 10003

We have used optically detected magnetic resonance (ODMR) to help characterize the local environment of 9,10-epoxy-7,8,9,10-tetrahydrobenzo(a)pyrene (BaPE) covalently bound to DNA. ODMR probes the three sublevels of the photoexcited triplet state, whose microwave frequency splittings and kinetics are sensitive to environmental factors. Our previous ODMR studies of the covalent DNA adducts of 9,10-epoxy-9,10,11,12-tetrahydrobenzo(e)pyrene and 7,8-dihydroxy-9,10-epoxy-7,8,9,10-tetrahydrobenzo(a)pyrene have indicated a quasi-intercalative environment for the pyrene triplet chromophore in the former and a solvent exposed conformation in the latter, based on zero field splittings in model systems and sensitivity of these splittings to denaturation and enzymatic digestion of the DNA adducts. In the case of BaPE, the photoexcited triplet adduct chromophore is highly perturbed by the presence of the nucleic acid; the phosphorescence is red-shifted nearly 25 nm from that of the model diol in the same solvent, both the D + E and 2E zero field transitions are down-shifted several tens of MHz, and the 77K phosphorescence lifetime is halved. These perturbations are much more drastic than those observed with BePE-DNA. Moreover, denaturation and enzymatic digestion have only a small effect on the ODMR of the adduct, in contrast to the results for BePE-DNA. Thus the predominant source of environmental perturbation in the BaPE-DNA case appears to be the base to which BaPE is covalently bound, rather than the double strand and single strand interactions which appear to cause most of the ODMR shift in BePE-DNA. Work supported by NCI Grant CA 20851. *Present address: Chemistry Division, Argonne Nat'l Lab., Argonne, IL 60439.

T-PM-B6 INDUCED CIRCULAR DICHROISM OF SOME POLYCYCLIC AROMATIC HYDROCARBONS IN THE DNA SOLUTIONS. Fu-Ming Chen (Intr. by David J. Puett), Department of Chemistry, Tennessee State University, Nashville, Tennessee 37203

Pyrene is found to exhibit strong optical activity in the DNA solutions as a result of intercalation of this planar molecule into the dissymetric environment of double helix. Dissociation of pyrene from DNA by the addition of sodium dodecyl sulfate (SDS) as well disruption of the duplex structure by denaturation can demolish such an induced optical activity. Circular dichroism (CD) measurements are carried out for pyrene saturated in various deoxypolynucleotide solutions (poly (dA-dT)·poly (dA-dT), poly (dG-dC)·poly (dG-dC), poly (dA)·poly (dT), and poly (dG)·poly (dC)) in order to elucidate the base sequence specific binding nature of intercalation. The results indicate that except for the poly (dA-dT)·poly (dA-dT), little or no CD is observed in these solutions (∿0.3mM in 0.01M NaCl). The large induced optical activity observed in the poly (dA-dT)·poly (dA-dT) solution coupled with the CD spectral similarity to that of pyrene in the native DNA solution serve to support our earlier conclusion through absorption spectral investigation that pyrene binds strongly to poly (dA-dT)·poly (dA-dT) by the intercalative mode but exhibits preference for the external mode and lesser binding ability for the other polynucleotides studied. The effect of salt concentration on the induced CD spectra are also investigated for other polycyclic aromatic hydrocarbons such as benzo(a)pyrene and 3-methylcholanthrene. (Supported by CA19817 and S06RR08092-09) of MBRS.)

T-PM-B7 Poly(dI-dC) · Poly(dI-dC):VACUUM ULTRAVIOLET CIRCULAR DICHROISM.*
John Clark Sutherland and Kathleen Pietruszka Griffin.
Biology Department, Brookhaven National Laboratory, Upton, NY 11973

We report the 180-300 nm circular dichroism (CD) of poly(dI-dC) in D_2O containing 20 mM potassium phosphate buffer at pD 7. The far ultraviolet (210-300 nm) CD has a negative maximum near 283 nm and a positive maximum near 260 nm, in agreement with previous reports (e.g. Mitsui et al., Nature 228, 1166-69; 1970). In the vacuum ultraviolet (vuv) region (wavelengths < 210 nm) we find a negative band at 203 nm and a very strong positive band at 188 nm. The far uv CD of poly (dI-dC) resembles the far uv CD of the high salt form of poly(dG-dC) (Pohl and Jovin, J. Mol. Biol. 67, 375-396; 1972), now known to correspond to the left-handed "Z" form of that polymer. The inverted far uv CD along with x-ray fiber diffraction patterns led Mitsui et al. (ibid) to speculate that poly(dI-dC) might adopt a left-handed double helical structure. In contrast, the vuv CD of poly(dI-dC) that we measured is similar to the vuv CD spectra of all of the right-handed double helical DNA's that have been reported to date and strikingly different from the vuv CD of left-handed "Z" DNA (Sutherland et al., Proc. Nat. Acad. Sci. 78, 4801-4804; 1981). Thus vuv CD, in agreement with more recent x-ray fiber patterns recorded at high humidity (Grant et al., Biochem. 11, 805-815; 1972 and Weslie et al., J. Mol. Biol. 143, 49-72; 1980) suggests that poly(dI-dC) adopts a right-handed B or B' double helical conformation in solution. Our results strengthen the proposal of Johnson (Ann. Rev. Phys. Chem. 29, 93-114; 1978) that vuv CD is a more reliable indicator of polynucleotide structure than is the more extensively studied far uv CD.
* CD spectra recorded using the SUPERB vacuum spectrometer at the National Synchrotron Light Source. This research, SUPERB and the NSLS are supported by the U. S. Department of Energy.

T-PM-B8 EXCHANGE OF THE HYDROGEN BONDED IMINO PROTONS IN CYTOSINE CONTAINING DNA AND RNA DUPLEXES.
Peter A. Mirau and David R. Kearns. Department of Chemistry, B-014, University of California San Diego, La Jolla, Ca, 92093.

The exchange rates of the hydrogen bonded imino proton in guanine-cytosine and inosine-cytosine containing DNA and RNA duplexes have been measured by ^1H NMR relaxation techniques in H_2O solution in an attempt to determine what relationships may exist between nucleic acid structure, conformation, and sequence and the base pair opening which results in exchange of the imino protons with the solvent. The spin-lattice relaxation rates of the imino protons are dominated by magnetic dipolar interactions at low temperatures and by exchange with the solvent at high temperatures. The exchange is limited by formation of the open state from which exchange occurs so these rates are a measure of the fluctuations in the double helix. Exchange from Z form polymers is very slow and exchange from similarly sequenced B form DNA polymers is faster than that from A form RNA or DNA-RNA duplexes. The more thermally stable alternating purine-pyrimidine duplexes exchange more rapidly at room temperature than do the homopolymer duplexes. Inosine containing duplexes exchange more rapidly than guanosine containing ones and methylation or bromination of the cytosine leads to slower exchange. Results will be presented for the B and Z forms of poly(dG-dC) and poly(dG-dm^5C), poly(dG)poly(dC), poly(dG)poly(rC), poly(rG)poly(dC), poly(rG)poly(rC), poly(dI-dC), poly(dI-dbr^5C), poly(dI)poly(dC), and poly(rI)poly(rC). A model for the open state from which exchange occurs which correctly predicts the exchange rates and activation energies will be presented.

T-PM-B9 IONIC STRENGTH DEPENDENCE OF PERSISTENCE LENGTHS AND EXCLUDED VOLUME PARAMETERS FOR T7 DNA.
J.A. Harpst and E.S. Sobel. Dept. of Biochem., Case Western Reserve Univ. Cleveland, OH 44106

Rayleigh light scattering (total intensity) measurements have been made on T7 bacteriophage DNA over a wide range of angles (4-135°) and concentrations of Na^+ (0.005-3.0 M) in a dilute sodium phosphate/EDTA buffer. Calibration of the instrument and subsequent treatment of the data have been based on the molecular weight of T7 DNA ($M = 26.43 \times 10^6$), recently determined by sequence analysis. The standard reciprocal intensity method of Zimm, utilizing linear least squares analyses by computer, provided root-mean-square radii (R), second viral coefficients (A_2), and experimental scattering curves [$P^{-1}(\theta)$] over the indicated angular range. Fitting these experimental curves to theoretical ones, calculated from wormlike coil theory with the equations of Sharp and Bloomfield, gave values of the persistence length (a) and excluded volume parameter (ε) as a function of ionic strength. The results obtained at three of the Na^+ concentrations studied were:

$[Na^+]$ (M)	R (nm)	$A_2 \times 10^4$ (mol cm^3 g^{-2})	a (nm)	ε
1	493	1.7	45	0.05
0.2	529	2.9	48	0.07
0.01	708	11.	74	0.12

These determinations of a and ε agree with some recent measurements of the parameters by other workers who used different techniques, and are consistent with recent theoretical considerations of changes in persistence length with ionic strength. (Supported in part by USPHS grants no. GM-29828 and GM-21946.)

T-PM-B10 THE BASE SEQUENCE DEPENDENCE OF DNA STIFFNESS, J.D. LEGRANGE,[+] R.H. AUSTIN,[++] M.E. HOGAN,[+] AND J. WANG[+] DEPARTMENT OF BIOCHEMICAL SCIENCES[+] AND THE DEPARTMENT OF PHYSICS,[++] PRINCETON UNIVERSITY, PRINCETON, NEW JERSEY 08544

We have used the large time range of triplet state anisotropy decay to study the torsional and bending motions of synthetic nucleotides of differing base pair composition. We have found large differences in the molecular stiffness of dG-dC, dA-dT, and dAC-dTG. The torsional spring constant and bending lifetime have been evaluated through simulations of the Brownian motions of duplex DNA of varying length using Schurr's expression. The torsional spring constant of dG-dC is roughly an order of magnitude larger than the values obtained for dA-dT, dAC-dTG, and random chicken DNA. The bending time constant for dG-dC is 40μsec which is roughly 10X larger than the value for dA-dT and a factor of 4 longer than the values for dAC-dTG and chicken. The implications of these results for the role of base composition in nucleic acid function are discussed.

T-PM-B11 **MOTION OF DNA THROUGH GELS.** **Charles P. Bean and Hubert Hervet, General Electric Research and Development Center, Schenectady, NY 12301 and College de France, Paris Cedex 75231, France.**

Gel electrophoresis is the standard method by which DNA molecules are separated according to molecular weight-either for analytical or preparative ends. Typically the gels, cast in ionic solution, have openings many times smaller than the length, L, of a subfraction of the more or less flexible charged DNA molecules. Under the influence of an electric field-typically volts per centimeter - a given subfraction of DNA will move with a characteristic mobility-typically ~10^{-4} cm^2/V-sec. If the molecules are presumed to move along their own contour, guided by the pores in the gel, one can derive[1] that the mobility, μ, is given by $\mu=\mu_o\langle R^2\rangle/L^2$. In this equation μ_o is the mobility of a segment short enough to be essentially stiff and R is the end-to-end vector of the DNA. If, further, one assumes that the configuration of the molecule is a random coil characterized by directional correlation or persistence, length, a, one can show[2] that $\langle R^2\rangle=2a^2(L/a-1+\exp(-L/a))$. Substitution of this expression in the earlier equation gives an explicit prediction for mobility as a function of contour length or molecular weight in terms of two parameters, μ_o and a.

Experiments using double stranded DNA in agarose and single strand DNA in polyacrylamide show-on extrapolation to zero field strength-very close agreement the theory given above. The effective persistence length is primarily a function of gel concentration.

1. O.J. Lumpkin and B.H. Zimm, Biopolymers (to be published) and our independent derivation.
2. e.g. L.D. Landau and E.M. Lifshitz, Statistical Physics, Pergamon Press, 3rd ed. 1980 p. 400.

T-PM-B12 THERMAL DENATURATION OF pBR322 DNA. L.T.Pratt, J.E.Knowles & R.D.Blake, Dept. of Biochemistry, Univ. of Maine, Orono, ME 04473.

High resolution melting profiles of Eco Rl restricted pBR322 DNA (4362 base pairs, Fgc=0.537) have been obtained by measuring the loss of hypochromicity at 260 nm and 282 nm as a function of temperature by the difference-approximation method (BBA,518,233(1978); Biopolymers, 19,681(1980)). Profiles were obtained at a variety of ionic strengths under equilibrium conditions. They reflect a wide range of domain base compositions in pBR322 (Fgc≈0.34-0.67) with numerous well resolved subtransitions. Profiles have been calculated for the published sequence (Sutcliffe,CSHSQB 43,77 (1979)) using the Fixman & Freire algorithm (Biopolymers 16,2693(1977)) with a wide range of values for the loop initiation and loop exponent parameters, and for three independently determined sets of stability constants for the ten nearest neighbors, and with modifications to the basic model. We have managed to achieve a vague representation of the experimental profile, however agreement is quantitatively inadequate, if not ambiguous. Therefore, we conducted direct analyses of experimental profiles by assuming that pBR322 dissociates as a collection of independent, non-degenerate, two-state subtransitions. Deconvolution results in 29±1 subtransitions on the basis of thermodynamic criteria. The size of domains varies between 64-215bp and is conserved over a wide range of ionic strengths. The results of attempts at determining loci of domains by their base composition and melting temperature and by electron microscopy will be discussed.
Supported by NIH (GM22827) and MAES(No.08402).

T-PM-B13 ENTHALPY BINDING IN AN ALLOSTERIC MACROMOLECULE: S. J. Gill, J. Wyman, B. Richey, and G. A. Bishop, Department of Chemistry, University of Colorado, Boulder, Co. 80309.

The concept of enthalpy binding has been developed for allosteric systems described by a set of states with specific enthalpies and standard free energies. Comparison of enthalpy with ligand binding reveals parallels in terms of the transition phenomena of allosteric reactions. However, the mass law for ligand binding reactions leads to ligand binding polynomials and the concept of cooperativity. Neither of these features are found in thermal binding.

We have applied the general thermal state theory to tRNA data (P. L. Privalov, and V. V. Filimonov (1978), J. Mol. Biol. 122, 447-464). The thermal state approach with six allosteric states fits the data as well as the original Privalov analysis based on five independent transitions. The relation between the two approaches is found in the population of significant states. The advantage of the thermal state treatment is that it is essentially model independent. Furthermore the salt concentration dependance of the equilibrium constants for the reactions between thermal states can be examined by linkage theory to determine the amount of sodium chloride which is expelled as the molecule denatures to higher enthalpy states.

Acknowledgement: We wish to acknowledge support of this work from NSF Grant PCM 77-20262 (J.W.) and NIH Grant 5 RO1 HL22325 (S.J.G.).

T-PM-C1 **IS THE Na-Ca EXCHANGE MECHANISM ELECTROGENIC?** By W.J. Lederer, S-S. Sheu, D.A. Eisner & R.D. Vaughan-Jones. Dept. Physiol. Univ. Maryland, Baltimore, MD 21201; Dept. Physiol., Univ.College London, London, England; Dept. Pharmacology, Oxford Univ. ,Oxford, England.

The Na-Ca exchange mechanism should transport net charge if it transports more than 2 Na^+ per Ca^{2+}. Such an electrogenic Na-Ca exchange has been reported. Since convincing blockers of Na-Ca exchange remain to be found, the activity of this transport mechanism can be most readily altered by varying the Na-gradient or the Ca-gradient across the sarcolemma. In sheep caridac Purkinje fibers, we measured intracellular sodium activity (a_{Na_i}) with a Na-selective micorelectrode and controlled membrane potential with a two-microelectrode voltage-clamp technique. After blocking the Na-pump, reducing Na_o or Ca_o produces a transient increase in tension and a fall in a_{Na_i} that is consistent with the activation of a Na-Ca exchange mechanism. Simultaneously, however, there is a transient activation of a "non-specific" conductance that has a reversal potential between approximately -20 and -60 mV. The Fig. shows current and tension records on changing Na_o from 145 to 0 mM for voltage clamp pulses to -38 and -78 mV from a holding potential of -55 mV. The activation of this conductance is seen when the Na-Ca exchange mechanism should also be activated and appears to depend on a rise of intracellular calcium. These results indicate that variations in membrane conductance may parallel the change in activity of the Na-Ca exchange mechanism and, consequently, interfere with the measurement of a putative Na-Ca exchange current.

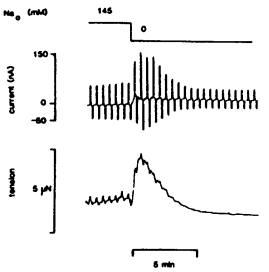

T-PM-C2 La^{3+} SELECTIVELY BLOCKS CALCIUM CURRENT IN SINGLE CELLS ISOLATED FROM BULLFROG ATRIUM. R. D. Nathan and W. Giles, Texas Tech University Health Sciences Center, Lubbock, Texas and The University of Texas Medical Branch, Galveston, Texas.

La^{3+} has been shown to inhibit the slow inward (Ca^{2+}/Na^+) current in multicellular cardiac muscle preparations, and to block Na^+-Ca^{2+} exchange in cardiac sarcolemmal vesicles. We have used a single microelectrode voltage clamp technique to characterize the actions of La^{3+} on transmembrane currents carried by Ca^{2+} and K^+ in individual cells obtained by trypsin and collagenase dispersion. TTX-resistant inward current (i_{Ca}) was reduced in a dose-dependent fashion by bath application of La^{3+} in HEPES-buffered Ringers (Ca^{2+}, 2.5 mM): 10^{-7} M reduced peak i_{Ca} by about 20% together with the overshoot and plateau of the action potential (resting potential, -90 to -96 mV). At 10^{-6} M, La^{3+} decreased i_{Ca} by about 70%, and at 10^{-5} M it completely blocked both inward (-40 to +50 mV) and outward (> +60 mV) current through the Ca channel. It is unlikely that this blockade is due to changes in surface charge, since La^{3+} (10^{-6} to 10^{-5} M) had no significant effect upon the voltage dependence of (i) steady-state inactivation of i_{Ca} (P_I = 300 ms, -90 to +10 mV; P_{II} = 150 ms, 0 mV), (ii) activation of the delayed rectifier K^+ current (-30 to +20 mV), and (iii) rate constants for the decay of K^+ tail currents (-90 to -40 mV). La^{3+} (10^{-5} M) produced no measureable changes in (i) the inwardly rectifying background K^+ current (-140 to -50 mV), (ii) the amplitude (-30 to +20 mV) or reversal potential of delayed potassium current. In summary, La^{3+} (10^{-7} to 10^{-5} M) produces a selective inhibition of i_{Ca} in amphibian atrial cells.

Supported by NIH Grants HL-27454 and HL-20708, and American Heart Association Grant 81-835.

T-PM-C3 IS Ca CHANNEL BLOCKAGE THE SAME AS Ca CHANNEL BONDAGE? A.M. Brown, H.D. Lux and A. Yatani. University of Texas Medical Branch, Galveston, Texas 77550 and Max-Planck-Institut, Munich, Germany.

The dihydropyridine Ca channel blocker nitrendipine binds with a very high affinity to nervous tissue (Gould et al, PNAS, 1982). The binding is reduced without a change of affinity when Ba is substituted for Ca. If the stoichiometry between binding and function is one, then the number, N, of Ba channels in a neuron should be less than N for Ca channels. We measured whole cell and elementary Ba and Ca currents in the same neuron and knowing the opening probability, calculated N. The experiments were done on isolated neurons of Helix. Whole cell clamp currents were measured with a two microelectrode voltage clamp and patch currents were measured with the gigaseal method. Na currents were suppressed by Tris substitution and K currents were suppressed by Cs substitution, TEA and 4-AP. Ba and Ca currents were produced in 40 mM extracellular divalent cation. Opening probabilities were estimated from tail current amplitudes at a return potential of of -50 mV following 5-8 msec steps over a range of potentials from -50 mV to +50 mV. Elementary currents at potentials from -20 to zero mV were determined from the mean values of the amplitude histograms and from the variance-mean ratio of ensembles of 25-50 patch clamp current records. The channel densities ranged from 2-9 μM^{-2}, and were the same for I_{Ba} and I_{Na}. Nitrendipine, between 10^{-8} and 10^{-9} M, blocked I_{Ba} and I_{Ca} equally well. We conclude that binding and blockage by nitrendipine are not equivalent. (A.M. Brown was a Josiah Macy Fellow; supported by NIH grant NS-11453)

T-PM-C4 INTRACELLULAR CA^{++} AND CA CURRENTS IN INTERNALLY PERFUSED SNAIL NEURONS. Lou Byerly and W. J. Moody, Dept. of Biol. Sci., USC, Dept. of Physiol., UCLA, and Dept. of Zool., U. of Wash.

Isolated neurons from the snail Lymnaea stagnalis were internally perfused and voltage clamped by the techniques of Byerly and Hagiwara (J. Physiol. 322:503, 1982). Intracellular concentration of Ca^{++} was measured with a Ca-sensitive microelectrode. The $[Ca^{++}]_i$ was not necessarily predictable from the $[Ca^{++}]$ of the perfusion solution. Perfusing with a solution that has 10 mM EGTA & no added Ca (0Ca-10EGTA) at pH 7.3 (100 mM HEPES), $[Ca^{++}]_i$ was $1\text{-}3\times10^{-7}$M, even though $[Ca^{++}]$ of the perfusion solution was well below 10^{-7}M. When the perfusion solution was changed to 5Ca-10HEDTA (10^{-6}M Ca^{++}), $[Ca^{++}]_i$ showed almost no change in a few cells, but in the majority of cells it rose rapidly to a value above 10^{-5}M. This surprisingly large increase in $[Ca^{++}]_i$ was accompanied by the development of an inward holding current at -50 mV. Removal of external Ca^{++} or addition of external Cd^{++} blocked the inward holding current and the large increase in $[Ca^{++}]_i$, suggesting that the Ca^{++} came from the external solution. Perfusion with 0Ca-10EGTA turned off the inward holding current and returned $[Ca^{++}]_i$ to $1\text{-}3\times10^{-7}$M. The Ca current "washed out" of these cells with internal perfusion. When $[Ca^{++}]_i$ was $<3\times10^{-7}$M, the Ca current appeared to be stable during the first 5-10 min of perfusion, but then fell to half its initial value after about 20 min of perfusion. When the cell was perfused with 9.4Ca-10EGTA ($[Ca^{++}]>10^{-6}$M), $[Ca^{++}]_i$ was about 10^{-6}M and the Ca current washed out much faster, falling to half in about 5 min. When the cell was returned to 0Ca-10EGTA after a few minutes of perfusion with a high Ca solution that brought the Ca current near zero, the Ca current showed very little recovery, although $[Ca^{++}]_i$ rapidly returned to a low value.
Supported by NS15341 and NS09012.

T-PM-C5 VOLTAGE-GATED CALCIUM CHANNELS IN MOUSE MYELOMA CELLS. Yasuo Fukushima and Susumu Hagiwara, Department of Physiology, Jerry Lewis Neuromuscular Research Center, UCLA Los Angeles, CA 90024.

At least two lines of evidence suggest that calcium ions play a role in the immune response. First, external Ca ions are required at the stage of target cell cytolysis by lymphocytes, when the lethal hit is thought to take place. Second, Ca ions are necessary for lymphocyte proliferation when stimulated by antigens and mitogens. Because of this Ca ion involvement, we wanted to investigate the possible role of the Ca channel in mediating the lymphocyte immune response. However, because of difficulties in keeping and recording from normal lymphocytes, we have started by examining the electrophysiological properties of mouse myeloma cells which are neoplastic lymphocytes. The myeloma cell line called S194 was examined, which synthesizes, but does not secrete, antibodies of the IgA class.

The whole cell was voltage-clamped with patch clamp technique and we found Ca current due to voltage-gated Ca channels. Ca inward current, which decayed exponentially after the peak, was activated around -50 mV and attained the maximum around -20 mV in 10 mM Ca solution. Outward current was negligible at least up to +30 mV. In these Ca channels, the Sr current was larger than Ba and Ca, and the inactivation kinetics were similar. Since the steady-state inactivation was clearly observed at potential levels more negative than those for inward Ca current activation, the inactivation of the Ca channel in mouse myeloma cells was considered to be voltage-dependent. For reasons which we have not yet understood, the amplitude of Ca currents varied greatly among cells.
Supported by USPHS grant NS 09012 and a grant from the MDA to S.H. and a MDA fellowship to Y.F.

T-PM-C6 Block Of Calcium Channels In Synaptosomes By Polyvalent Cations. D.A. Nachshen, Dept. Physiology, University of Maryland School of Medicine, Baltimore, MD 21201

Voltage-dependent ^{45}Ca influx was measured in synaptosomes (isolated presynaptic nerve terminals) from rat brain, that were depolarized by raising the extracellular potassium concentration. Influx was terminated at one sec, so that most of the uptake was mediated by inactivating ('fast') Ca channels (Nachshen and Blaustein, 1980, J. gen. Physiol. 76, 709-728). This influx was blocked by polyvalent cations with half-inhibition constants (K_I) that were clustered in three distinct groups: 1) K_I = 0.2 - 1 μM (Cd, Y, Pb, and the lanthanides, group I), 2) K_I = 50 - 100 μM (Mn, Co, Ni, Zn, and Hg, group II), or 3) K_I > 1 mM (Mg, Sr, and Ba, group III). Most inhibitory ions had little effect on synaptosome membrane potential (monitored with a voltage-sensitive fluorescent dye), or on the voltage-dependence of Ca influx, at concentrations close to their K_I. Lineweaver-Burke type experiments showed that all of the blockers competed with Ca for the channel site involved in ion transport. This site appears to have a high affinity for cations with an ionic radius close to that of Ca, and with a high charge/radius ratio. The low efficacy of Mg may indicate that small, highly hydrated cations are excluded from the channel. Supported by NIH grant NS-16461.

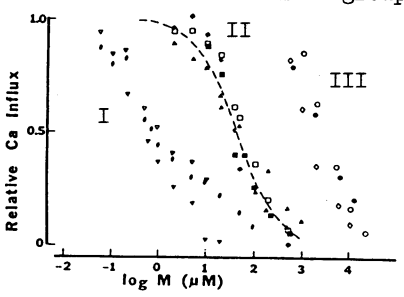

T-PM-C7 CALCIUM CHANNELS FROM PARAMECIUM CILIA INCORPORATED IN A PLANAR LIPID BILAYER.
B.E. Ehrlich, A. Finkelstein, M. Forte*, C. Kung*. Department of Physiology and Biophysics, Albert Einstein College of Medicine, Bronx, NY and *Laboratory of Molecular Biology, University of Wisconsin, Madison, WI.

We have been able to incorporate voltage-dependent Ca^{++} channels into a planar lipid bilayer. The Paramecium was chosen for these reconstitution studies because voltage-dependent Ca^{++} channels exist on the cilia only and because it is possible to prepare large quantities of pure ciliary membrane vesicles. In addition, the suitability of Paramecium to electrophysiological, biochemical genetic, and behavioral studies makes it possible to compare many characteristics of the in situ and reconstituted channel. On a macroscopic level the reconstituted currents are comparable to in situ Ca^{++} currents in ionic selectivity, in degree of blockage by metal ions, and by the lack of Ca^{++} currents in one mutant. For example, when an ionic gradient of Ca^{++}, Ba^{++}, or Sr^{++} is imposed across the bilayer, currents are measured at V = 0. A Mg^{++} gradient does not produce a detectable current. On a microscopic level, at least two channels that carry divalents have been observed with single channel conductances of 35 pS and 1.5 pS, respectively. Both of these channels are ideally selective for cations over anions and are voltage-dependent. However, only the smaller channel selects among the divalents with a selectivity sequence similar to the in situ channel and responds to voltage as expected for the Ca^{++} channel.

Supported by NIH grant GM 29210, NSF grant BNS-7918554, and a Muscular Dystrophy Foundation Postdoctoral Fellowship to BEE.

T-PM-C8 ION-ION INTERACTIONS IN THE Ca CHANNEL OF SINGLE HEART CELLS.
Peter Hess, Kai S. Lee and Richard W. Tsien, Department of Physiology, Yale University School of Medicine, New Haven, CT 06510.

A single binding site for divalent cations within the Ca channel has been used successfully by Hagiwara et al. to explain saturation of I_{Ca} at high Ca_o and block of I_{Ca} by inorganic ions such as Co^{2+} or Ni^{2+}. In agreement with this theory, I_{Ca} in dialyzed guinea pig ventricular cells is less sensitive than I_{Ba} to block by Cd^{2+}, as expected since Ca^{2+} binds more strongly than Ba^{2+}. However, the opposite is true for D600, diltiazem and nitrendipine: I_{Ca} is more sensitive than I_{Ba} to drug block. This behavior is not expected for a simple, lone binding site. Another argument comes from observations of ion-ion interactions. Peak inward current does not change monotonically as Ca_o is replaced by Ba_o (Ca_o+Ba_o=10 mM). In solutions with 1-3 mM Ca_o (9-7 mM Ba_o), the current reaches a minimum which is considerably smaller than the current seen in either 10 mM Ca_o or 10 mM Ba_o (Figure). Such an "anomolous mole fraction effect" has been reported for gramicidin channels or inward rectifier K channels, but not so far for Ca channels. The blocking effect of Ca ions was also seen with Ba_o kept constant. Like the organic drug effects, the interactions between permeant ions call for modification of the single binding site model. The Ca channel might be simultaneously occupied at two or more binding sites with different ionic preference, or it might contain a single site whose properties are influenced by the previous history of ion permeation.

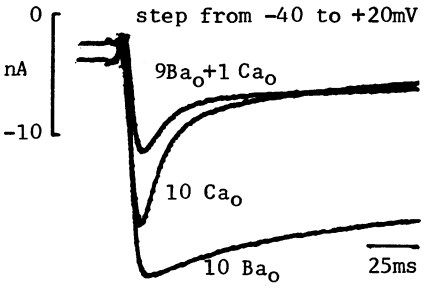

T-PM-C9 ACTIVATION AND INACTIVATION OF TWO VOLTAGE-DEPENDENT Ca CHANNELS
Joachim W. Deitmer, Abteilung Biologie, Ruhr-Universität, D-4630 Bochum, FRG

The two-intracellular-microelectrode technique was applied to investigate membrane currents in the hypotrich ciliate Stylonychia mytilus. The fast, early inward current was carried by Ca ions (or Sr or Ba ions). The inward current-voltage relationship, I_{in}-V, had two peaks, one at -45 mV, and the other at -15 mV (holding potential -50 mV). The Ca permeability at -45 mV was calculated according to the constant field theory to be about one order of magnitude smaller than at -15 mV. When the cell released its membranellar band (row of compound cilia at the anterior), the inward current peak at -45 mV disappeared. At the same time the two-peak action potential lost one component and changed to a single-peak action potential. Similar changes in early inward current and action potential could be obtained by surgically removing the anterior, but not the posterior, cell end. Reducing the K outward current with tetraethylammonium or 4-amino-pyridine did not change the course of the I_{in}-V relationship. Co^{2+} inhibited both Ca currents, but with different efficacies. When Ba^{2+} was used as charge carrier, the I_{in}-V relationship was similar as in Ca, although the kinetics of activation and inactivation of the two types of currents were affected differently by Ba. It is concluded that the membrane of Stylonychia contains two, spatially separated classes of voltage-dependent Ca channels. The existence of two Ca channels may be related to the independent motor control of the two main groups of ciliary organelles in this cell.

- Supported by the Deutsche Forschungsgemeinschaft, SFB 114 TP A5

WITHDRAWN

T-PM-C11 ELECTRICAL RECORDING OF A VOLTAGE DEPENDENT Ca CONDUCTANCE IN THE SQUID AXON. Caputo, C., DiPolo, R. and Bezanilla, F. (Intr. by L.Mateu). C.B.B., IVIC, Apartado 1827, Caracas 1010A, Venezuela. Dept. Physiology. UCLA. Los Angeles, CA 90024 and MBL Woods Hole, MA 02543, USA.

We report the measurement of TTX insensitive Ca currents in freshly dissected, voltage clamped squid axons (L. pealei) under internal dialysis or perfusion. Prolonged exposure to K-free internal and external media, was used to eliminate the flow of Ca^{++} through K channels and TTX prevented its flow through the Na channels. Unspecific leakage currents were diminished by using solutions prepared with large organic ions (tris, N-methylglucamine and Methanesulfonate). Membrane resistance reached values close to 80 $K\Omega cm^2$. In some experiments signal averaging and subtracting procedures were also used. Under these conditions inward currents, dependent on the presence of external calcium and blocked by cadmium could be visualized. The magnitude and time course of the currents is voltage dependent. Noticeable activation occurs at -40 mV and the current is maximum at about 0 mV. The mean values of the maximal inward current was 2.9 $\mu A/cm^2$ in 80 mM Ca_o (at 0 mV) and 0.93 $\mu A/cm^2$ in 10 mM Ca_o (at -10 mV). The peak value of the currents at 0 mV was attained in less than 10 msec. With relatively long pulses (up to 70 msec) no noticeable inactivation was observed, However steady depolarization to 0 mV membrane potential, caused the currents to inactivate 50% in about 45 sec. Ba ions could substitute for Ca causing only a small shift in the I-V curve toward less positive potentials. These currents demonstrate the presence of a voltage dependent Ca conductance in the squid giant axon which may play a role in the total Ca entry during depolarization. Supported by PHS GM 30376 and IDEA.

T-PM-C12 EVIDENCE FOR AN INCREASED VOLTAGE-DEPENDENT CA^{++} CURRENT IN HERMISSENDA B PHOTORECEPTORS DURING RETENTION OF ASSOCIATIVE LEARNING. J. Farley*, W. Richards* and D.L. Alkon. *Dept. Psych. Princeton, and Sect. Neural Systems, Lab. of Biophysics, NINCDS, MBL, Woods Hole.

An early, voltage-dependent K^+ current (I_A) in the Type B photoreceptors of Hermissenda, is selectively reduced during retention of associative learning (Alkon et al., Science, 215: 693, 1982). Here, we present evidence for a complementary training-induced increase of an inward calcium current. Following conditioning of intact animals, light-induced peak (26.2 mV vs. 21.0 mV) and steady-state generator potentials (23.3 mV vs. 15.4 mV), as well as dark input resistances, were greater for isolated B cells from associatively-trained vs. control animals ($p<.05$). A 10 sec, 40 mV depolarizing current step prior to the light step, causing inactivation of I_A, (Shoukimas and Alkon, in prep.), enhanced the between-group differences in light responses (31% vs. 9.4% increases in peak response), and also increased the delay-to-peak response (58% vs. 0% increase) for associatively-trained animals vs. control ($p<.05$). These results suggest that associative training produces a long-term enhancement of an inward Ca^{++} current (also enhanced by the preceding depolarizing current step). The results are inconsistent with changes in any of the other major B cell conductances. For example, previous research (West et al., J. Neurophysiol., 48: 1243, 1982) indicated that I_{Na} is unchanged by training. In addition, prolonged depolarization of the B cell would be expected to have little or no effect upon the delayed outward K^+ (I_B). Associative training-induced effects on Type B light responses and membrane conductances in the presence of 4-aminopyridine will also be discussed.

T-PM-C13 EFFECTS OF LOW-FREQUENCY AMPLITUDE MODULATED RADIOFREQUENCY WAVES ON THE CALCIUM EFFLUX OF THE HEART. J.L. Schwartz*, J. Delorme† and G.A.R. Mealing* (Introduced by S.L. Jacobson°), *Division of Biological Sciences, National Research Council of Canada, Ottawa, Canada, †Department of Biology, University of Ottawa, Ottawa, Canada, and °Department of Biology, Carleton University, Ottawa, Canada.

The effects of low level 240 MHz electromagnetic radiation, both continuous and amplitude modulated at heart natural beating frequencies and at 16 Hz, were examined. Frog hearts, stimulated at their natural beating frequency throughout the experiments, were loaded with $^{45}Ca^{2+}$ for 30 min, rapidly rinsed, and then exposed for 30 min in vials filled with non-radioactive Ringer solution in a TEM irradiation cell at specific absorption rates between 0.15 and 3.0 μW/g (incident power between 0.5 and 10 W). Radioactive calcium counts of washout solutions and hearts were compared to those obtained from sham-irradiated samples.

The results indicate that under certain conditions low level electromagnetic energy significantly increases the calcium efflux from heart by about 19%. This effect could only be detected when the carrier wave was modulated at 16 Hz, the incident power being 1 Watt. It was not seen for either continuous or heart natural frequency modulated waves. The absorbed power levels seem to exclude possible gross heating of the hearts. Our results will be discussed in relation to findings by other investigators on calcium efflux changes in brain tissue exposed to microwaves.

T-PM-C14 ELECTRICAL ESTIMATES OF Ca CHANNEL DENSITY IN HEART CELL MEMBRANES. Bruce P. Bean, Martha C. Nowycky and Richard W. Tsien, Departments of Physiology and Neuroanatomy, Yale University School of Medicine, New Haven CT 06510.

In patch clamp studies of Ca channel activity in neonatal rat heart cells, we have compared two different approaches for estimating the number of functional Ca channels (N_f): (1) Many-channel recordings under similar conditions as single channel recordings of unitary current amplitude, and (2) ensemble fluctuation analysis. In (1), whole cell recordings of Ca channel current (I) were obtained in near-isotonic Ba_o (~100 mM). For steps to the inward peak of the I-V relation, we found $\langle I_{max}\rangle$=494 pA and $_2\langle c_m\rangle$=31 pF (7 cells). This gives a current density of 16 pA/pF (=16 V/s) or, assuming 1 uF/cm^2, 16 uA/cm^2. With a rough estimate of $(i\cdot p)_{max}$ as ~0.5 pA (Reuter, Stevens, Tsien & Yellen, 1982), $N_f=I_{max}/(i\cdot p)_{max}$ is ~1000 channels per cell (range: 250-1800). In (2), fluctuation analysis of whole-cell current records gave plots of variance vs. mean current fitted by var=iI-I^2/N_f. In two cells in isotonic Ba_o, depolarizations to +40 or +50 mV gave i=0.22 and i=0.25 pA (in harmony with the earlier unitary current data), and N_f ~750 and ~2500. In 5 other cells in 10 Ca_o or 10 Ba_o, the range for N_f was 1700 to >7500. Clearly, further analysis is needed. Methods (1) and (2) have different limitations. Combining whole-cell and single-channel data is simple in principle, but high Ba_o or Ca_o is needed for resolution of i, and membrane potential in cell-attached patches is not directly measured. Ensemble fluctuation analysis is adequate for low as well as high Ba_o or Ca_o, but its accuracy is limited by even small drifts. It will be important to find out what contribution run-down makes to the variability in N_f, and to see how N_f compares with the number of (3H)-nitrendipine binding sites.

T-PM-C15 SURFACE CHARGES AND CALCIUM CHANNEL SATURATION IN SKELETAL MUSCLE MEMBRANE OF THE FROG. G. Cota and E. Stefani. Department of Physiology and Biophysics, Centro de Investigación del IPN, Apartado Postal 14-740, México, D.F. 07000, México.

Current clamp experiments were performed at 23°C in the cutaneous pectoris muscle from Rana pipiens. Muscles were incubated in a K^+-free TEA and Cs-containing solution prior to experiments to further block K outward currents. The recording solution was (mM): TEA-CH_3SO_3 120, $Ca(CH_3SO_3)_2$ 2-30 and sucrose 290-374 (pH 7.0). Ca was isotonically substituted by Ba. We used the maximum rate of rise ($\dot{V}_{max}$) of the Ca (or Ba) action potential as a measure for I_{Ca} (or I_{Ba}). $\dot{V}_{max}$ showed saturation at high divalent cation concentration. Following Michaelis-Menten kinetics, K_m and $\dot{V}_{max-s}$ (the saturated $\dot{V}_{max}$) were respectively 7±1 mM and 2.0±0.2 V/seg with Ca(5-10 fibres), and 25±5 mM and 4.5±0.8 V/seg with Ba (7-13 fibres). The membrane potential (E_m^*) at $\dot{V}_{max}$ and the spike threshold shifted to more positive values with increasing divalent cation concentration. For example, E_m^* shifted from +25.0±1.0 mV (3) to +32.1±3.0 mV (3) when Ca was increased from 10 mM to 30 mM (with Ba, E_m^* was respectively +9.9±1.7 mV (7) and +16.1±1.5 mV (5)). These shifts were fitted following the Gouy-Chapman-Stern theory. Binding constant of divalent cation to charged groups on the surface membrane was zero for Ba and 39±3 M^{-1} for Ca. The free surface charge density and surface potential (Ψ) were 0.20±0.03 e$^-$/μm^2 (Ψ=-30.3 mV) with 10 mM-Ba, and 0.09±0.01 e$^-$/μm^2 (Ψ=-15.0 mV) with 10 mM-Ca. The $\dot{V}_{max}$ vs. Ca and Ba surface concentration curves also showed saturation. Corrected values for K_m and $\dot{V}_{max-s}$ were respectively 65±5 mV and 3.5±0.3 V/seg with Ca, and 450±50 mM and 6.5±0.5 V/seg with Ba. In conclusion, saturation of I_{Ca} or I_{Ba} could involve both surface charges effects and internal binding site(s) in the calcium channel.

T-PM-D1 CORRELATION OF THE INTERACTION PROPERTIES OF CHICKEN GIZZARD TROPOMYOSIN WITH ITS PRIMARY STRUCTURE. Clive Sanders and Lawrence B. Smillie, MRC of Canada Group in Protein Structure and Function, Dept. of Biochemistry, University of Alberta, Edmonton, Canada, T6G 2H7.

Chicken gizzard tropomyosin (gTM) and rabbit striated muscle α-tropomyosin (αTM) have been compared with respect to their ability to polymerize head-to-tail and to interact with rabbit skeletal F-actin and troponin. While the binding of gTM and αTM to F-actin is affected similarly by increasing [Mg^{2+}] and reaches a level of 1 TM to 7 actin monomers, the head-to-tail polymerization of gTM is more extensive than αTM as indicated by both viscosity and sedimentation equilibrium measurements. The binding of troponin to gTM is weaker than to αTM (affinity chromatographic and viscosity evidence). The latter observation is consistent with the demonstration (Pearlstone & Smillie (1982) J. Biol. Chem. 257 10587-10592) that the T1 fragment of troponin-T binds less strongly to gTM than to αTM whereas the T2 fragment binds similarly to both. These interaction studies can be correlated with amino acid sequence differences in the two proteins at their COOH-terminal ends. Whereas their primary structures are highly homologous from residues 1 to 260, significant differences, including the absence of Tyr-261 and Tyr-267 in gTM, are present from residues 261 to 284, the region of binding of the troponin-T1 fragment to αTM (Mak & Smillie (1981) J. Mol. Biol. 149 541-550).

(Supported by MRC of Canada.)

T-PM-D2 THREE-DIMENSIONAL ASPECTS OF THE REPETITIVE STRUCTURE OF TROPOMYOSIN. G. N. Phillips, Jr., Dept. of Physiology & Biophysics, University of Illinois, Urbana, IL 61801

Tropomyosin is a two-stranded α-helical coiled-coil molecule that winds around the actin filaments of muscle. These molecules have a length such that each one can span seven actin monomers. McLachland and Stewart (J. Mol. Biol. 103, p. 271) have analyzed the amino acid sequence as a one dimensional object and concluded that there are not seven, but fourteen, quasi-equivalent repeats along the length of tropomyosin. This finding has led to the suggestion that one set of seven sites is used for the 'on' state of muscle, and the other set for the 'off' state.

Using results from X-ray crystallography and known aspects of the stereochemistry of α-helical coiled-coils, atomic coordinates have been generated for the tropomyosin molecule. These coordinates are being used to examine the spatial distribution of amino acid side chains along the molecule. The sequence repeats give rise to structural repeats with intervals ranging from 52 Å to 63 Å, with an average of 59 Å. The irregularities in the periodic spacing have led to the suggestion that "flexible links" are necessary to attach tropomyosin to the actin helix. The lengths of the intervals require, furthermore, that tropomyosin bind to the actin helix at a fairly large radius (∿45 Å). Because actin monomers consist of two distinct domains, it may be that an "outer" domain of actin can move relative to an inner "helix-contact" domain, thus providing a binding site at large radius and contributing to the deviations from regularity required for tropomyosin-actin interactions.

Supported by a Beckman Research Award to G.N.P. and by NIH, MDA and NSF grants to C. Cohen.

T-PM-D3 TROPOMYOSIN INHIBITS THE RATE OF ACTIN POLYMERIZATION. S. E. Hitchcock-DeGregori and J. Maris. Dept. of Biological Sciences, Carnegie-Mellon Univ., Pittsburgh, PA 15213.

Addition of rabbit skeletal αβ-tropomyosin (TM) to purified skeletal actin monomer (A) inhibits the rate of actin polymerization but not the final extent in the following ionic conditions: 50mM or 100mM KCl, 50mM KCl + 2mM $MgCl_2$, 2mM $MgCl_2$ (all in 5mM TrisHCl pH 7.5, 0.1mM $CaCl_2$, 0.1mM ATP, 0.5mM DTT, 0.1mM NaN_3). Tropomyosin binds to F-A in these ionic conditions (determined by cosedimentation). In the presence of 0.5mM $MgCl_2$ there is a small but variable activation of the rate of polymerization. Inhibition of polymerization has been detected using high shear viscometry in Ostwald viscometers and right angle light scattering in a spectrofluorometer with excitation and emission set at 400 nm. Inhibition, measured as the time to reach half maximal viscosity or scattering, is due to a longer lag as well as a smaller slope during the period of maximal rate of increase in polymer. The effect is more striking when polymerization is followed using viscometry. The inhibition of polymerization by TM is saturated at a TM:A molar ratio of 1:7. Nucleation with F-A partially overcomes inhibition by TM, but polymerization is still slower than control A with nuclei. Since TM affects polymerization at low stoichiometric ratios to monomeric A, we suggest it is not acting directly on the actin monomer. The results indicate that TM exerts its effect at an early stage of polymerization, after formation of nuclei, and may in addition inhibit filament elongation. Our results are in contrast to earlier work reporting activation of polymerization by TM (Pragay and Gergely, 1968, Arch.Biochem.Biophys. 125, 727-733).

(Supported by grants from NIH (GM 28830 and AM 00914) and MDA).

T-PM-D4 FILAMENT "CUTTING" BY VILLIN. A. Weber, T. Walsh, M. Mooseker, E. Bonder. Department Biochemistry and Biophysics, University of Pennsylvania and Biology Department, Yale University. Villin added to F-actin shortens filaments and thus increases the filament number. Although that is generally attributed to cutting, i.e., villin-induced breakage, it could also be caused a) by nucleation followed by redistribution of monomers between original filaments and nuclei or b) to capping of filaments which without villin are in a steady state of breaking and reassociation. We used a depolymerization assay (at 0.05 uM actin) to distinguish cutting from a and b. Villin capping of barbed ends results in a reduction of the off-rate (1) equally at Ca 3-200 uM with villin less than 1 nM, i.e., no Ca effect on rate constants and (2) at villin up to 55 nM only at low Ca (3-10 uM) for a brief period. Interrupting villin action by EGTA restored control off-rate, i.e., no change in filament number. With high Ca (above 100 uM) and villin above 1 nM : the off-rate increased with time and in proportion to villin concentration. After interruption with EGTA off-rates exceeded control rates, i.e., filament number had been increased. Actin 20 X below critical ruled out (a) as cause for the increase in filament number. If (b) plays a role filament number must increase with dilution since reassociation should depend on square of filament concentration. Control off-rates were identical at 0.06 and 0.03 uM actin and at 10 and 200 uM Ca. Thus villin must have caused filament breakage. Tropomyosin (0.034 uM) protected against cutting over a 2 hr periods without inhibiting capping. Supported by NIH Grant HL-15-835.

T-PM-D5 FLUORIMETRIC STUDIES OF BINDING INTERACTION OF TROPONIN WITH TROPOMYOSIN. Tsung-I Lin and Robert M. Dowben, Muscle Research Laboratory, Baylor University Medical Center, Dallas, Texas 75246.

The binding interaction between troponin and tropomyosin has been studied fluorimetrically using tropomyosin labeled with N-(iodoacetyl-aminoethyl)-5-naphthylamino-1-sulfonic acid and troponin labeled with 5-iodoacetamidofluorescein. The binding curve, which was obtained by monitoring the steady-state fluorescence anisotropy or intensity changes, showed a simple binary complexing mechanism for troponin-tropomyosin binding interaction. Using labeled tropomyosin titrated with troponin, the apparent dissociation constants in the presence and absence of calcium ions were determined to be 0.532±0.192 μM and 0.587±0.287 μM respectively. Similar results were obtained for labeled troponin titrated with tropomyosin. The binding curve for labeled troponin titrated with calcium ions was biphasic indicating two classes of calcium binding sites. The apparent binding constants of calcium for troponin calculated from the midpoints of the transitions were approximately 1.25×10^7 $M^{-1}$and 1.58×10^6 M^{-1}. This work was supported by NIH grant HL-26881.

T-PM-D6 HETEROGENEITY OF THIN FILAMENT CALCIUM REGULATORY PROTEINS OF RABBIT SKELETAL MUSCLES. Margaret M. Briggs and F.H. Schachat. Department of Anatomy, Duke University Medical Center, Durham NC 27710. (Introduced by Darrell R. McCaslin).

Differences in the distribution of α and β tropomyosin species as well as heterogeneity of α subunits has been reported in rabbit skeletal muscles (Bronson and Schachat, J. Biol. Chem. (1982) 257, 3937). The species of both tropomyosin and troponin in fifteen rabbit skeletal muscles have now been evaluated by $NaDodSO_4$-polyacrylamide gel electrophoresis with and without 3.5M urea. Complex and heterogeneous patterns of expression were observed for both proteins. The muscle-to-muscle variations do not correspond to differences in fiber type determined by histochemical procedures. Experiments using intact muscle and homogenates indicate that the heterogeneity does not arise from proteolysis. In addition to the tropomyosin species previously reported, four species of troponin T (TnT) were found, two in fast muscles and two in slow muscles. The two fast troponin T species have been purified and designated TnT_{1f} and TnT_{2f}, according to their mobility on $NaDodSO_4$-polyacrylamide gels. Their amino acid compositions have been determined, and peptide mapping by gel and HPLC performed. These data combined with phosphorylation studies indicate that the two species are not interconvertible, suggesting that they do not result from the only known reversible post-translational modification of TnT. These two fast TnT species more likely result from the expression of different genes. This heterogeneity of troponins and tropomyosins makes clear that there is substantially more variability in thin-filament Ca^{+2} regulatory proteins than previously supposed.

This work was supported by a grant from the NIH (NS18228) to F.H.S.

T-PM-D7 BINDING OF TROPONIN C AND TROPONIN I AND FLUORESCENCE ENERGY TRANSFER STUDIES OF THEIR COMPLEX. Chien-Kao Wang and Herbert C. Cheung, Graduate Program in Biophysical Sciences and Department of Biochemistry, University of Alabama in Birmingham, Birmingham, AL 35294.

The association constant for complex formation between troponin I (TNI) and troponin C (TNC) labeled at Cys-98 with 5'-iodoacetamidoeosin (IAE) was determined in the presence (5.6×10^9 M^{-1}) and absence (6.7×10^5 M^{-1}) of Ca^{2+}. The difference in the corresponding free energy changes (-5.2 kcal) is the free energy coupling for binding of 4 moles of Ca^{2+} and one mole of TNI to the labeled TNC. We previously determined the distance between Met-25 and Cys-98 in TNC from energy transfer studies with dansylaziridine (DNZ) attached to the former residue and IAE to the latter (Biochemistry (1982) 21:5135). This work has been extended to include (1) the distance between Cys-48 and Trp-158 in TNI and (2) four intermolecular distances between the four residues of TNC and TNI in their binary complex. The minimum intramolecular distance of TNC in the TNC·TNI complex was 23Å. Ca^{2+} binding increased this distance to 27Å. The minimum intramolecular distance in isolated TNI was 14Å, with Trp-158 as the donor and 1,5-IAEDANS as the energy acceptor. The four distances between TNC and TNI were determined with DNZ attached to Met-25 and either 1,5-IAEDANS or IAE to Cys-98 in TNC, and IAE to the -SH in TNI. The following minimum separations were obtained in the absence (and presence) of Ca^{2+}: (1) Met-25 and Cys-48, 26Å(31Å); (2) Cys-98 and Trp-158, 17Å(17Å); (3) Cys-98 and Cys-48, 44Å(39Å); and (4) Met-25 and Trp-158, 15Å(15Å). The distances (1) and (3) are sensitive to Ca^{2+} binding. These results and the intramolecular distance in TNC suggest that Ca^{2+} binding to TNC induces structural perturbations in more than one regions of the TNC·TNI complex. (Supported by NIH AM-25193).

T-PM-D8 IDENTIFICATION OF AN ACTIVE SITE PEPTIDE OF MYOSIN AFTER PHOTOAFFINITY LABELING, Yoh Okamoto and Ralph G. Yount, Biochemistry/Biophysics Program and Department of Chemistry, Washington State University, Pullman, WA 99164-4630

The active site of myosin has been labeled by a new photoaffinity analog of ADP, N-(4-azido,2-nitroanilino)ethyl diphosphate (NANDP). [β-^{32}P]NANDP was trapped stoichiometrically (0.73 mole/mole) at the active site of subfragment one (SF_1) by crosslinking SH_1 and SH_2 using the Co(II)/Co(III) phenanthroline system [J. Wells and R. G. Yount, PNAS (1979), 76, 4966]. After photolysis for 2 min, 66% of the trapped NANDP was bound covalently to SF_1. Gel electrophoresis and radioautography showed only the 95K heavy chain fragment was labeled. Similar experiments after limited trypsin digestion further localized the modification site to the N-terminal 25K peptide. Extensive trypsin and subtilisin BPN' digestion of labeled SF_1 yielded two major radioactive hydrophobic peptides, P_1 and P_2, which were separated by reverse phase HPLC. Amino analysis of P_2 gave a composition of 1 Asx, 2 Pro, 2 Val, 1 Leu, 2 Tyr and 1 ε-N-trimethyl Lys, assuming [^{32}P] NANDP was incorporated 1:1 in the peptide. Peptide P_1 had a similar composition but was less pure. Both peptides gave Val on N-terminal analysis by dansyl chloride/TLC techniques. Recently S. W. Tong and M. Elzinga (in press) have sequenced the 25K peptide (residues 1-204) of rabbit myosin heavy chain. This fragment, which contains one of the two trimethyl lysines known to exist in myosin, has a peptide sequence Val_{125}-Asn-Pro-Tyr-$(Me)_3$Lys-Trp-Leu-Pro-Val-Tyr_{134} which fits the composition of P_2 almost exactly. Determination of the exact location of NANDP in the peptide is in progress. Supported by an MDA Fellowship to Y.O. and NIH grant AM-05195 to R.G.Y.

T-PM-D9 STRUCTURE OF MYOSIN/PARAMYOSIN FILAMENTS FROM A MOLLUSCAN SMOOTH MUSCLE. Loriana Castellani, Peter Vibert, Carolyn Cohen, Rosenstiel Basic Medical Sciences Research Center, Brandeis University, Waltham, MA 02254.

Molluscan smooth muscles are characterized by thick filaments that consist of a large core of paramyosin and a surface layer of myosin. Certain of these muscles display an unusual contractile activity known as "catch"; but the role of paramyosin and the design of these filaments in relation to the catch mechanism is still uncertain. We have analyzed the structure of thick filaments from a non-catch muscle from Mytilus edulis (Pedal Retractor Muscle) by X-ray diffraction and electron microscopy. The myosin crossbridge array in the relaxed state is characterized by a set of X-ray layer lines at 38, 24, 10.4nm. Direct observation of the crossbridge lattice in isolated, negatively-stained thick filaments shows that these layer lines come from a helical arrangement of bridges with 8/3 symmetry. Selective extraction of myosin performed on both systems confirms this conclusion. Isolated filaments, shadowed with platinum, demonstrate that the crossbridge helix is right-handed. The helical tracks run at a steep angle of about 17° to the filament axis and indicate a rotational symmetry of about 9-fold. The paramyosin core, revealed when the myosin is removed, shows features consistent with the model advanced by Elliott (1979) and Bennett and Elliott (1981) of a paracrystalline structure composed of planar sheets. We find, however, that the filament cores undergo some distortion upon removal of myosin. Our results on PRM indicate that the helical myosin surface lattice cannot be related in a simple manner to that of the paracrystalline core. These studies are being extended to other molluscan thick filaments.

Supported by grants from NIH, NSF, MDA and by a Fellowship from MDA to L.C.

T-PM-D10 CONFORMATION AND ASSEMBLY OF SMOOTH MUSCLE MYOSIN. Kathleen M. Trybus and Susan Lowey. Rosenstiel Science Center, Brandeis University, Waltham, MA 02254.

Filaments formed from dephosphorylated smooth muscle myosin from the calf aorta (10 mM KP_i, pH 7.5/0.15 M KCl/5 mM $MgCl_2$) are in equilibrium with 10S monomer. The 10S monomer is a bent or folded conformation in which the LMM region of the rod is bent back onto the S-2 region near the heads (Trybus et al., 1982; Suzuki et al., 1982; Onishi & Wakabayashi, 1982). The effect of light chain phosphorylation on the equilibrium between 10S monomer and polymer was investigated. Thiophosphorylation of the 20,000 dalton light chain does not change the sedimentation coefficient of the slow-moving boundary, suggesting that monomeric phosphorylated myosin can also form the bent 10S conformation. Phosphorylation shifts the equilibrium distribution in favor of polymer, however, both in the presence and absence of MgATP. A mixture of phosphorylated and dephosphorylated myosin, each having different aggregation properties, could account for the apparent lack of a critical concentration in the polymerization of smooth muscle myosin (Megerman & Lowey, 1981). The effect of phosphorylation on the size and shape of smooth muscle myosin filaments was investigated by electron microscopy. Filaments were assembled starting from different buffer conditions and states of myosin--monomeric myosin in high or low ionic strength, or from "minifilaments," small aggregates of smooth muscle myosin similar to those described by Reisler (1980) for skeletal muscle myosin. Despite the many similarities between smooth muscle myosin and skeletal myosin, there are distinct differences in the conformation of the monomer, the size of the minifilaments, the structure of the synthetic filaments, and the effects of nucleotide and phosphorylation on filament stability.

T-PM-D11 ARE MYOSIN SUBUNITS IN DYNAMIC EQUILIBRIUM. Guillermina S. Waller* and Susan Lowey. Rosenstiel Center, Brandeis University Waltham, Massachusetts 02254.

The subunits of myosin subfragment 1 (S1) have been shown to dissociate reversibly at 37°C in 10mM MgATP (Sivaramkrishnan and Burke, 1981). This raises the question of whether the myosin light chain (LC) heterodimer (a molecule containing both LC1 and LC3) can be generated by an exchange of light chains between two homodimeric species (a myosin containing 2 moles of LC1 or LC3). To resolve this problem myosin homodimers were isolated by immunoadsorbents specific for the N-terminal sequence of LC1 (anti Δ1) and LC3 (anti Δ2) (Silberstein and Lowey, 1981). Conditions for light chain exchange were incubation at 37°C, 10mM MgATP of equal concentration of LC1 and LC3 homodimers, or only one type of homodimer with a 20-fold molar excess of heterologous light chain. Hybrid formation was monitored by electrophoresis on polyacrylamide gels in a non-denaturing buffer. We find that under these conditions there is little or no light chain exchange. However, as reported previously, extensive exchange of light chains occurs in the presence of a dissociating agent such as 4.7M NH_4Cl (Wagner and Weeds, 1977). One possible explanation for the lack of exchange in myosin as compared to S1, might be a stabilizing effect of the LC2 (or DTNB) light chain which is absent in chymotryptic S1. We conclude, therefore, that the light chains are firmly bound to the myosin heavy chains, and it is highly unlikely that a dynamic equilibrium exists between the myosin subunits in a living muscle. (Supported by grants from NIH, NSF, and the Muscular Dystrophy Association)

T-PM-D12 MYOSIN FILAMENT ASSEMBLY AND SUPRAMOLECULAR STRUCTURE GENERATION.
Julien S. Davis, Department of Biology, The Johns Hopkins University, Baltimore, MD, 21218.

Pure myosin from vertebrate skeletal muscle can spontaneously self-assemble between pH 7.8 and 8.5 into thick filaments having a narrow length distribution and a morphology similar to the native filament.

Kinetic and equilibrium experiments in the pressure-jump were used to study the assembly and length-regulation mechanisms (Davis, J. S. (1981) Biochem. J. 197, 301-308, 309-314). The association reaction was found to be independent of filament length and occurs via a 44 nm parallel-dimer intermediate (Davis, J. S. et al. (1982) FEBS Lett. 140, 293-297). The rate of the dissociation reaction, on the other hand, increases exponentially by a factor of 500 as the filament grows bidirectionally from the central bare-zone out to its full length. Filament growth ceases at the point where equilibrium between the 'on' and 'off' rates is established.

These experiments show clearly that it is possible to assemble a complex 3-dimensional structure from like subunits alone. The full course of assembly including the nucleation stage relies on so-called emergent properties which appear sequentially during filament growth; the final phase of the process being the control of the apparently open-ended polymerization reaction described above. The mechanism is quite different from previously characterized polymerizing systems that are regulated by externally introduced information (copolymerizing proteins, etc.) or by simple geometrically imposed limits on polymer size (icosahedral viral coats and subunit enzymes).

T-PM-E1 RATE AND EQUILIBRIUM MEASUREMENTS OF THE LINKED BINDING OF MgADP AND ACTIN TO CARDIAC MYOSIN-S1. Raymond F. Siemankowski and Howard D. White, Dept. Biochemistry, University of Arizona, Tucson, AZ 85721.

We have measured the rate and equilibrium constants shown below for the linked equilibria between bovine ventricle (BV) myosin-S1 and ADP by stopped flow measurements. (Conditions: 100mM KCl, 5 mM MOPS, 2mM $MgCl_2$, pH 7, 15°). The Kassoc of BV actomyosin-S1 is ca. ten fold larger than for rabbit skeletal (RS) actomyosin-S1, due to the ten-fold lower rate of dissociation. The Kassoc of ADP to BV actomyosin-S1 is ca. 20 fold greater than to RS actomyosin-S1, due primarily to an eight-fold or greater decrease in the rate constant for the dissociation of ADP from BV actomyosin-S1. The antagonism between ADP and actin for binding to cardiac-S1 is only ca. one third that observed for RS S1. Although the rate of ADP dissociation from BV actomyosin-S1 is not the rate limiting step of ATP hydrolysis, (kcat=$6s^{-1}$), it is sufficiently slow to be the limiting step of S1 dissociation from actin by ATP in vitro and of cross bridge detachment in muscle. Moreover, the rate of dissociation of ADP may potentially limit the rate of contraction of an unloaded muscle. (Supported by grants from the Arizona Heart Association and PHS HL20984). In the figure, numbers in parentheses are from Flamig, D. and Cusanovich, MA., JBC, in press.

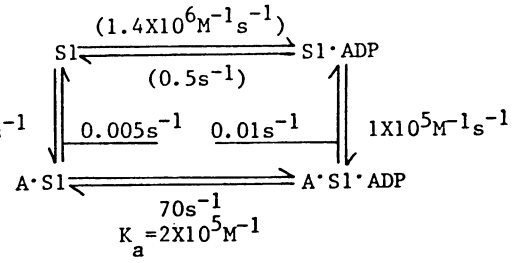

T-PM-E2 ADP BINDS TO MYOFIBRILS AND ACTOMYOSIN-S1 WITH EQUAL AFFINITIES. Robert E. Johnson and Raymond F. Siemankowski, Department of Biochemistry, University of Arizona, Tucson, Arizona 85721.

We have measured the binding of Mg^{++}ADP to bovine cardiac acto-S1 by utilizing the ability of ADP to competitively inhibit the rate of acto-S1 dissociation by ATP. This is an extension of the work by White (Biophys. J. 17, 40a (1977)) who measured the ADP affinity of rabbit skeletal acto-S1. For skeletal acto-S1 K_d = 200 μM (20 °C, 100 mM KCl, 10 mM Tris (pH 8), 5 mM $MgCl_2$) and for cardiac acto-S1 K_d = 5 μM (15 °C, 100 mM KCl, 5 mM MOPES (pH 7), 2 mM $MgCl_2$). In a parallel set of experiments we have measured the binding of Mg^{++}ADP to rabbit skeletal and bovine cardiac myofibrils by adding varying amounts of ADP, spinning down the myofibrils, and measuring the ADP left in the supernatant. With skeletal myofibrils about 90% of the ADP bound with a K_d = 200 μM (25 °C, 80 mM KCl, 30 μM $A_{p5}A$, 5 mM HEPES (pH 7.5), 5 mM $MgCl_2$). With cardiac myofibrils K_d = 7 μM (0 °C, 80 mM KCl, 30 μM $A_{p5}A$, 5 mM HEPES (pH 7.5), 5 mM $MgCl_2$).

Marston et al (J. Mol. Biol. 128, 111 (1979)) have proposed that tension can change the conformation of a cross-bridge and its affinity for nucleotides without dissociation from the actin thin filament. Cooke (Nature 294, 570 (1981)), however, has shown that at least part of the cross-bridge in rigor muscle fiber does not change conformation under stress. The equality of ADP binding affinities between acto-S1 and myofibrils implies that either (1) the cross-bridges in rigor myofibrils are not constrained to be in a conformation other than that which it would be in if the thick filaments were removed; or (2) ADP binding is not sensitive to cross-bridge conformation. (Supported by grants from NIH and AHA Arizona Affiliate).

T-PM-E3 FLUORESCENCE CHANGES INDUCED BY MYOSIN SUBFRAGMENT-1 (S-1) BINDING TO IODOACETAMIDO-FLUORESCEIN-MODIFIED REGULATED ACTIN. Lois E. Greene, NIH, Bethesda, MD 20205.

The model of Hill et al. (PNAS 77, 3186) suggests that regulated actin exists in two states, a state which binds S-1 weakly and a state which binds S-1 strongly, with Ca^{2+} and S-1 shifting the equilibrium toward the strong state. As a test of this model, the proportion of tropomyosin-actin units in the strong state was examined by using a fluorescent probe (IAF) on troponin I (Trybus and Taylor, PNAS 77, 7209). This model predicts that S-1 should induce a fluorescence change in the presence and absence of Ca^{2+}, but Trybus and Taylor only observed the change in the absence of Ca^{2+}. It was found that, both with and without Ca^{2+}, the binding of S-1 causes a fluorescence change. In the absence of Ca^{2+}, the fluorescence change slightly precedes the saturation of all actin sites by S-1, while in the presence of Ca^{2+}, the fluorescence change greatly precedes the saturation by S-1. This result agrees with the prediction of this model that the shift to the strong state occurs at a much lower level of S-1 binding to actin with Ca^{2+} than without Ca^{2+}. In addition, pPDM-S-1, a stable analogue of S-1·ATP which binds to regulated actin with only slight cooperativity, was examined to determine whether it induces a fluorescence change. In the presence of ATP and without Ca^{2+}, there was no fluorescence change when pPDM-S-1 bound to regulated actin. This suggests that under this condition, pPDM-S-1 binds nearly identically to the weak and strong states of regulated actin. However, in the absence of ATP, pPDM-S-1 did induce a fluorescence change. This is probably due to 2-fold stronger binding of pPDM-S-1 to the strong state than to the weak state of regulated actin. Nucleotide bound to S-1 thus appears to affect the relative binding strength of the S-1 to the weak and strong states of regulated actin.

T-PM-E4 BINDING OF FLUORESCENT NUCLEOTIDE TO SUBFRAGMENT-1 AND ACTO-SUBFRAGMENT-1. S.S. Rosenfeld and E.W. Taylor, Dept. of Biophysics and Theor. Biol., University of Chicago, Chicago, IL 60637.

The binding of εATP and εADP to skeletal or smooth muscle subfragment 1 (SF-1) yields a large increase in fluorescence when observed in the presence of 200 mM acrylamide (Ando et al., Biophys.J., 37, 46a (1982)). Both smooth and skeletal SF-1 hydrolyze εATP at a rate of 0.25/s, and at a rate of 1.5/s in the presence of 200μM actin. Skeletal SF1-A1 binds to actin in the presence of εATP at low ionic strength with a dissociation constant of 20μM. Mixing either class of SF-1 with εATP or εADP produces biphasic fluorescence transients. The apparent second order rate constants for the first transition and the maximum rates for the second transition are very similar to the values obtained by monitoring the tryptophan fluorescence transients after mixing either class of SF-1 with ATP or ADP. Mixing SF-1+εATP with excess ATP produces a fluorescence transient with a rate constant of 0.25/s--identical to the rate of steady state hydrolysis. Acto-SF-1 is dissociated by εATP; and the rate of this dissociation, as measured by light scattering, is equal to the rate of enhancement of εATP fluorescence. Actin accelerates the rate of release of εADP from SF-1. The maximum rate at infinite actin is 20/s. for smooth muscle and 550/s. for striated muscle SF-1. When SF-1+εATP is mixed with actin+ATP, a rapid decrease in fluorescence is observed (100/s for SF1-A1) followed by a slower process whose rate depends on actin concentration. We have examined the binding of εATP to cross-linked acto-SF-1 (Mornet et al., Nature,292, 301 (1981)). Actin enhances the rate of dissociation of εATP and increases the accessibility of bound nucleotide, as measured by solute quenching and interpreted by Stern-Volmer plots. These results show that εATP is a useful probe of the intermediate states in the myosin and actomyosin ATPase cycle.

T-PM-E5 THE RATE-LIMITING STEP IN THE ACTOMYOSIN ATPase CYCLE. Leonard A. Stein, Lois E. Greene, P. Boon Chock and Evan Eisenberg, NIH, Bethesda, MD 20205.

Although there is agreement that actomyosin can hydrolyze ATP without dissociation of the actin from myosin, there is still controversy about the nature of the rate-limiting step in the ATPase cycle. Previous work has shown that P_i release cannot be rate-limiting because K_{ATPase} is stronger than $K_{binding}$ (Stein, Biophys. J. 37, 264a). Therefore, we suggested that the rate-limiting step is a conformational change which occurs before P_i release but after the ATP hydrolysis step. However, the data were also consistent with the ATP hydrolysis step ($AMT \rightleftarrows AMD \cdot P_i$) being rate-limiting. A prediction of this latter alternative, but not the former, is that almost no acto·S-1·ADP·P_i complex will form when ATP is mixed with acto·S-1 because acto·S-1·ADP·P_i occurs after the rate-limiting step. In the present study we determined the amount of acto·S-1·ADP·P_i formed when ATP is mixed with S-1 cross-linked to actin (Mornet et al., Nature 292, 301). This cross-linked acto·S-1 hydrolyzes ATP at V_{max}. The amount of acto·S-1·ADP·P_i was determined both from fluorescence and direct measurement of P_i. We found that at μ=.013M the fluorescence magnitude was ~60% of the value with S-1 alone, while at μ=.07M the fluorescence magnitude was ~80% of that with S-1 alone. If ATP hydrolysis were rate-limiting the fluorescence magnitude should be less than 10% of that with S-1 alone. Control studies showed that almost none of the fluorescence increase was due to ATP binding. Furthermore, direct measurement of P_i corroborated the fluorescence studies. We conclude that ATP hydrolysis is not the rate-limiting step in the acto·S-1 ATPase cycle. Rather both S-1·ADP·P_i and acto·S-1·ADP·P_i, which are in rapid equilibrium, undergo a rate-limiting conformational change before P_i release but after the ATP hydrolysis step.

T-PM-E6 KINETIC ANALYSIS OF MG^{2+} AND ATP INHIBITION OF ACTO-S1 ATPASE OF FAST MUSCLE MYOSIN ISOZYMES. M. Balish, D. Richards, and P. Dreizen. Biophysics Graduate Program and Department of Medicine, SUNY Downstate Medical Center, Brooklyn, N.Y.

It is well known that at high concentrations of MgATP, actomyosin undergoes dissociation with concomitant loss of ATPase activity. This paper explores the kinetics of inhibition by Mg^{2+} and ATP of acto-S1 ATPase for the light chain isozymes, S1-L1 and S1-L3, of rabbit fast muscle myosin. At low ionic strength, plots of velocity against Mg^{2+} concentration, at constant ATP, show that free Mg^{2+} is an inhibitor of acto-S1 ATPase. Double reciprocal plots of velocity against actin concentration indicate a classical pattern of competitive inhibition by Mg^{2+}; however, replots of these data indicate two distinct Mg^{2+} inhibition sites with equivalent inhibition constant K_{Mg}. Comparison of K_{Mg} values for the light chain isozymes shows significantly greater inhibition for acto S1-L1 than acto S1-L3. A similar analysis of velocity profiles for acto-S1 ATPase at different ATP concentrations reveals that free ATP is also a competitive inhibitor, with two distinct and apparently equivalent inhibition sites for ATP. The ATP inhibition constant K_{ATP} is stronger than K_{Mg}. However, K_{ATP} values are approximately the same for S1-L1 and S1-L3, in contrast with Km and K_{Mg} values, which differ for the light chain isozymes. Mg^{2+} and ATP do not cause significant inhibition of S1 Mg-ATPase, in the absence of actin. The findings are most simply interpreted in terms of a kinetic model in which two distinct pairs of Mg^{2+} and ATP binding sites are involved in modulating the dissociation and reassociation of acto-S1, and the light chain isozymes differ with respect to Mg^{2+} sensitivity. (Supported by grants from N.Y. Heart Association, N.I.H., and fellowship from Insurance Medical Scientist Scholarship Fund).

T-PM-E7 AMP AND ADP INHIBIT ATP HYDROLYSIS BY F-ACTIN AT STEADY STATE BUT HAVE NO EFFECT DURING POLYMERIZATION. Stephen L. Brenner and Edward D. Korn, NIH, Bethesda, MD 20205.

AMP and ADP inhibit the hydrolysis of ATP in solutions of F-actin at steady state. The inhibition is competitive with ATP. In solutions containing 24 μM actin, 50 mM KCl, 0.1 mM $CaCl_2$, at 25°C, pH 7.5, the K_m for ATP is about 600 μM and the K_i values are 9 μM for AMP and 44 μM for ADP. In the presence of 200 μM ATP, ATP hydrolysis was inhibited 64% by 50 μM AMP and 96% by 1 mM AMP. GMP, UMP, and P_i had no effect. Under these conditions, 50 μM AMP had no effect on the time course of actin polymerization, the hydrolysis of ATP during polymerization, or the critical actin concentration. Simultaneous measurements of G-actin/F-actin subunit exchange and incorporation of radioactivity from [α-^{32}P]ATP into F-actin at steady state showed that nucleotide incorporation occurred more rapidly than subunit exchange. AMP inhibited the incorporation of radioactivity from [α-^{32}P]ATP, but the total nucleotide incorporated (AMP + ADP from ATP) was invariant. We conclude that the relative affinity of F-actin for adenine nucleotides is AMP > ADP > ATP, the reverse of that of G-actin. The data also suggest that the hydrolysis of ATP in F-actin solutions is not necessarily associated with monomer-polymer interactions. Hydrolysis may occur along the sides of filaments or at spontaneous breaks. In either case, nucleotide exchange and ATP hydrolysis can occur in the absence of subunit exchange. The inhibition of ATP hydrolysis by AMP in the absence of an effect on the critical concentration suggests that, under these ionic conditions, either (1) the subunit association and dissociation reactions that determine the critical concentration do not involve hydrolysis of ATP or (2) only a small, AMP-insensitive, fraction of ATP hydrolysis events at steady state is associated with monomer-polymer end interactions.

T-PM-E8 ACTIVITY PROFILE OF THE L2 LIGHT CHAIN OF SKELETAL MYOSIN WITH F-ACTIN AS COFACTOR. Suzanne M. Pemrick, Dept. of Biochemistry, S.U.N.Y., Downstate Medical Center, Brooklyn, NY 11203.

This investigator demonstrated that skeletal L2 enhanced the regulated actomyosin ATPase activity and the Ca2+-sensitivity of the thin filament by increasing the steady state concentration of active complexes (Biochemistry (1977) 16: 4047). An apparent contradiction to these findings was reported by Srivastava, Cooke and Wikman-Coffelt (BBRC (1980)92:1), who, working with F-actin noted that both the actomyosin ATPase and tension generation by actomyosin threads was unaffected by loss of L2. It was, therefore, imperative to analyze the modifier capabilities of L2 with non-regulating actin (F-actin). For native myosin (2 moles L2/mole) both the Kapp for actin and the Vmax were increased 2- to 3-fold by lowering the apparent Mg2+ concentration (at 1 mM MgATP) from 1 to 0.02 mM, in the absence of Ca2+. This effect was not readily apparent for 50% L2-deficient myosin. By comparing the apparent inhibitory effect of high Mg2+ at 0.6, 1 and 2 mM MgATP, it was possible to prove that millimolar concentrations of free ATP had an activating effect on the acto-myosin ATPase with native myosin, and nearly no effect with L2-deficient myosin. Therefore, L2 modifies the actomyosin ATPase activity in both actin systems, it is merely that the conditions are different. The activating effect of free ATP is retained for phosphorylated myosin (P-myosin) and F-actin. However, the ability of P-myosin to decrease the Kapp for actin (Pemrick (1980) J. Biol. Chem. 255:8836) is probably conformation dependent and is best observed at high Mg2+ and ambient Ca2+. One word of caution: an inhibitory effect of L2 upon Vmax can be observed if there is also an increase in the apparent Mg2+ concentration.

Supported by USPS Grant HL22401.

T-PM-E9 NORMAL AND DYSGENIC MURINE SKELETAL MUSCLE MYOSIN M.T.Anderson and S.P.Scordilis, Dept. Biol. Sci., Smith College, Northampton, Mass. 01063

Muscular dysgenesis in the mouse (mdg/mdg) is an autosomal recessive mutation characterized by a lack of muscle contractility in the embryo. Myosin was column purified from normal (+/+) and heterozygote (+/mdg) adult skeletal muscle and from normal (+/+) and dysgenic (mdg/mdg) 18 day embryos. Two dimensional gel electrophoresis demonstrated that the major myosin light chains are shared by the myosins of all four tissues and are characteristic of fast skeletal muscle; LC-1 23.3 kD, LC-2 18.9 kD, LC-3 15.0 kD. Comparison of the high ionic strength EDTA-activated ATPase activities demonstrated significant differences between these myosins. The adult myosins had +/+ 2.98 umol/min/mg and +/mdg 1.35 activities at 37 C, whereas the embryonic myosins had +/+ 3.5 and mdg/mdg 2.06 activities. The physiologically relevant low ionic strength actin-activated ATPase activities were analyzed by a weighted linear regression analysis. The adult tissue activities were +/+ 3.17 and +/mdg 1.06 at 37 C. The actin-activation of the embryonic myosins appears to be dependent on the extent of phosphorylation of the P-light chain. Corresponding to the change in regulation observed from the embryonic to the adult myosin (from phosphorylation dependent to phosphorylation independent), the myosin light chain kinase changes from a calcium independent form in the embryos to a calcium dependent form in the adult tissues.

Supported by N.I.H. NS-16681, the MDA and Smith College Blakeslee Fund.

T-PM-E10 CALCIUM DEPENDENT PROTEOLYSIS IN THE MOUSE E.B.Goodwin and S.P.Scordilis, (Intr. B. Walcott) Dept. Biol. Sci., Smith College, Northampton, Mass. 01063

The developmental expression of calcium dependent proteolysis has been studied in 18 day embryos, newborns, 1, 2, 4, and 8 week old mice from the inbred strain 129/ReJ. The calcium dependent proteolytic activity was monitored on SDS slab gels by the ability of an extract of skeletal muscle to degrade purified rabbit skeletal myosin heavy chain over a 24 hour period at 37C. Two proteolytic activities were found: a calcium independent one and a calcium dependent one. First, it became necessary to determine the degree of inactivation of the proteolytic activities which was due to thermal degradation during the 24 hr incubation period. It was found that the calcium independent proteolysis lost almost 80% of its activity by hour 16. Concomitant with this decrease, the calcium dependent proteolytic activity increased by almost 60%. Therefore, at the start of the incubation the majority of proteolytic activity was non-calcium dependent though, more thermally labile than the calcium dependent proteolysis. Consequently, the developmental expression of the calcium dependent proteolysis was monitored after 14 hours of incubation. Virtually no expression of calcium dependent proteolysis was detected at one week after birth, though it was detected at two weeks. This implies that calcium dependent proteolysis is not expressed until somewhere between one and two weeks of age, whereas calcium independent proteolysis is unchanged.

This work was supported by grants from the N.I.H. NS-16681, Muscular Dystrophy Association and the Blakeslee Fund of Smith College to S.P.S.

T-PM-E11 NATURAL ABUNDANCE ^{13}C NMR SPECTRA OF DISEASED HUMAN MUSCLE.
M. Bárány, D.D. Doyle*, G. Graff*, V.C. Mougios*, D. L. Spencer*, E. Abraham*, W. M. Westler*, and J. L. Markley. College of Medicine, University of Illinois at Chicago, IL 60612 and Department of Chemistry, Purdue University, West Lafayette, IN 47907

^{13}C NMR spectra of human surgical muscle samples have been obtained at 50 and 118 MHz. Numerous sharp peaks in the ^{13}C spectrum have been assigned to carbon atoms of soluble metabolites and fatty acyl chains of neutral fats and membrane-phospholipids. Comparisons have been made of ^{13}C NMR spectra of normal and diseased muscles after removal of neutral fats by extraction with isopentane. Creatine, lactic acid, glucose, phospholipids, and free fatty acids are not removed from muscles by isopentane. The most striking difference between ^{13}C NMR spectra of isopentane-extracted normal and diseased muscle samples was the size of the residual 30.5 ppm methylene carbon resonance: small in normal muscles and in non-specific muscle diseases, but large in myogenic and neurogenic muscle diseases. In addition, differences were also found between normal and diseased muscles in their creatine content and in their ability to produce lactic acid. By deoxycholate treatment of isopentane extracted diseased muscles we estimated that about 1/5th of the total phospholipids are highly mobile. T_1 and NOE measurements indicated that the differences in peak height for the 30.5 ppm resonance between normal and diseased muscle are due only to difference in the amount of higly mobile fatty acyl chains in the muscle and not due to differences in relaxation parameters. ^{13}C NMR of isopentane-extracted muscle appears to permit differentiation of normal from diseased muscle and, within diseased muscle, grading of the severity of the disease. (Supported by MDA, Shriners Hospitals, NIH RR-01077, NIH GM-28894, and NSF CHE 79-16100).

T-PM-E12 EARLY AND LATE CHANGES IN MEMBRANE EXCITABILITY AND LYSOSOMAL ACTIVITY IN EXPERIMENTAL STEROID MYOPATHY. R.L. Ruff, M.D., Ph.D., Department of Physiology and Biophysics, University of Washington, Seattle, Washington 98195.

Groups of 300g male Sprague-Dawley rats received daily subcutaneous injections of dexamethasone (D) 1.5mg/kg or saline (C). During the first 3 weeks: 1) D rats developed significant total body and muscle atrophy despite similar food intake and activity levels to those of C rats, 2) Leupeptin, a lysosomal protease inhibitor, did not prevent muscle atrophy, 3) muscle $[K]_i$ and $[Na]_i$, and in vivo measured membrane potentials and action potentials in fast and slow twitch muscles were not altered by steroid treatment. After 4 weeks some D rats showed accelerated muscle atrophy associated with: 1) depolarization and diminished excitability of fast-twitch muscle fibers, 2) reduced $[K]_i$ and increased $[Na]_i$, and 3) fever. At necropsy, the rapidly wasting rats had systemic bacterial infections with multiple organisms. Both acetamenophen and indomethacin reduced fever in D rats, but only indomethacin decreased muscle wasting. Leupeptin also reduced atrophy in septic rats. The findings are compatible with the following scheme: initially, dexamethasone produced muscle atrophy by decreasing protein synthesis. Prolonged glucocorticoid treatment resulted in immunosuppression and sepsis. In septic rats, accelerated atrophy and deterioration of surface membrane function occurred due to prostaglandin (PG) E_2 activation of lysosomal protease (Rodeman et al., J. Biol. Chem. 257:8716). SOL muscle may have been relatively spared from the accelerated atrophy with sepsis because PG $F_{2\alpha}$ increased protein synthesis. The data suggests that caution be exercised in attributing the muscle atrophy associated with prolonged steroid treatment solely to direct glucocorticoid effects. Supported by NIH grants NS00498, NS16696.

T-PM-F1 ANALYSIS OF NMR RELAXATION DATA ON MACROMOLECULES. Attila Szabo, Laboratory of Chemical Physics, NIADDK, National Institutes of Health, Bethesda, Maryland, 20205.

Recent developments and applications of the model-free approach[1] to the interpretation of nuclear magnetic relaxation times in macromolecules is presented. This approach is based on the realization that, at currently available magnetic fields, the information contained in relaxation parameters on fast internal motions is limited because of the nature of the NMR experiment. In fact, the unique information on fast internal motions can be completely described by just two parameters (a generalized order parameter (S^2), and an effective correlation time (τ_e) which are measures of the spatial restriction and the time scale of the motion) that can be simply extracted from the data. Once these parameters are obtained they can be readily modelled (in a variety of ways) if a physical picture of the motion is desired. Thus, the model-free approach can be regarded as a data reduction scheme, which actually simplifies the processes of modelling data. The validity of the approach is illustrated by showing that elimination of a part of a data set (i.e. relaxation parameters at several magnetic fields) does not significantly alter the values of S^2 and τ_e. Finally, the relation to the work of Jardetzky and coworkers is discussed.

[1] G. Lipari and A. Szabo, J. Am. Chem. Soc. 104, 4546, 4559 (1982).

T-PM-F2 THE STUDY OF ENZYME CATALYZED REACTIONS BY TWO DIMENSIONAL NMR. H.L. Kantor, R.S. Balaban and J.A. Ferretti*. NHLBI, LKEM, LC*, NIH, Bethesda, MD 20205

Two-dimensional magnetization transfer FTNMR spectroscopy is a useful technique for studying rates of enzyme catalyzed reactions. This study describes results of two enzyme mediated reactions: (1) the creatinephosphokinase catalyzed reaction of adenosine triphosphate (ATP) with creatine to produce creatine phosphate and adenosine diphosphate, and (2) the adenylate kinase catalyzed conversion of adenosine diphosphate (ADP) to ATP and adenosine monophosphate (AMP). In the "2D" experiment all exchange pathways are observed simultaneously in a single study, which can amount to a significant savings in time. The experimental procedure for measuring rates by 2D FTNMR was first described by Jeener et al.[1] and involves determining the amount of material which reacts in a fixed interval of time, T_{mix}. Systematic variation of T_{mix} in the creatine phosphokinase catalyzed reaction yielded curves which could be fit to a single one step scheme. In contrast to this result, the data obtained on the adenylate kinase catalyzed reaction could not be fit to such a simplified scheme. Here the reversible exchange between ADP and AMP could be modeled by a one step scheme but the reversible formation of ATP from the same ADP was observed to occur only after an induction period. The mechanistic implications based on the 2D FTNMR as well as the potential and limitations of the technique will be discussed.

[1] Jeener, J., Meier, B.H., Bachman, P., Ernst, R.R. J. Chem. Phys. 71:4546, 1979.

T-PM-F3 LANTHANIDE INDUCED PEPTIDE FOLDING: VARIATIONS IN LANTHANIDE AFFINITY AND INDUCED PEPTIDE CONFORMATION. Jean Gariépy, Brian D. Sykes and Robert S. Hodges, Department of Biochemistry and the MRC Group in Protein Structure and Function, University of Alberta, Edmonton, Alberta, Canada T6G 2H7.

The diamagnetic lanthanides lutetium and lanthanum have proven to be useful metal binding probes for a synthetic 13 residue fragment representing the calcium binding site 3 of rabbit skeletal troponin C (residues 103-115). The peptide conformation induced by these metals was monitored by proton magnetic resonance at 270 MHz. The peptide affinity for these rare earths is 50 to 400 times higher than for calcium (K_{Lu3+}, 1.3 x $10^4 M^{-1}$; K_{La3+}, 1.1 x $10^5 M^{-1}$; K_{Ca2+}, 3 x $10^2 M^{-1}$) which is related to the change in cation charge from +2 to +3. The peptide conformation induced by the presence of La^{3+} generates a different ^1H NMR spectrum than the one observed for the lutetium saturated peptide. Thus, it appears that these metals do not fold the peptide into exactly the same conformation. The resonance shifts observed during the Lu^{3+} titration are much smaller than in the case of La^{3+} addition. The fact that lutetium binds less tightly than lanthanum to the peptide may be linked directly or indirectly to the difference in ionic radii between these metals (Lu^{3+}, 0.85 Å; La^{3+}, 1.06 Å). This may in turn indicate that the peptide primary sequence encodes for some aspects of metal ion specificity. The ^1H NMR results also demonstrate that glycine 108 adopts a restricted geometry in the absence of metal such that its two alpha-carbon protons are in different environments which are further affected by the addition of either metal.

(Supported by MRC of Canada)

T-PM-F4 ^{1}H-NMR OF THE AMIDE PROTON OF HYALURONIC ACID IN H_2O. M.K. COWMAN,[+] D. COZART*, K. Nakanishi, and E.A. Balazs*. Eye Research and Dept. of Chemistry, Columbia Univ., New York, N.Y.

Proton NMR spectroscopy has been used to investigate the amide protons of a low molecular weight hyaluronic acid segment (HAseg, DP=14-20) and smaller highly purified oligosaccharides (DP=2-5) derived from HA, studied in H_2O at pH 2.5 and pH 5.5. A single amide proton resonance was observed for HAseg. The smaller oligosaccharides showed separate resonances, corresponding in relative peak area to the interior and end G1cNAc residue amide protons. For the α- and β-anomers of C3-linked G1cNAc end residues of $(G1cUA\text{-}G1cNAc)_n$ oligosaccharides, the amide protons appear 0.10-0.20 ppm downfield of the corresponding interior residue peak. For the C1-linked G1cNAc end residues of (G1cNAc-G1cUA) oligosaccharides, the amide proton occurs approximately 0.10 ppm upfield of the interior residue peak. The interior residue amide proton peak for all oligosaccharides occurs at approximately the same chemical shift (8.1 ppm at pH 2.5, 8.0 ppm at pH 5.5) as the HAseg amide proton. This chemical shift differs only slightly from that for β-G1cNAc or Me β-G1cNAc, as a result of the opposing environmental effects of G1cNAc linkage to G1cUA at both C1 and C3.

The coupling constants (~8.8-9.6 Hz) determined for the amide proton resonances appear to be independent ofchain length, sequence, residue position, and solvent pH. The large coupling constant suggests a nearly trans arrangement of the amide proton with respect to the proton at C2.

No large magnitude change in chemical shift or coupling constant which might be indicative of hydrogen bonding from the amide N-H to the carboxyl(ate) of the adjacent G1cUA was observed.

(Supported by NIH Grants EY 01747, EY 04156, and CA 11572).

[+]Present address: Department of Chemistry, Polytechnic Institute of New York, Brooklyn, N.Y.

T-PM-F5 FLUORESCENCE DEPOLARIZATION BY ANISOTROPIC ROTATIONAL DIFFUSION OF A FLUOROPHORE AND ITS CARRIER MOLECULE. Thomas P. Burghardt and Daniel Axelrod, CVRI, Univ. of California, San Francisco, CA 94143, and Dept. of Physics, Univ. of Michigan, Ann Arbor, MI 48109.

We derive an analytical expression for the polarization anisotropy of a luminophore undergoing rotational diffusion about a single axis while attached to a nonluminescing, rotationally diffusing asymmetrical carrier molecule. In contrast to previous related calculations, we allow the rotation axis of the luminophore to assume an arbitrary orientation relative to the carrier. Additionally, we have measured the polarization anisotropy of bovine serum albumin (BSA) labeled with dansyl, NBD, tetramethylrhodamine, or eosin that is: (a) surface adsorbed to a glass/buffer interface, using a variation of the technique of total internal reflection fluorescence spectroscopy (TIRFS); or (b) bulk dissolved, using conventional transmitted illumination fluorescence spectroscopy.

With our theory, using previously published values for the rotational diffusion coefficients of BSA and fluorescence lifetimes of the fluorophores, we estimate the rotational diffusion coefficient of the covalently bound probes from our measured anisotropy values. Our results indicate a wide variability in the rotational diffusion coefficients of the probes (from $\sim 10^7$ sec^{-1} for dansyl to $\sim 10^9$ sec^{-1} for eosin) attached to either surface adsorbed or bulk dissolved states of BSA. Contrasting the rotational diffusion coefficients for each probe for surface adsorbed BSA vs. bulk dissolved BSA indicates that surface adsorption of the BSA molecule can hinder the rotational motion of the probe. These results have important consequences in the interpretation of results from other fluorescence techniques, such as singlet-singlet energy transfer, where the rotational mobility of the probe is important. Support by NS 14565 and HL 24039.

T-PM-F6 BIOCHEMICAL KINETICS OF PROTEIN SURFACE BINDING STUDIED AT EQUILIBRIUM WITH TOTAL INTERNAL REFLECTION FLUORESCENCE. Nancy L. Thompson and Daniel Axelrod, Dept. of Chem., Stanford Univ., Stanford, CA 94305 and Biophysics Res. Div., Univ. of Michigan, Ann Arbor, MI 48109.

The molecular details of specific and nonspecific interactions of a soluble protein at a cell surface are central to the rate of reaction with membrane-bound receptor. We have employed total internal reflection fluorescence to study the equilibrium kinetics of rhodamine-labeled immunoglobulin molecules (R-IgG) nonspecifically binding to fused silica coated with bovine serum albumin (BSA-glass); of rhodamine-labeled insulin (R-insulin) nonspecifically binding to BSA-glass; and of rhodamine-labeled anti-dinitrophenyl (DNP) myeloma protein MOPC 315 (R-MOPC) specifically binding to fused silica coated with DNP-conjugated bovine serum albumin (DNP-BSA-glass). An internally reflected laser beam, illuminating primarily surface bound molecules, is combined with fluorescence photobleaching recovery (TIR/FPR) and fluorescence correlation spectroscopy (TIR/FCS) to measure surface binding kinetics. TIR/FPR shows that R-IgG at .023 mg/ml binds to BSA-glass with irreversible and reversible components. TIR/FCS shows that one reversible component has characteristic time 6.3 ms and is limited by the rate of bulk diffusion, and that the equilibrium surface concentration of this component equals 65 IgG/μm^2. Comparatively, R-insulin at ∿.002 mg/ml reversibly binds to DNP-BSA-glass with slightly longer characteristic time. Bivalent R-MOPC at ∿.05 mg/ml specifically binds to DNP-BSA-glass with characteristic desorption time >10 min. Univalent R-MOPC fragments appear to specifically bind to DNP-BSA-glass, but exhibit a large fraction of nonspecific binding. These results suggest that rapidly reversible nonspecific binding between soluble proteins and a cell surface may accompany or precede specific binding with membrane receptors.

T-PM-F7 FLUORESCENCE QUENCHING OF INDOLE DERIVATIVES AND PROTEINS BY SUCCINIMIDE. M.R. Eftink, R. Mallinson, and C. Ghiron, Department of Chemistry, University of Mississippi, University, MS 38677 and the Department of Biochemistry, University of Missouri, Columbia, MO 65201.

Quenching of the fluorescence of tryptophanyl residues in proteins by acrylamide has been successfully used to determine the degree of solvent exposure of these residues. Another polar quencher that can be used for such studies is succinimide. In contrast to acrylamide, however, the quenching of indole fluorescence by succinimide is not 100% efficient. We have also found the quenching efficiency of succinimide, γs, to be quite solvent dependent, as compared to the efficiency of acrylamide, γ_A, which is approximately 1.0 in all solvents. The ratio $\gamma s/\gamma_A \tilde{\sim} \gamma s$ (measured as the ratio of the Stern-Volmer constants for succinimide and acrylamide quenching of indole) varies from ~0.7 in water to ~0 in the non-polar solvent dioxane. While there appears to be no direct correlation between γs and solvent polarity (i.e. dielectric constant), the values of γs depend most noticeably on whether the solvent is protic or aprotic. For all protic solvents $\gamma s > 0.1$; for aprotic solvents $\gamma s \lesssim 0.1$. In similar comparative studies of the quenching of single tryptophan containing proteins we also have found the ratio of Stern-Volmer constants for succinimide and acrylamide to vary from 0.6 to 0.7 for those having solvent exposed tryptophanyl residues to 0.1 to 0.2 for those having buried residues. In connection with the above studies with indole, these results indicate that the quenching of buried residues in proteins proceeds by dynamic penetration of the quenching into the globular protein matrix, as opposed to the periodic exposure of such residues due to segmental unfolding events. (This research was supported by NSF grants PCM 77-26614.)

T-PM-F8 THERMODYNAMIC AND FLUORESCENCE STUDIES OF THE pH DEPENDENCE OF THE BINDING OF NAD^+ TO LIVER ALCOHOL DEHYDROGENASE. M.R. Eftink, M. Riggins and W. Cromwell, Department of Chemistry, University of Mississippi, University, MS 38677.

Previous studies of the interaction of liver alcohol dehydrogenase (LADH) with the coenzyme NAD^+ have demonstrated the involvement of a group on the protein having a pKa of 9-10, which is decreased by about 2 pH units upon coenzyme binding. Also the fluorescence of LADH undergoes an alkaline quenching due to the ionization of a group with pKa ~9.8. These effects appear to involve the same amino acid residue, but the identity of this group is uncertain. To further characterize the nature of this linkage between NAD^+ binding and proton dissociation we have studied a) the pH dependence of the proton release upon NAD^+ binding, b) the pH dependence of the $\Delta H°$ (calorimetric) of NAD^+ binding and c) have determined the $\Delta H°$ (van't Hoff) for the ionization of the group involved in the alkaline quenching effect. Our work is consistent with the shift in the pKa a single group from 9.6 to 8.0 on NAD^+ binding. A $\Delta H°$ value of 7.5 ± 1.5 kcal/mole is found for the alkaline quenching group. This $\Delta H°$ value is consistent with the pattern we find for the pH dependence of the $\Delta H°$ for NAD^+ binding. The pKa of the alkaline quenching group is also found to be ionic strength independent. Our results, particularly the magnitude of the $\Delta H°$ found for the ionizing group, are most consistent with this group being a tyrosine or cysteine residue. Supported in part by grants from the Research Corporation and the National Science Foundation (PCM 79-23031).

T-PM-F9 INTERACTION OF HYDROPHOBIC INHIBITORY LIGANDS WITH CALMODULIN. J. David Johnson, Department of Pharmacology and Cell Biophysics, University of Cincinnati College of Medicine, Cincinnati, Ohio 45267

Dansylchloride labeled Calmodulin, CDR_{DANS}, undergoes a large (80%) fluorescence increase with the binding of hydrophobic inhibitory ligands. This fluorescence increase occurs only in the presence of Ca^{2+} and is independent of Mg^{2+}. Apparent dissociation constants were determined for each ligand: R24571 (2-3nM), fendiline and prenylamine (0.5-0.7μM), felodopine (3μM), W-7 (4μM), TFP (5μM), D-600 and verapamil (30μM), and diltiazem (80μM). TFP, felodopine and ANS bind to CDR with similar Ca^{2+} dependence as the CDR induced activation of phosphodiesterase and myosin light chain kinase. This suggests that Ca^{2+} binding to Ca^{2+} specific regulatory sites on CDR exposes hydrophobic sites which bind hydrophobic ligands and CDR-binding proteins. Our studies of fluorescent hydrophobic ligands binding to calmodulin suggest that some ligands show selectivity in binding to some of the 3-4 hydrophobic binding sites on calmodulin and that ligand binding to certain sites can increase ligand binding at other sites perhaps by an allosteric mechanism. If Calmodulin activation of different proteins occurs by interaction of these proteins with specific hydrophobic sites on Calmodulin then it might be possible to direct ligands to a specific site to abolish or even potentiate certain Calmodulin mediated events. Ca^{2+} binding to Ca^{2+} specific sites on other Ca^{2+} binding proteins including Troponin C and scallop Ca^{2+} binding protein exposes similar hydrophobic domains for protein-protein or protein-ligand interactions. This suggests that Ca^{2+} binding to Ca^{2+} specific sites and the subsequent exposure of allosterically interacting hydrophobic sites to facilitate protein-protein and/or protein-ligand interactions may be a general feature of the mechanism of action of Ca^{2+} binding proteins. Grant support- The Muscular Dystrophy Association.

T-PM-F10 FLUORESCENCE RECOVERY TECHNIQUES FOR MONITORING SLOW ROTATIONAL MOTIONS. William A. Wegener, Muscle Research Laboratory, Baylor University Medical Center, Dallas, Texas 75246 and Rudolf Rigler, Department of Medical Biophysics, Karolinska Institute, Stockholm, Sweden.

Besides measuring translational motions of a particular probe, fluorescence photobleaching recovery (FPR) experiments also monitor rotational motions. Since FPR is not restricted by the fluorescent lifetime, it is well suited for observing extremely slow rotations previously inaccessible to luminescence techniques. We discuss several methods for independently extracting rotational and translational contributions in complex systems where both effects may occur on comparable timescales. One design uses 2π or 4π collection optics to enhance the fluorescence signal and eliminate directionality dependence of the emission. Suitable alignment of the bleaching pulse polarization relative to the polarization of the subsequent monitoring beam eliminates orientational effects from recovery of fluorescence, while combinations of alignments isolate orientational dependence. A novel design is then described involving more readily available set-ups in which fluorescence signal is detected at right angles using an additional polarizer. This design also allows rotational motions of a label's absorption dipole and emission dipole to be independently observed. Several extensions of standard FPR are examined which involve initial depletion by a reversible process like triplet formation and bleaching pulse wavelength different from that of the monitoring beam.

(Supported by a Swedish Medical Research Fellowship to W.A.W.)

T-PM-G1 ELECTRICAL PROPERTIES OF SHEEP PURKINJE STRANDS: IMPEDANCE MEASUREMENTS AND VOLTAGE CLAMP SIMULATIONS INCLUDING ELECTRODIFFUSION. R. A. Levis, R. T. Mathias, and R. S. Eisenberg. Dept. of Physiol., Rush Medical College, Chicago, Illinois 60612.

The impedance of sheep Purkinje strands was measured from ~1 Hz to 3-5 kHz, and was interpreted with circuit models based on morphology. Three models of the clefts were considered. A lumped model, in which all of the cleft membrane is in series with ~100 Ωcm^2, only fits the data below about 20 Hz. Two distributed models, referred to as the 'pie' and 'disc' models, both provide good fits to the data, at all frequencies, with similar membrane parameters but with different values of the cleft luminal resistivity.

The average linear parameters obtained from curve fitting to the distributed models were used in computer simulations of the currents flowing during voltage clamp. Simulations included nonlinear ionic currents as well as radial variation of voltage, current, concentration and membrane flux. As expected, these computations show that voltage across the cleft membranes can not be controled during the rapid sodium current. Substantial control of potential across the cleft membranes is possible during the smaller slower secondary inward (calcium) and potassium currents; however, cleft concentration of calcium and potassium can not be controlled. The combined effects of intracellular accumulation and cleft depletion of calcium are sufficient to turn off calcium current even if conductance is maintained. (Supported by NIH grant # HL20030 and American Heart # 79-851)

T-PM-G2 **WHAT CONTROLS INTRACELLULAR SODIUM ACTIVITY IN CARDIAC MUSCLE?** By S-S. Sheu and W.J. Lederer, Dept. Physiology, University of Maryland School of Medicine, 660 W. Redwood St., Baltimore, MD 21201.

When the Na-pump is completely blocked in sheep cardiac Purkinje fibers, intracellular sodium activity (a^i_{Na}) rises from about 6 mM to between 20 and 35 mM. If the Na-pump were the only transport system responsible for extruding Na from the intracellular compartment, a^i_{Na} should rise towards its electrochemical equilibrium value (about 1 M at a membrane potential of -60 mV). Because of the dependence of a^i_{Na} on Ca_o when the Na-pump is blocked, Deitmer & Ellis (J. Physiol. 277: 437, 1978) have suggested that the Na-Ca exchange mechanism keeps a^i_{Na} well below its "equilibrium" level under these conditions. We have examined this proposal by testing the action of several agents that have been reported to block the Na-Ca exchange mechanism. In sheep cardiac Purkinje fibers we measured a^i_{Na} with a Na-sensitive microelectrode and controlled membrane potential with a two-microelectrode voltage clamp. After blocking the Na-pump with 10 uM strophanthidin and 0 mM K_o, a relatively stable level of a^i_{Na} (between 20-35 mM) was reached. We then applied lanthanum chloride (1 mM), adriamycin (100 uM) or quinidine (100 uM). None of these substances led to a dramatic rise of a^i_{Na}. Such results suggest one or both of the following conclusions: 1. These agents do not block the Na-Ca exchange mechanism; 2. A transport system other than the Na-Ca exchange is responsible for keeping a^i_{Na} at a relatively low level when the Na-pump is blocked. Supported by NIH(HL25675), American Heart Association and its Maryland State Affiliate, the March of Dimes Birth Defects Foundation.

T-PM-G3 EFFECTS OF $(K^+)_o$ AND NOREPINEPHRINE ON INTRACELLULAR SODIUM ION ACTIVITY AND TWITCH TENSION OF CANINE CARDIAC PURKINJE FIBERS. W-B. Im*, M.S. Pecker* and C.O. Lee, Department of Physiology, Cornell University Medical College, New York, N.Y. 10021.

Intracellular Na ion activity (a^i_{Na}) and twitch tension (T) of canine cardiac Purkinje fibers electrically driven at 1 Hz were measured simultaneously and continuously during decreases or increases of $(K^+)_o$ from 5.4 mM to 1.0 (n=6), 2.0 (n=7), or 8.1 (n=6) mM and restoration of $(K^+)_o$ to 5.4 mM. K^+ produced concentration-dependent changes in a^i_{Na} and T as shown in the Figure. A change in a^i_{Na} always accompanied a change in T. During onset of and recovery from changes in $(K^+)_o$, the time course of the change in a^i_{Na} was similar to that of the change in T. An apparent hysteresis in the relationship of a^i_{Na} and T was often observed during changes of $(K^+)_o$ from 5.4 to 1.0 mM and back to 5.4 mM. Such a hysteresis was not observed with changes of $(K^+)_o$ between 5.4 and 2.0 or 8.1 mM. These results indicate that changes in a^i_{Na} are related to changes in T, perhaps by means of changes in intracellular Ca level due to a Na-Ca exchange. We also measured a^i_{Na} during exposure of the fibers to 10^{-6} M norepinephrine in 0, 5.4 and 16.2 mM K^+ solutions. Norepinephrine in 16.2 and 5.4 mM K^+ solutions decreased a^i_{Na} by 0.7±0.5 (mean±SD;n=5) and 1.5±0.3 (n=4) mM respectively, while it had no effect on a^i_{Na} in K^+-free solution. The result supports the hypothesis that norepinephrine stimulates the Na-K pump in cardiac cells. (Supported by USPHS HL 21136).

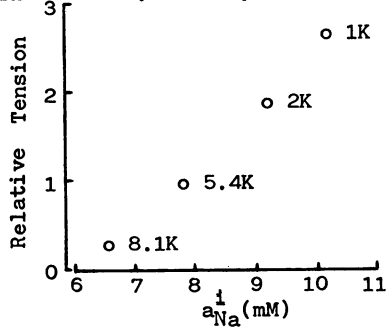

T-PM-G4 SLOW INACTIVATION IN CALCIUM CHANNELS OF CARDIAC PURKINJE FIBERS. T. Scheuer and R.S. Kass, Department of Physiology, University of Rochester, Rochester, NY 14642

A component of calcium current inactivation that develops over several seconds was characterized in calf cardiac Purkinje fibers. After blocking overlapping outward currents by intracellular injection of tetrabutylammonium ion (TBA), shortened (.5-1 mm) preparations were voltage clamped using two microelectrodes. Tetrodotoxin (10 μM) was present to eliminate sodium current. After a change in voltage, calcium current inactivation develops with a biphasic time course that was measured using train or double pulse protocols. Control experiments indicate that the slow component is not caused by TBA injection and is not altered by substitution of barium for calcium in the external solution or by intracellular injection of EGTA. Time constants for slow inactivation are voltage dependent, reaching a maximum near -40 mV with faster changes occurring at more positive and negative potentials. While measured time constants varied between fibers they ranged from 10-20 s near -40 mV to 2-4 s near -70 and -18 mV, the extreme potentials studied. Fast, but not slow, inactivation could be removed by a 150 ms hyperpolarizing interpulse to -70 mV. The voltage dependence of slow inactivation was measured using 8 s inactivation curves that incorporated such a hyperpolarizing interpulse. This dependence was altered in the presence of the calcium channel blocking compound, diphenylhydantoin, suggesting that interactions with slow inactivation may contribute to the action of some calcium current inhibitors. Supported by NIH Grants HL-21922 and HL00556.

T-PM-G5 OPTICAL QUENCHING OF CALCIUM CURRENT BLOCK IN THE CARDIAC PURKINJE FIBER. R. S. Kass and M.C. Sanguinetti, Department of Physiology, University of Rochester, Rochester, NY 14642.

We report experiments in which we have investigated the effects of light on calcium current inhibition brought on by several different organic compounds. We find that block by some, but not all, of these drugs can be completely reversed by exposure to light of the appropriate intensity and energy. A two microelectrode voltage-clamp technique was used to measure membrane current and action potentials in shortened (.5 to 1 mm) isolated calf Purkinje fibers. Light from an halogen incandescent lamp, passed through an infrared rejection filter, was collimated and focused on preparations by a long-working distance microscope objective. Wavelengths of light were selected with narrow band interference or wide band long pass filters. Calcium current was first completely blocked by applying drugs at previously determined concentrations. A beam of light was then focused on the fiber while membrane current was continuously monitored. Exposure to light completely removes calcium current block by the dihydropyridine derivative nisoldipine within 3 min. When the light is turned off, complete block redevelops within 5-7 min. These effects, not observed at incident light wavelengths greater than 450 nm, were confirmed in action potential and twitch tension experiments in which illumination readily modulates the effects of nisoldipine on these parameters. After quenching nisoldipine block with light, we find that the recorded calcium current responds to norepinephrine and shows a voltage-dependence characteristic of currents measured under drug-free conditions. We find similar optical modulation of calcium current blockade by nifedipine, but not by nitrendipine, or by D600. Supported by NIH Grants HL21922 and HL00556.

T-PM-G6 SLOW INACTIVATION IN GUINEA PIG VENTRICULAR MYOCARDIUM. Craig W. Clarkson, Jay W. Mason, Tetsu Matsubara, James W. Moyer, and Luc M. Hondeghem. Department of Pharmacology, University of California, San Francisco, CA 94143.

Recent evidence indicates that cardiac Na channels may undergo a process of slow inactivation which is dependent upon both time and membrane voltage. Characterization of this process may be of some importance since the effect of many drugs on Na channels has been shown to depend upon the state of the Na channel. We have used the maximum upstroke velocity of the action potential ($\dot{V}_{max}$) to investigate the rate of development of slow inactivation in guinea pig ventricular myocardium. A single sucrose gap method was used to clamp the membrane at holding and plateau potentials. The free-running action potential upstroke was differentiated to obtain $\dot{V}_{max}$. The rate of development of slow inactivation was determined using a two pulse protocol. Results indicate that slow inactivation of $\dot{V}_{max}$ at -20 to +20 mV develops with a time course that can be well approximated by an exponential function having a time constant of approximately 9 to 12 seconds. Slow inactivation of $\dot{V}_{max}$ could be reversed by holding at well polarized membrane potentials for several seconds. TTX (2 μM) increased both the rate of development and magnitude of inhibition of $\dot{V}_{max}$ at -20mV and +20mV. These results suggest that cardiac Na channels in mammalian ventricular muscle can exist in a slow inactivated state at depolarized levels of membrane potential. The presence of slow inactivation could contribute to the controversy over the mechanism of action of TTX on cardiac tissue, and deserves further investigation.

T-PM-G7 DEPOLARIZATION INDUCED POTENTIATION OF NOREPINEPHRINE CONTRACTIONS CAN BE BLOCKED BY NIFEDIPINE. Luc M. Hondeghem and Michael J. Ayad, Department of Pharmacology, University of California, San Francisco, California 94143.

Coronary vascular spasm can be effectively controlled by nifedipine. The origin of vascular spasm and its prevention by nifedipine was studied in isometric rabbit aortic rings. At normal resting potentials the EC_{50} of norepinephrine (NE) is 10 nM, whereas in muscles depolarized by 20 mM potassium the EC_{50} is reduced to 1 nM. Thus the effect of NE is markedly potentiated by potassium depolarization. This potentiation is most marked (> 75% of maximum contraction) for the combination of small doses of NE and potassium, which by themselves result in little or no contraction. Small doses of nifedipine (3 nM) have little effect upon NE contractions, block potassium contractures by 50%, and virtually abolish the potassium induced NE potentiation. We propose that a major mechanism of action of nifedipine is to prevent coronary spasm resulting from physiological concentrations of catecholamines in depolarized muscle.

T-PM-G8 DOES THE "PACEMAKER CURRENT" GENERATE THE DIASTOLIC DEPOLARIZATION IN THE RABBIT SINO-ATRIAL NODAL CELLS? A. Noma, M. Morad & H. Irisawa, Nat'l. Inst. for Physiol. Sci., 444, Okazaki, Japan

Sino-atrial cells generate a time-dependent inward current when voltage-clamped to potentials negative to -40mV. There is some question as to the role of this current (known as I_h, I_f, I_c) in generation of diastolic depolarization. Recently, Cs^+ was shown to selectively block I_h, but had little effect on the rate of diastolic depolarization (Maylie and Morad, 1981, Biophys. J. 33:11a). This finding suggests that either I_h plays a minor role in pacemaking or that Cs^+ blocks the I_h channel in a voltage-dependent manner. In this study small preparations of spontaneously beating rabbit sinoatrial node were voltage clamped with the two-microelectrode technique. The effects of 0.25-5 mM Cs^+ on the spontaneous pacing rate and the time-dependent inward "pacemaker" current, i_h, were studied. In the presence of 2 mM Cs^+, the spontaneous pacing rate decreased only slightly even though i_h was strongly depressed at potentials negative to -60 mV. Cs^+ had little or no effect on other time-dependent currents observed with clamp pulses less negative than -50 mV. Since no voltage-dependence of the Cs^+ action on i_h could be measured, it was considered unlikely that the lack of Cs^+ effect on the rate of diastolic depolarization results from a voltage-dependent effect of Cs^+ on the i_h channel. Adrenaline produced a marked positive chronotropic effect in the Cs^+-treated preparations. This effect was accompanied by marked enhancement of the slow inward current (i_{si}) with no change in the Cs^+-blocked i_h current. These results are consistent with the idea that i_h plays a minor role in generation of pacemaker depolarization, and suggests a more prominent role of i_{si} in the nodal cells.

T-PM-G9 TRANSMEMBRANE IONIC CURRENTS IN SINGLE CARDIAC PACEMAKER CELLS. E. Shibata and W. Giles (Intr. by R. B. Clark) University of Texas Medical Branch, Galveston, Texas 77550.

Enzymatic dispersion (elastase, collagenase, trypsin) has been used to isolate single pacemaker cells from the sinus venosus of the bullfrog, Rana catesbeiana. A modified suction microelectrode technique was used to record spontaneous pacemaker activity and to apply the voltage clamp. This myogenic pacemaker response is insensitive to tetrodotoxin (TTX, 10^{-6} M). A prominent pacemaker potential develops from a maximum diastolic potential near -70 mV; the subsequent action potential peaks near +35 mV, and is approx. 450 msec in duration at -50 mV. Voltage clamp measurements reveal two distinct time- and voltage-dependent ionic currents: (i) A TTX-insensitive transient inward current: threshold, -55 mV; peak amplitude ≅ 200 pA at 0 mV; apparent E_{rev}, approx. +50 mV. (ii) A slow, maintained outward K^+ current: activation range, -30 mV to +20 mV; E_{rev} in 2.5 mM $(K^+)_o$, -95 mV; slope of E_{rev} versus $\log_{10}(K_o)$, 50 mV/decade.

Kinetic studies indicate that each K^+ tail current decays as single exponential; and that the development of the pacemaker potential is modulated by both i_K and activation of the inward current. (Supported by NIH (HL-27454) and AHA (81-835)).

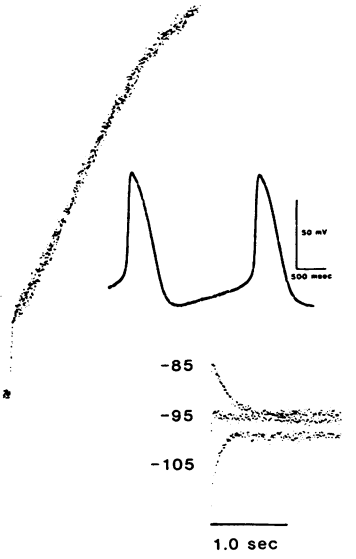

T-PM-G10 VOLTAGE-DEPENDENT INACTIVATION - REACTIVATION OF TTX-RESISTANT INWARD CURRENT IN SINGLE CELLS FROM BULLFROG ATRIUM. D. L. Campbell, K. Robinson and W. Giles (Intr. by M. Andresen). Department of Physiology and Biophysics, University of Texas Medical Branch, Galveston, TX 77550

A single microelectrode voltage clamp technique was used to study the kinetics of the TTX-insensitive (3 μM) inward current (I_{Ca}) in single cells enzymatically isolated from bullfrog atrium. I_{Ca} records were digitized for signal averaging and curve-fitting. The applicability of the Hodgkin-Huxley formalism for inactivation-reactivation was tested in two different protocols. (1) Recovery of I_{Ca} was studied using 100 msec paired pulses (P_I, P_{II}) to -10 mV to avoid activation of the delayed rectifier. Curve-fitting analysis show that the recovery time-course is a single exponential (τ = 117±8 msec, n=7, H.P. -90 mV) and that all individual current records inactivate with a fixed single exponential time-course (τ = 29.3±0.8 msec, n=34), despite 90% variation in amplitude. (ii) Steady-state inactivation (H.P. -80 or -90 mV) was studied using 500 msec prepulses to varying potentials followed by a 100 msec test pulse to 0 mV. A conventional inactivation curve (see Figure) was obtained: V_h = -29.0 ± 1.05 mV, slope factor, 6.23 ± 0.18 mV (n=6). In summary, in atrial cells, i_{Ca} exhibits conventional inactivation within the physiological range of potentials.

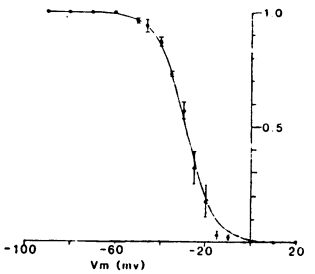

(Supported by NIH HL-27454 and AHA-81-835).

T-PM-G11 AN INWARDLY RECTIFYING K^+ CURRENT IN BULLFROG ATRIAL CELLS. Y. Momose, G. Szabo, and W. Giles, Dept. of Physiology and Biophysics, Univ. of Texas Medical Branch, Galveston, Tx. 77550.

Individual cells from bullfrog atrium were isolated by enzymatic dispersion. A K^+ current which regulates the resting potential was studied, using both whole-cell single microelectrode voltage clamp, and patch clamp techniques. Quasi-instantaneous voltage clamp measurements show that this current exhibits prominent inward rectification. When $(K^+)_o$ is raised in the range 10 to 113 mM (i) E_{rev} changes with a slope of 49 mV/10-fold $\Delta(K^+)_o$. (ii) Negative to E_{rev} the I-V's are linear with slopes proportional to the square root of $(K^+)_o$. (iii) 'Cross-over' of the I-V curves is observed positive to 0 mV.

Patch clamp recordings ($(K^+)_o$ 10 to 113 mM) consistent of discrete transitions between only two levels of current. The single channel I-V curve is linear and its slope exhibits a square root dependence on $(K^+)_o$, with $\gamma \cong 19$ pS in 113 mM K^+_o. The absence of discrete transitions positive to the calculated E_K, and the weak voltage-dependence of the channel life-times, suggest that inward rectification is a fundamental property of a single channel.

The spectral density of the macroscopic cell current fluctuations (113 mM $(K^+)_o$; E_m -130 mV) closely approximates a single Lorentzian (F_o, 1.5 Hz) which is consistent with directly recorded single channel properties. Combination of the macroscopic current data and the single channel measurements give an estimate of K^+ channel density, 1500±200 per cell, or 1 per 2 μm^2.

Ba^{++} (50 to 250 μM) produces a significant voltage-dependent block of the macroscopic current. Single channel recordings suggest that this arises mainly from a reduction in mean open time.

Supported by NIH Grants HL-27454 and HL-24820 and by Am. Heart. Grant 81-835.

T-PM-G12 TIME-DEPENDENT OUTWARD CURRENT IN ISOLATED GUINEA PIG ATRIAL AND VENTRICULAR MYOCYTES. J.R. Hume, Department of Pharmacology/Toxicology, Michigan State University, East Lansing, MI 48824.

Quiescent cells from guinea pig atria and ventricles were isolated using a collagenase dispersion technique. Resting potentials and action potentials characteristic of intact atrial and ventricular preparations can be recorded. A single suction micropipette voltage clamp technique (Hume and Giles, J. Gen. Physiol. in press) was used to study time-dependent outward current(s) in these cells.

TTX (10^{-5} M) and a holding potential of -50 mV were used to eliminate the fast inward Na^+ current. Under these conditions, when voltage clamp steps to the plateau range of potentials are applied, a time-dependent outward current is activated following i_{Ca}. In both atrial and ventricular cells (Fig.) examination of outward tail currents at room temperature reveals: an isochronal (2-5 sec) activation range extending from -30 to +30 mV and a monoexponential decay of outward tail currents which reverse near -80 mV (when $[K]_o$ = 5mM). These results suggest that a single component of delayed rectification which is carried primarily by K^+ is present in both cell types. (Supported by USPHS grant, HL 30143.)

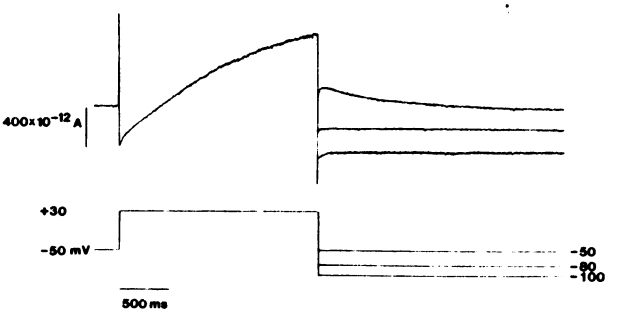

T-PM-G13 FURTHER EVIDENCE THAT I_{K_2} IN CHICK EMBRYONIC HEART CELLS IS A POTASSIUM ION CURRENT. J.R. Clay[1] and A. Shrier[2]. [1]Lab. of Biophysics, NINCDS, MBL, Woods Hole, MA 02543, USA; [2]Dept. of Physiology, McGill University, Montreal, PQ, Canada H3G 1Y6.

We recently reported a time-dependent pacemaker current in aggregates of ventricular cells derived with tissue culture techniques from 7-day old chick embryonic hearts which was nearly absent from 17-19 day old hearts (A. Shrier and J.R. Clay, 1980. Nature. 283:670; J.R. Clay and A. Shrier, 1981. J. Physiol. 312:471; Ibid. 312:490). We concluded that the ionic constituent of the current was potassium, primarily because the time dependence was absent during a voltage step to E_K. The kinetic and rectifier properties of the current were similar to those of I_{K_2} in mammalian cardiac Purkinje fibers originally reported by D. Noble and R.W. Tsien (1968. J. Physiol. 195: 185). However, D. DiFrancesco (1981. J. Physiol. 314:359) has recently reinterpreted I_{K_2} in Purkinje fibers as an inward current, I_f. Moreover, D. DiFrancesco and D. Noble (1982. J. Physiol. 326:65P) have carried out computer simulations which suggest that our measurements may also be consistent with I_f. Our steady state IV's in K_o = 1.3 mM are, in fact, consistent with their model. However, our IV's in K_o = 3.5 mM show a net developmental loss of outward current and a loss of negative slope conductance. Both of these changes are inconsistent with I_f. Moreover, 2 mM Cs blocks the time dependence at 7 days, while revealing a significant time-independent inward current, as predicted by the I_{K_2} model. Finally, we note that the simulations of DiFrancesco and Noble (1982) indicate a biphasic current response in the vicinity of E_K, which we did not observe experimentally. Therefore, we conclude that, on balance, our evidence supports I_{K_2} in our preparation rather than I_f. Supported by the Medical Research Council, Canada.

T-PM-G14 MICROSPIKE POTENTIALS IN AGGREGATES OF EMBRYONIC CHICK CARDIAC CELLS. Ronald L. Seaman* and Robert L. DeHaan+, *Biomedical Research Division, Georgia Tech EES, Atlanta, GA 30332, and +Dept. of Anatomy, Emory University, Atlanta, GA 30322. Intr. by David B. Dusenberry.

The small transient depolarizing potentials that appeared spontaneously in TTX-treated (10^{-7} gm/ml) aggregates of cultured 7-day embryonic ventricle cells were termed microspikes (DeHaan and DeFelice, Fed. Proc. 37: 2132-2138, 1978). In a recent analysis, microspikes with amplitudes of 0.2 - 8.0 mV were recorded at frequencies of 0.3 to 8 per min. Microspikes had an exponential rising phase with a time constant of 150 msec. Minimum time-to-peak (140 msec) was seen in microspikes of about 1 mV. Return of the microspike potential to baseline was non-exponential and slower. It lasted 0.3 to 8 sec, and often included an undershoot of the original resting potential. Microspike potentials could result from a transient increase of 2-50 nA/cm^2 in an inward current or a similar decrease in an outward current. In some preparations, the stable resting potential was interrupted by brief flurries of TTX-resistant action potentials. Such bursts occurred with frequencies and duration similar to those of large microspikes. We are currently testing the hypothesis that microspikes result from spontaneous transient increases in intracellular free calcium which activates an increase in net inward current. We propose that the slow decay of the microspike potential reflects the return of calcium to low levels. The cross-spectral density of two-electrode recordings of membrane potential that contained microspikes had a peak at 0.1 - 0.5 Hz. Thus, these events may contribute to the low frequency content of voltage and current noise reported in other cardiac preparations under calcium overload conditions. (Supported by U.S.A.F. School of Aerospace Medicine)

T-PM-G15 SMALL SIGNAL IMPEDANCE AND TRANSIENT CURRENTS IN VOLTAGE CLAMPED CLUSTERS OF CHICK HEART CELLS. L. Ebihara, Dept. of Pathology, Univ. of Colorado, Denver, Colorado 80262 and R.T. Mathias, Dept. of Physiology, Rush Medical College, Chicago, Illinois 60612.

Voltage clamp studies were performed on small spherical clusters of embryonic chick heart cells grown in tissue culture. In these studies the fast Na^+ current was either inactivated or blocked by tetrodotoxin, so only plateau or pacemaker currents were studied.

The linear frequency domain representation of a voltage and time dependent channel has two components: (a) a steady conductance determined by the d.c. voltage; (b) a frequency dependent admittance due to opening and closing of channel gates in proportion to small applied voltage fluctuations. We identified four distinct voltage and frequency dependent components of the impedance. The pharmacology, voltage dependence and rate constants of these cmponents correlated with: (1) the gating of the pacemaker channel; (2) the gating of the delayed K^+ channel; (3) the on gating of the slow inward Ca^{++} channel; and (4) the turn off of the slow inward current. However, impedance component (4) did not correspond to voltage dependent inactivation gating of the slow inward channel, rather the impedance suggested that accumulation/depletion of Ca^{++} is primarily responsible for the inactivation phase of the slow inward current in this tissue. (Supported by AHA grant #79-851 and NIH grant HL29205).

T-PM-G16 ELECTROPHYSIOLOGICAL CHARACTERISTICS OF CA^{++} TOLERANT SINGLE FELINE VENTRICULAR MYOCYTES. Steven R. Houser and Lewis H. Silver, Department of Physiology, Temple University School of Medicine, Philadelphia, Pa. 19140

Myocytes were isolated from normal cat hearts by perfusing the coronary arteries with a Krebs-Henseleit solution (KHS) containing low levels of Ca^{++} and collagenase. Following isolation, myocytes were placed in KHS containing Ca^{++} (1-2.7mM). Myocytes in these solutions maintained normal structural characteristics and responded to extracellular stimulation with brisk contractions. These myocytes were impaled with 3M KCl filled microelectrodes. During these studies the cells were superfused with Tyrode solution (35^{o}-37^{o}C) gassed with 95% O_2 - 5% CO_2. All cells were quiescent before impalement. Upon insertion of microelectrodes cells became spontaneously active for short time periods but eventually became quiescent. The mean resting potential (n = 17) was -79.4 + 0.8mV. Myocytes were stimulated intracellularly and action potentials (AP) recorded. These $\overline{AP}$'s were similar to those previously reported for intact tissue. The mean value for AP plateau height was 105 + 3.2mV yielding an overshoot of + 25 + 2.7mV. Cells stimulated at different rates demonstrated $\overline{t}$ypical rate dependent shortening of $\overline{th}$e AP at the 80% repolarized level (APD_{80}). At stimulation rates of 30, 60, and 120/min, the mean values of APD_{80} were 364, 338, and 230 mSec respectively. The results demonstrate that these isolated myocytes retain electrophysiological characteristics that are representative of those described in intact ventricular muscle. (Supported by NIH #HL22673 and HL07193).

T-PM-Pos1 CHLORIDE ION TRANSPORT AND ITS INHIBITION IN THYLAKOID MEMBRANES by V. Vambutas, Department of Biochemistry, Mount Sinai School of Medicine, New York, N.Y. 10029

Cl^- translocation across energized and non-energized thylakoid membranes was blocked by piretanide, an inhibitor of active Cl^- transport in fish intestinal epithelial cells. Cl^- transport in non-energized thylakoids was dependent on cation (K^+) concentration of the medium. N,N'-dicyclohexylcarbodiimide (DCCD) and carbonyl cyanide m-chlorophenyl hydrazone (CCCP) did not inhibit Cl^- transport. Piretanide (1 mM) had no effect on photophosphorylation catalyzed by phenazine methosulfate or on Ca^{2+}-dependent ATPase activity of isolated chloroplast coupling factor (CF_1). It is proposed that piretanide specifically inhibits a H^+-independent translocation mechanism of Cl^- in thylakoid membranes.

Preliminary evidence indicates that the anion transporter in thylakoid membranes is a protein(s). Detergent extracts of thylakoid membranes, when reconstituted into azolectin/cholesterol vesicles, stimulated piretanide sensitive Cl^- efflux from vesicles (measured with a Cl^- sensitive electrode). Trypsin-treated extracts had no activity, while valinomycin had only a small stimulatory effect. Preliminary evidence indicates that anion efflux in reconstituted vesicles is coupled to cation efflux. (Supported by NSF Grant PCM-8115652)

T-PM-Pos2 SPECTRAL PROPERTIES OF CHLOROPHYLL AND PORPHYRIN DERIVATIVES, AND THEIR RELATION TO REACTION CENTER SPECTRA. Joseph Eccles and Barry Honig - Department of Biochemistry, Columbia University, 630 West 168th Street, New York, N.Y. 10032

The spectroscopic properties of several chlorophyll and bacteriochlorophyll derivatives have been examined in the CNDO/S approximation. The enol tautomers of Chl *a* and BChl *a* are compared with the standard keto forms. The enol form is found to have a new long wavelength absorbance in each case. The calculated intensities are found to be very dependent upon the assumed geometry of the fifth ring of the enol.

Protonated and unprotonated Schiff's bases of Chl *a* and BChl *a*, as well as the 4,8-formylvinylporphinato metal (II) compound examined by Ward *et al.*[1], are also examined.

The spectra of photosynthetic reaction centers are discussed in light of these results.

[1]B. Ward, P.M. Callahan, R. Young, G.T. Babcock and C.K. Chang, submitted to J.A.C.S.
Supported by NSF PCM 82-07145.

T-PM-Pos3 REDUCTION IN THE SIZE OF THE PHOTOSYSTEM I CHLOROPHYLL ANTENNA IN IRON DEPRIVED CELLS OF *ANACYSTIS NIDULANS*. Himadri Pakrasi and Louis A. Sherman, Division of Biological Sciences, Tucker Hall, University of Missouri, Columbia, MO 65211.

Deprivation of iron from the growth medium results in major changes in the photosynthetic membranes of the cyanobacterium, *Anacystis nidulans* R2. Iron-starved cells are different from normal cells in their: 1) chlorophyll a absorption peak, 2) low temperature fluorescence emission peaks, 3) room temperature fluorescence kinetics, and 4) chlorophyll-protein complexes of lithium dodecyl sulfate (LDS) solubilized membranes as revealed by LDS-PAGE analysis. The ultrastructural parameters of iron-deprived cells are also changed markedly. However, the electron transport rates for photosystem I (DAD/Ascorbate $\rightarrow$ Methyl viologen), photosystem II ($H_2O \rightarrow$ DCBQ) and the whole chain ($H_2O \rightarrow$ MeV) are normal in these cells. To investigate the changes in the organization of iron-deprived thylakoids, we measured the light saturation characteristics of PSI and PSII electron transport rates. The saturation of the PSI rate was found to be much faster in these cells, indicating a smaller antenna size for PSI. In order to obtain a conclusive value for the size of the PSI antenna pool, the rate of photooxidation of P700 (the reaction center of PSI) was measured by difference absorption spectroscopy under limiting light conditions at room temperature. Whole cells were incubated with DCMU and cyanide to block electron donation to PSI (Melis, A, Arch. Bioch. Bioph. 217: 536-545, 1982). Results indicate that the chlorophyll a antenna pool serving PSI is decreased in *A. nidulans* cells grown in iron-deprived conditions. This feature correlates well with the absence (in iron-deprived cells) of high molecular weight chlorophyll-protein complexes thought to be associated with PSI. This research was supported by NIH Grant GM21827.

T-PM-Pos4 PHASE SEPARATION OF NON-BILAYER LIPIDS IN THYLAKOID MEMBRANES OF CHLOROPLASTS.
K. Gounaris, A. Sen, A.P.R. Brain, P.J. Quinn and W.P. Williams, Chelsea College, University of London, London SW3 6LX, U.K.

Monogalactosyldiacylglycerol (MGDG), the major lipid component of chloroplast membranes is known to form inverted hexagonal structure in aqueous dispersions (Sen et al. (1981) Biochim. Biophys. Acta 663:380). Inverted lipid micelles and other non-bilayer structures have been reported in freeze-fracture studies on mixed lipid dispersions containing MGDG (Sen et al. (1981) Nature 293:488; (1982) Biochim. Biophys. Acta 685:297). Similar non-bilayer structures are also observed in total polar lipid extracts of chloroplasts dispersed in presence of salts (Gounaris et al. (1983) Biochim. Biophys. Acta, in press). No such non-bilayer structures have been reported in freeze-fracture replicas of chloroplasts which tend to suggest that protein-lipid interactions may play an important role in stabilizing chloroplast membrane structures. To test this hypothesis chloroplasts were heated to different temperatures and examined using freeze-fracture electron microscopy. Normal structures were observed up to 45°C. Dramatic changes occurred when chloroplasts were heated to 50°C for 5 min, 74% of all chloroplasts examined in freeze-fracture replicas had phase separated lipids very similar in morphology to inverted hexagonal structures. Low temperature fluorescence and functional studies on preheated chloroplasts showed a differential effect of lipid phase separation on PSI and PSII. These results strongly suggest a very important structural/functional role of Hex_{II} forming MGDG in chloroplast membranes.

T-PM-Pos5 POLARIZED INFRARED SPECTROSCOPY OF THE BACTERIAL REACTION CENTER LM COMPLEX
E. Nabedryk, D. Tiede, P.L. Dutton, J. Breton, S. Biophysique, CEN Saclay 91191 Gif-sur-Yvette cédex, France and Dept. Biochem. and Biophys. U. of Penna., Philadelphia PA 19104

A comparison of the protein structure was made between the native bacterial photosynthetic reaction center of Rps. sphaeroides R-26 (containing LM and H subunits) and the fully functional LM complex derived from it. These LMH and LM complexes were reconstituted into lecithin vesicles and oriented multilayers for infrared (IR) dichroism analysis were formed by air-drying onto CaF_2 discs. Polarized IR difference spectra ($A_{//}-A_{\perp}$) of the reconstituted LM and LMH multilayers show a similar positive signal (i.e. a preferential absorption of light polarized parallel to the plane of incidence) for the amide A (3300 cm^{-1}) and the amide I (1656 cm^{-1}) bands, attributable to oriented α-helix segments. A corresponding negative signal is seen for the amide II band (1543 cm^{-1}). However, a small negative signal at 1630 cm^{-1} likely associated with protein β-structures is only detected with the LMH complex. Preliminary analysis of the UV circular dichroism spectrum of the LM complex in detergent solution show that the extent of the α-helix content is comparable to that in the LMH complex. From these data, it is concluded that : i) in both the reconstituted LMH and LM complexes, the α-helix segments tend to be aligned along the normal to the membrane ii) all of the oriented α-helices are found in the photoactive LM subunit while oriented β-structure appears localized in the H subunit.

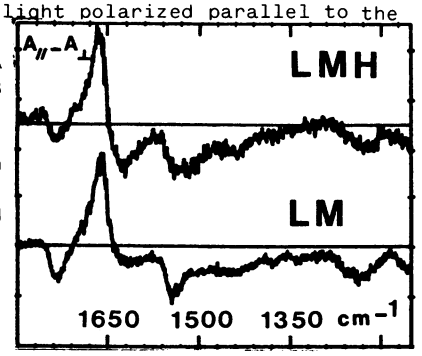

T-PM-Pos6 ORIGIN OF SIGNAL II IN SPINACH CHLOROPLASTS AND ITS ROLE IN THE WATER SPLITTING PROCESS.
P.J. O'Malley* and G.T. Babcock, Department of Chemistry, Michigan State University, E. Lansing, MI 48824-1322.

The primary donor to $P680^+$, generally termed Z, gives rise, in its oxidized state, to a characteristic EPR signal termed IIvf. Previous model compound studies of Signal II have centered on the immobilized anionic and neutral forms of semiquinone radicals. These radicals, however, exhibit an essentially structureless band shape in contrast to the partially resolved five line pattern observed for Signal II. We now show that certain cationic semiquinone radicals exhibit partially resolved hyperfine structure similar to Signal II. For example, the 2,5-dimethylhydroquinone cation radical exhibits a band shape and microwave power saturation characteristics similar to Signal II. The band shape for both the *in vitro* and *in vivo* species is attributed to stabilization of the antisymmetric orbital. The greater splitting between the resolved peaks for the *in vivo* species suggests a greater contribution from the antisymmetric orbital in this case. *In vivo* ENDOR data also support the quinone origin of this signal. Resolution of three bands in the 10-20 MHz range is in accord with the unique saturation characteristics of semiquinone radicals in protic solvents. The large positive electrode potential of cationic quinone radicals ($\simeq$1.0 V) *in vitro*, together with the known donor properties of Z to $P680^+$, suggests an active role for a plastoquinone cation radical in the water splitting process (supported by USDA CRGO).

T-PM-Pos7 ELECTRON SPIN RESONANCE STUDIES OF THE ORIENTATION OF THE CAROTENOIDS IN RHODOPSEUDOMONAS SPHAEROIDES WILD TYPE. Harry A. Frank, John Machnicki and Paul Toppo, Department of Chemistry, University of Connecticut, Storrs, CT 06268.

The triplet state ESR spectra of chromatophores of Rhodopseudomonas sphaeroides wild type dried flat on mylar strips display a marked dependence of the intensity of the ESR signals on the orientation of the mylar plane with respect to the static ESR field direction. These orientation effects have previously been observed for the triplet state signals assigned to the primary donor of bacterial photosynthesis (H. A. Frank, et al BBA 547 (1974) 484, and B. J. Hales, et al Biophys. J. 37 (1982) 229a). We present here triplet state spectra from Rps. sphaeroides wild type recently assigned to carotenoids (H. A. Frank, et al JACS 102 (1980) 4893) which also display large orientation effects. The data are discussed with regard to the orientation of the carotenoids both in the membrane and with respect to the primary donor species.

T-PM-Pos8 EXCITON CALCULATIONS IN BACTERIOCHLOROPHYLL PROTEIN. Leland C. Mayne & Bruce S. Hudson, Department of Chemistry and Institute of Molecular Biology, University of Oregon, Eugene, OR 97403

The bacteriochlorophyll protein antenna complex from Prosthecochloris aestvarii strain 2K provides an array of well characterized chromophores with a single low energy transition. The X-ray structure of this complex has been determined by Fenna and Matthews[1] providing an excellent system for testing exciton calculations. Pearlstein and Hemenger[2] made calculations of the absorbance and CD spectra and found that they could not reproduce experimental line shapes as long as they assumed the lowest Bchl transition was y-polarized as has been accepted. We have recently made calculations using extended dipoles and point monopole arrays varying the dipole strength, dipole separation, band width and the ratio of dipole strength to quadrupole strength. These calculations were carried out for both x- and y-polarized absorptions and in some cases for the protein trimer as well. Our results seem to show best agreement with experimental line shapes assuming the conventional y-polarization for the low lying transition of Bchl but with a slightly higher dipole strength than that used by Pearlstein and Hemenger. Results of calculations based on the protein trimer are not markedly different from those calculated for the monomer.

[1] B.W. Matthews et al. J. Mol. Biol. 131, 259-285 (1979).
[2] R.M. Pearlstein & R.P. Hemenger, Proc. Natl. Acad. Sci., USA 75, 4920-4924 (1978).

T-PM-Pos9 GROUND-STATE INTERACTIONS ON ANTENNA B800, B850 AND B870 BACTERIOCHLOROPHYLLS OF RHODOSPIRILLACEAE. Marc Lutz, Bruno Robert, André Vermeglio and Roderick K. Clayton*, Département de Biologie, CEN Saclay, 91191 Gif-sur-Yvette cédex France, *Division of Biological Sciences, Cornell University, Ithaca, NY 14853, USA

Resonance Raman (RR) spectroscopy permits selective observations of bacteriochlorophylls (BChls) involved in chromatophores and in antenna pigment-protein complexes of photosynthetic bacteria, and yields information about ground-state interactions assumed by these molecules (1,2). However, the contributions of individual BChls presently cannot be distinguished by this technique.The recent finding that BChl absorbing at 800 nm can be reversibly extracted from the B850-800 antenna complex from Rps spheroides (3) was applied to the study of environmental interactions specifically assumed by B800, using low-temperature, difference RR spectra excited at 363.8 nm. Two carbonyl stretching modes were observed at 1636 and 1702 cm^{-1}, corresponding to one bound acetyl C=O and one free ketone C=O, respectively. These RR spectra also showed that the reinsertion of a B800 into the complex can be structurally perfect : the bound molecule indeed most probably recovers its native network of bonds.

BChl pairs present in the B850(800 depleted) complex from Rps spheroides and in the B870-type complexes of Rps rubrum and Rps spheroides assume slightly but definitely different ground-state interactions, concerning in particular the binding sites of their acetyl carbonyls. The proposal that only two distinct types of antenna complexes should occur in purple bacteria can also be tested on a molecular level.

(1) M.Lutz, A.J.Hoff, L.Bréhamet (1982) BBA,679,331-341. (2) M.Lutz (1981) Photosynthesis, G.Akoyunoglou ed., Balaban, vol.3, 461-476. (3) R.K.Clayton, B.J.Clayton (1981) ibid.377-386.

T-PM-Pos10 AN HYPOTHESIS ON THE ORIGIN OF THE 695nm FLUORESCENCE (F695) OF CHLOROPLASTS AT 77K. Jacques Breton, Service de Biophysique, CEN-Saclay, 91191 Gif-sur-Yvette, France.

At 77K the emission spectrum of chloroplasts consists of 3 main bands located at 735nm (F735) 695nm (F695) and 685nm (F685). A small shoulder can also be detected at 680nm (F680) which is originating from the light-harvesting complex (LHC). F735 is associated with PS1 while F685 and F695 are related to PS2. By analyzing the orientation of the Qy dipoles responsible for these emission bands we found that they were all oriented at a small angle to the membrane plane, with the exception of F695 which is oriented perpendicular to this plane. We have also shown that all the emission bands of isolated LHC, including a band at $\sim$ 698nm, were oriented parallel to the plane of the membrane. By comparing the linear dichroism spectra of chloroplasts to the ones of isolated PS2 particles we have observed that all the Qy transitions of the PS2 core antenna were oriented parallel to the plane of the membrane. A similar orientation has been observed for P680, the primary donor of PS2. However the pheophytin (Phe) intermediary acceptor has its Qy transition oriented perpendicular to this plane.

The variable fluorescence is attributed to charge recombination in reaction centers where the first stable quinone (Q) acceptor is reduced. At room temperature it is commonly supposed that the charge recombination on P680 creates an exciton which returns to the antenna system. We propose that at 77K some of these excitons are created on Phe and leave the RC directly without returning to the antenna bed. A similar proposal involving P680 can be made for at least a fraction of the F685 emission. A new model pointing towards a common origin for all of the PS2 emission (both constant and variable fluorescence) at low temperature will be discussed.

T-PM-Pos11 REDOX TITRATION OF THE SLOW ELECTROCHROMIC PHASE IN CHLOROPLASTS. M.E. Girvin and W.A. Cramer, Dept. of Biological Sciences, Purdue University, W. Lafayette, IN 47907. (Intr. by P. Argos)

The slow (msec) component of the 515 nm electrochromic band shift has been associated with electron transfer from plastoquinol through the cytochrome b_6-f-Rieske center complex. This would be part of a Mitchellian "Q-loop" that could allow an H^+/e^- ratio greater than one to be generated in this region of the electron transport chain.

In order to determine the redox potentials of the plastoquinol donor and first electron acceptor to this postulated loop, we have titrated the amplitude of the slow phase as a function of ambient potential between +230 and -250 mV at pH 7. The operating redox system was calibrated by titrating FMN. The amplitude of the slow phase is very small at positive potentials, begins to increase below +200 mV, and shows a mid-point of +110 mV that is associated with that of the plastoquinol donor. With the donor fully reduced, the half-time of the slow phase was 3-4 msec. Dark reduction of cytochrome b_6 did not cause a decrease in slow phase amplitude, which remained constant as the potential was decreased to the range, -100- -150 mV. Below this redox level the amplitude decreased slightly, but at least 75% of the maximum remained at -250 mV with a half-time of 4 msec. It is concluded that reduction of cytochrome b_6 is not responsible for generation of the slow phase, a conclusion previously reached by J. Whitmarsh and M. Selak. Furthermore, if the electron acceptor giving rise to the slow phase is accessible to the reduced redox dyes, then it must have a midpoint potential more negative than -250 mV. (Supported by NSF grant PCM-8022807).

T-PM-Pos12 COHERENCE AND LOCALIZATION OF EXCITONS IN MOLECULAR ARRAYS. Robert F. Goldstein and William Bialek, Department of Biophysics and Medical Physics, University of California, Berkeley, California 94720

We apply radiationless transition theory(1), including a rigorous treatment of vibrational relaxation(2), to energy transfer in large molecular arrays. For short times after creation of the exciton, apparent inhomogeneous vibrational broadening may hinder exciton mobility via Anderson localization(3), although exciton coherence has not decayed. We examine the decay of coherence in a representation-independent fashion, and show localization and coherence to be independent on all time scales. The time and extent of coherence decay are temperature dependent; in particular, exciton coherence is expected to last much longer than vibrational coherence under several conditions, including low temperature. These results call into question our current understanding of rapid energy-transfer in photosynthetic antennae--coherence may play an important role in the effecient trapping of excitons.

1. Soules, T.F. & C.B. Duke, Phys. Rev. B 3:262 (1971).
2. Bialek, W. & R.F. Goldstein, Biophys. J. 37:225a (1982).
3. Anderson, P.W., Phys. Rev. 109:1492 (1958).

Supported by the NSF (PCM 78-22245 and pre-doctoral fellowship to W.B.) and the U.S.D.O.E. through the Lawrence Berkeley Laboratory.

T-PM-Pos13 INVOLVEMENT OF SLOWLY EQUILIBRATING PROTONS IN PHOTOSYSTEM II STABILITY. James D. Johnson, Valerie R. Pfister, and Peter H. Homann, Institute of Molecular Biophysics, Florida State University, Tallahassee, FL 32306.

Exposure of the water-oxidizing site of the photosynthetic system II to moderately alkaline conditions is known to cause its inactivation. Several other deleterious processes involving this site also require a pH > 7, for example the inhibition by Cu^{2+} and the release of functional Cl^-. We have found that, in intact thylakoids, all these treatments are facilitated in osmotically swollen thylakoids. Parallel measurements of H^+-equilibration between thylakoids and the external bulk solution have identified two metastable H^+-pools, one readily released by uncouplers, and the other not. Both pools could be monitored with fluorescent pH probes like 9-aminoacridine and atebrin. This led to the unexpected observation of an uncoupler-insensitive, slow recovery of the probe fluorescence which was accompanied by a proton release. The pH at the water-oxidizing site appeared to be determined by the uncoupler-insensitive protons. During thylakoid swelling, essentially all metastable protons became releasable by uncoupler-addition.

This explains why the water-oxidizing site was more susceptible in hypotonic media to treatments requiring an elevated pH. Osmotic swelling appears to have alleviated an obstruction of protonated buffering groups including those which determined the pH at the site of water oxidation.

Supported by grant #8011755 from the National Science Foundation.

T-PM-Pos14 A POLYNUCLEAR MANGANESE CENTER IN O_2 EVOLVING PHOTOSYNTHETIC MEMBRANES OF SCENEDESMUS OBLIQUUS. B. Upadrashta, D. Abramowicz and G. C. Dismukes, Princeton University, Dept. of Chemistry, Princeton, NJ 08544

EPR spectra at 4.2 K of two mutants of S. obliquus have been compared to the wild type (WT) cells. Light sensitive peaks at g' 1.18 and 0.87 in WT cells are suppressed in a PS-II lacking mutant (PS-X-C14) and a low fluorescent (LF-1) mutant, both of which cannot evolve O_2 (Fig.). These resonances also occur in a binuclear Mn(III) protein from spinach thylakoids which is believed to function as the water oxidizing enzyme. They are fine structure peaks for an $S \geq 1$ spin state. A peak at g' 2.74 in WT cells is 3-4x larger than in the LF-1 and PS-X-C14 mutants, and also exhibits at least 17 lines of hyperfine structure with average A=39G (inset). This peak occurs at the half-field $\Delta M_S=2$ "forbidden" region for the binuclear Mn(III) protein in spinach. It is strong evidence for a polynuclear Mn cluster with $S \geq 1$. The absence of these peaks in LF-1 and PS-X-C14, along with a concomitant x 2 increase in the g' 2.0 peak characteristic of mononuclear Mn(II), indicates that Mn in these mutants is not present as EPR detectable clusters, unlike WT. Supported by USDA-CRGO and Searle Scholars grants.

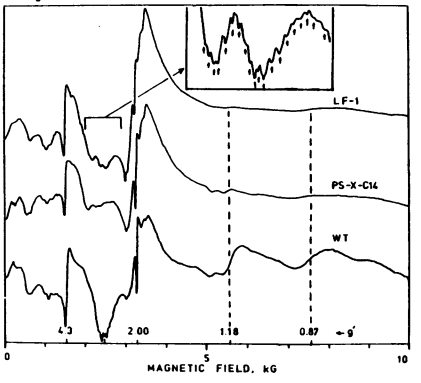

T-PM-Pos15 ELECTRON SPIN RESONANCE SPECTRA OF THE CYTOCHROME B_6F COMPLEX OF SPINACH CHLOROPLASTS

J.W. McGill,G.C. Gerstle,J.A. Ribes,O.N. Malbec,J.C. Salerno Biology Dept.,Rensselaer Polytechnic Institute,Troy,N.Y. 12180 The ESR spectra of low spin cytochrome b_{559} component(s) have been detected in purified preparations of the cytochrome b_6f complex.A broad component with g near 3.65 is reduced by dithionite but not by ascorbate;it resembles the spectra of the mitochondrial b cytochromes in modified preparations of the bc_1 complex. Weak signals observed in chloroplast membrane fragments suggest that two b_{559} components may be resolved in the intact system.Antimycin effects on spectra are weak or absent, although oxidant induced reduction was observed.Detailed ESR spectra of cytochrome f reveal some asymmetry of the g_z=3.5 peak,and a broad g_y between 1.7 and 1.8;the third feature is probably below 1.0. Complete spectra of the Rieske type Fe/S center have been obtained.Antimycin shifts the position of the g_z peak from 2.02 to higher field,and also shifts the g_y feature from 1.90 to slightly lower field. This effect is probably mediated by a shift in the redox or binding state of another component. UHDBT sharpens the g_z peak and shifts it to lower field; the broad g_y feature at g=1.8 is further broadened by UHDBT,the opposite of the effect seen in some other systems. Little or no cytochrome b_{563} was seen in our preparations of b_6f complex; the signals near g=2.95 attributed to b_{563} in purified preparations by other workers may be due to modified b_{559} type cytochrome. Using membrane fragments,the g_x feature of b_{563} was detected;it is very broad and centered between 1.3 and 1.4. This implies that the tetragonal and rhombic crystal field terms are respectively about 3.3 and 1.5 times the spin orbit coupling,since the other features have been reported near g=3.1 and 2.15.

T-PM-Pos16 LOCALIZATION OF CYTOCHROME b_{559} IN THE PHOTOSYNTHETIC APPARATUS. P. Usharani, L. V. M. Rao, K. T. Tokuyasu and W. L. Butler, Dept. of Biology, University of California, San Diego, La Jolla, California 92093

We have used immunohistochemical techniques to localize cytochrome b_{559} in the photosynthetic apparatus of spinach leaves. Cytochrome b559 was purified from spinach as a high molecular weight lipoprotein and used for the production of antibodies in rabbits. The antibodies were immunopurified by affinity chromatography. Ultrathin frozen sections of spinach leaves, suitable for electron microscopy, were stained first with the purified antibodies against cytochrome b_{559} and then with either ferritin-conjugated goat antirabbit IgG or with gold-conjugated protein A which also binds to the rabbit IgG. Electron microscopy shows that the electron dense label is associated almost exclusively with the grana regions of the photosynthetic apparatus.

T-PM-Pos17 PHOSPHOLIPID ENRICHED CHROMATOPHORES: CHARACTERIZATION OF THE ELECTRON TRANSFER AND ENERGY CONSERVING PROPERTIES. Rita Casadio,G.Venturuli and B.A.Melandri.Inst.of Botany, Via Irnerio 42, 40126 Bologna,Italy.

Chromatophores of Rhodopseudomonas spaeroides GA cells grown photoheterotrophically were fused with phospholipid vesicles by means of a freeze- thaw-sonication technique.Vesicles with a diminished number of intramembranous protein particles per lipid surface area with respect to the untreated chromatophores were still active in light induced proton uptake,generation and mantainance of a transmembrane potential and electron transport,as detected by means of fast spectroscopy. The half life time of the reaction center(RC) complex rereduction by cyclic electron flow,in vesicles characterized by the same cyt. c/ RC molar ratios,ranged from 1 to 3 ms in control chromatophores to 16- 19 ms in fivefold phospholipid enriched chromatophores when measured at 50 $\pm$ 10 mV ambient redox potential. The diminished electron flow rates parallelled the increased phospholipid-ubiquinone 10 molar ratios; a fast electron trasport could be restored in the phospholipid enriched fractions by addition of exogenous ubiquinone 5 in ethanolic solution.

The data are indicative of the dissociation of the RC and b/c_1 complexes following dilution with phospholipids and of the role of the ubiquinone pool in controlling the intercomplex electron transfer processes in this system, in agreement with what has been suggested for the inner membrane of mitochondria on the basis of steady state kinetic experiments.

T-PM-Pos18 OXIDATION KINETICS OF THE PS II SECONDARY QUINONE ACCEPTOR (Q_B) FROM PEA CHLOROPLASTS. H.H. Robinson and A.R. Crofts, Department of Biophysics, University of Illinois, Urbana.

The oxidation kinetics of the primary quinone acceptor (Q_A) depend upon the oxidation state of the secondary quinone acceptor (Q_B/Q_B^-). Q_A^- is oxidized with a half time of 100μs by Q_B, and with a half time of 200μs by Q_B^-. All of the centers are put into the state Q_B^- with a flash of light, then incubated in the dark, and then assayed for the remaining Q_B^-. The property of two different oxidation rates of Q_A^- allows for a linear measure of the extent to which oxidation of Q_B^- occured during the dark incubation. When the donor side of PS II is mostly in the state S_2, the oxidation half time of Q_B^- is 22s, and the reaction is first order. This back reaction is sensitive to the state of the PS II donors. 30μM NH_2OH or 5μM FCCP in the absence of O_2 extends the oxidation half time to 30 minutes. The 22s back reaction half time from Q_B^- to S_2 measured here is consistant with previously measured times for the resetting of the oxygen evolving complex of PS II (the return of S_2 to S_1) in the absence of inhibitors. When DCMU is present the back reaction half time from Q_A^- is 1.5s. Assuming that DCMU has not modified Q_A^-, the ratio of these half times (22s/1.5s) determines an equilibrium constant of 15 for the couple $Q_A^-Q_B \rightleftharpoons Q_AQ_B^-$. If the redox potential of the couple Q_A/Q_A^- is taken to be -30mV then the couple Q_B/Q_B^- is 40mV (all at pH 7.6). The stability constant for the semiquinone at the Q_B site is then $3.4 \cdot 10\text{-}2 \cdot K_o/K_r$, where K_o and K_r are the equilibrium constants for binding of oxidized and fully reduced plastoquinone from the pool to the Q_B site.

T-PM-Pos19 INHIBITION OF THE B-C_1 COMPLEX OF RPS. SPHAEROIDES BY A NEW ANTIBIOTIC, MYXOTHIAZOL
S.W. Meinhardt and A.R. Crofts, Department of Physiology and Biophysics,Univ. of Illinois, Urbana

A recently isolated antibiotic, myxothiazol, has been shown to affect electron transport through the mitochondrial b-c_1 complex (1,2). In chromatophores from Rps. sphaeroides strain Ga myxothiazol inhibits the flash induced reduction of cyts b_{566}, b_{561}, c_1, and c_2. Titrations have shown 1 binding site/b-c_1 complex, independent of antimycin. The extent of cyt c oxidation following a flash was less with myxothiazol present than with UHNQ or UHDBT (3). Redox titrations of the extent of flash induced cyt c oxidation in the presence of myxothiazol or UHNQ showed a difference which gave a curve indicating a single component with an $E_{m7} \sim 290$ mV, n=1. Addition of excess myxothiazol to chromatophores inhibited by UHDBT or UHNQ reversed the extra oxidation of cyt c after a flash. Between pH 6 and 9, addition of myxothiazol to chromatophores reduced by dithionite in the presence of PMS produces a blue shift, maxima and minima at 562 and 568 nm respectively, centered at 566 nm, which was independent of antimcyin. These results can be explained by suggesting that UHNQ, UHDBT, myxothiazol, and ubiquinol (4) are competing for the same reaction site, and that myxothiazol can displace the other reactants. The reaction site is formed at the interface between the cyt b_{566}-protein and the FeS-protein and catalyzes the oxidation of QH_2 and a concerted reduction of cyt b_{566} and FeS (5).
1)Becker, W. F., Von Jagow, G., Anke, T., Steglich, W., FEBS Lett. 132, 329-3332) Von Jagow, G. and Engel, W. D., FEBS Lett. 136, 19-24. 3) Meinhardt, S. W. and Crofts, A. R., FEBS Lett. in Press. 4)Bowyer, J. R. et al., (1982) 2nd EBEC Short Reports, p. 201-202. 5)Crofts, A. R. et al. (1982) 2nd EBEC short Reports, p. 327-328

T-PM-Pos20 CONSTRUCTION OF A LIGHT-DEPENDENT ELECTRON DONATION SYSTEM USING AN OXYGEN-EVOLVING PHOTOSYSTEM II PREPARATION--APPLICATION TO THE STUDY OF THE BOVINE MITOCHONDRIAL CYTOCHROME b-c_1 COMPLEX. Eric Lam, Department of Biophysics and Division of Molecular Plant Biology, University of California, 313 Hilgard Hall, Berkeley, CA 94720.

Light-dependent reduction of cytochrome c can be demonstrated in the presence of the mitochondrial cytochrome b-c_1 complex and an oxygen-evolving Photosystem II preparation from chloroplasts. This photoreduction requires the cytochrome b-c_1 complex and is sensitive to inhibitors of photosynthetic and mitochondrial electron transport, such as DCMU, antimycin A and myxothiazol. Addition of micromolar amounts of duroquinone enhances the extent and rate of the photoreduction about five-fold. Double reciprocal plot analysis of the reduction process for cytochrome c identified two apparent binding sites with K_m of 0.47μM and 10.2 μM at a b-c_1 concentration of 0.8 μM.

In the absence of cytochrome c, relatively small changes of absorbance were observed for the cytochromes in the cytochrome b-c_1 complex. However, with the addition of micromolar amounts of duroquinone, a rapid reduction of cytochrome c_1, and a biphasic reduction of cytochrome b can be observed upon illumination. The effects of antimycin A, myxothiazol, ascorbate and their combined actions on the kinetics of reduction of these cytochromes were studied. The results are discussed in terms of possible mechanisms of electron transfer through the cytochrome b-c_1 complex and the mode of action of antimycin A and myxothiazol.

(This research has been supported in part by a grant from the National Institute of Health to Dr. R. Malkin.)

T-PM-Pos21 CHLOROBIUM CHLOROPHYLLS: STRUCTURES, AGGREGATIONS, CONFORMATIONS AND CHIRALITY.
K. M. Barkigia, J. Fajer, D. A. Goff, L. A. Kehres and K. M. Smith. Brookhaven National Laboratory, Upton, NY 11973 and the University of California, Davis, CA 95616.

1) Bacteriochlorophylls c, d and e aggregates in hexane exhibit large optical red-shifts which provide viable models for the antenna chlorophylls of green and brown photosynthetic bacteria. Chemical modification studies clearly implicate the hydroxy group of the 2-(1-hydroxyethyl) substituent as the promoter of the aggregations and thus offer a rationale for the presence of that group in BChls c, d and e.

2) The structures of three homologues of methyl bacteriopheophorbide d, derived from the green sulfur bacterium Chlorobium vibrioforme, were determined by X-ray diffraction. The 4,5- diethyl (I) and 4-isobutyl, 5-ethyl (II) derivatives crystallized from hexane to yield cofacial dimers connected by hydrogen bonds. The newly isolated 4-neopentyl, 5-ethyl compound (III) crystallized from methanol to form chains connected by hydrogen bonds. I and II exhibit considerable nonplanarity in contrast to III which is nearly planar. These differences typify the wide range of conformations packing forces can induce in chlorophylls and, by extrapolation, exemplify the structural effects protein environments can impose on the chromophores.

3) Compounds I, II and III, although isolated from the same organism, display different chiralities at the 2-(1-hydroxyethyl) substituent. It is R for I and S for II and III, i.e. bulky groups at position 4 cause a switch from R to S at position 2 and thus raise intriguing questions regarding the biosynthetic pathways.

(Work supported by the Department of Energy and the National Science Foundation.)

T-PM-Pos24 BIOSYNTHESIS OF SUCCINATE DEHYDROGENASE IN *BACILLUS SUBTILIS*.
L. Hederstedt*, K. Magnusson and L. Rutberg. (Intr. by Y. Hatefi)
Department of Bacteriology, Karolinska Institutet, S-104 01 Stockholm, Sweden

Composition. Succinate dehydrogenase (SDH) is a membrane-bound iron-sulfur flavoprotein having a similar structure in mammals, yeast, *Neurospora crassa* and bacteria (1). The enzyme is composed of two different polypeptides; Fp (M_r, 60-70K) and Ip (M_r, 25-30K). Both subunits contain non-heme iron and acid-labile sulfide. The Fp subunit also contains a covalently bound FAD. SDH is in the membrane of the aerobic bacterium *Bacillus subtilis* and is structurally and functionally complexed to cytochrome b_{558} (M_r, 19K). Biogenesis of SDH has been studied in *B. subtilis* mutants deficient in SDH, cytochrome b_{558} and heme (1,2).

Topology. Cytochrome b_{558} spans the bacterial membrane and anchors SDH to the inner surface (3).

Genetics. The structural genes for Fp, Ip and cytochrome b_{558} are part of an operon, the *sdh* operon (2). The *sdh* genes seem to be transcribed in the order cytochrome b_{558}, Fp, Ip.

Membrane binding. A model for the biosynthesis of SDH in *B. subtilis* has been proposed and to a large extent experimentally verified (1,2). Fp and Ip subunits are made in the cytoplasm as soluble proteins that later become membrane-bound. The location of newly synthesized apocytochrome b_{558} is not known, but this hydrophobic polypeptide is thought to be inserted into the membrane in concert with its synthesis. When holocytochrome b_{558} appear, binding site(s) on the cytochrome for soluble SDH subunits are exposed and an active membrane-bound SDH-cytochrome b_{558} complex is formed.

1. Hederstedt, L. and L. Rutberg (1981) Microbiol. Rev. 45, 542. 2. Hederstedt, L. et al. (1982) J. Bacteriol. 152, 157. 3. Hederstedt, L. and L. Rutberg (1983) J. Bacteriol. 153.

T-PM-Pos25 REACTION OF CYTOCHROME OXIDASE WITH O_2 AT LOW TEMPERATURES: RELATIONSHIP TO PROTON PUMPING. Vincent, J-C.*; Kumar, C., Naqui, A. and Chance, B., Johnson Res. Fdn.,Univ. of Penna., Phila., PA 19104: *Universite de Rouen, E.R.A., 471C N.R.S., France

In an attempt to understand whether the steps in the formation and decay of low temperature O_2 intermediates of cytochrome oxidase (A,B_1,B_2 [1,2]) are coupled to proton uptake and release by cytochrome oxidase, we have studied the pH-dependence of the various steps in the O_2-cytochrome oxidase reaction. We also used a pH-indicator to monitor small changes in pH in the medium associated with proton uptake or release while spectral monitoring shows the formation or decay of any of the enzyme intermediates.

The kinetics of interconversion of the various intermediates during the reaction of reduced mitochondrial cytochrome oxidase with oxygen shows that the conversion from Compound A to B_2 seems to occur through two separate pathways, as suggested by double maxima in the reaction rate vs. pH plots. Compound B_1 is found at a greater concentration in the quasi-steady state at -100°C at acidic pH suggesting that conversion to B_2 occurs with release of protons by the enzyme. This is supported by pH measurements under similar low temperature conditions using bromothymol blue as an indicator. The insensitivity of heme a and Cu_{a3} oxidation to pH, as measured by EPR, suggests that the proton interactions occur close to the active site of the protein: the heme a_3-Cu_{a3} couple.

Supported by NIH 37476, PCM-80-26684. JCV was awarded a NATO fellowship.

[1] Chance, B., Saronio, C. and Leigh, Jr., J.S. (1975) J. Biol. Chem. 250:9226-9237.
[2] Chance, B., Saronio, C. and Leigh, Jr., J.S. (1975) Proc. Natl. Acad. Sci. 721635-1640.
[3] Clore, G.M. and Chance, E.M. (1978) Biochem. J. 173:799-810.

T-PM-Pos26 STRUCTURAL BASIS FOR THE PEROXIDATIC AND CATALATIC ACTIVITIES OF CYTOCHROME OXIDASE. Chance, B., Institute for Structural & Functional Studies, 3401 Market St., Phila., PA, Kumar, C., Naqui, A., Johnson Res. Fdn., Univ. of Penna., Phila., PA, Powers, L., and Ching, Y., Bell Tel. Laboratories, 600 Mountain Ave., Murray Hill, NJ

Identification of the structure of the pulsed oxidase as a non-sulfur bridged form [1] permits interpretation of the reactions of the enzyme with ligands of the ferric state, particularly peroxides and cyanide. The pulsed oxidase cyanide compound has structural features of the first shell very similar to other low spin compounds such as the yeast peroxidase cyanide compound. Intermediates identified in the peroxidatic/catalatic cycle of the cytochrome oxidase have been formed and characterized by X-ray absorption studies. The structure of the peroxide compounds of cytochrome oxidase and those of the peroxidase Compounds I, II and III are compared. Based upon the first shell homologies of the iron EXAFS in the pulsed oxidase to that of horseradish peroxidase, yeast peroxidase, catalase and cytochrome o, similar homologies of pulsed oxidase peroxide are observed in comparison with Compound II of HRP and Complex ES of yeast peroxidase.

Supported by NIH GM 27308, 27176, 38385 and SSRL Project 623B (DOE,BES,NSF,DMR and NIH,BRP,DRR).

[1] Powers, L., Ching, Y., Chance, B. & Muhoberac, B. (1982) Biophys. J. 37:403a.

T-PM-Pos27 INHIBITION MECHANISM OF CYTOCHROME OXIDASE BY NICKEL(II) ION. Naqui, A., Gabbidon, E., Kumar, C. and Chance, B., Johnson Research Foundation, University of Pennsylvania, Phila.,PA 19104

Insertion of a heavy metal (e.g., Ni^{2+}) into the cytochrome oxidase active site near the Fe,Cu atoms could assist in the study of this enzyme by X-ray absorption spectroscopy. So far, Beinert and Palmer [1] have found that urea (6 M) is necessary for the insertion of Hg. Here we have studied the kinetics of O_2 uptake and reduction of cytochromes c,a,a_3 of mitochondria and purified cytochrome oxidase at different concentrations of added Ni^{2+}. Ni^{2+} is a noncompetitive inhibitor with respect to O_2 (K_i 1 x 10^{-3} M). A kinetic model has been proposed to explain this phenomenon. The kinetics of reduction of cytochromes c,a and a_3 in presence of Ni^{2+} shows that cytochromes c and a both are reduced instantly while a_3 remains oxidized for a much longer time. On the basis of the crossover theorem of Chance, et al [2], it has been concluded that Ni^{2+} mainly blocks the electron transfer between cytochromes a and a_3 and thus may be within range of an EXAFS study.

Supported by NIH GM 27308, GM 28385, GM 27476 and SSRL Project 623B (DOE,BES,NSF,DMR and NIH, BRP,DRR).

[1] Beinert, H. and Palmer, G. (1965) in Oxidases and Related Redox Systems (King, T.E., et al., eds.) John Wiley, NY. pp. 567-590.
[2] Chance, B., Williams, G.R., Holmes, W.F. & Higgins, J. (1955) J. Biol. Chem. 217:439-451.

T-PM-Pos28 STRUCTURAL BASIS FOR MODIFIED FORMS OF PURIFIED CYTOCHROME OXIDASE. Powers., L, Ching,Y. Bell Tel. Labs., Murray Hill, NJ; Chance, B.; Kumar, C., Johnson Res.Fdn.,Univ.of Penna., Phila.PA and Hartzell, C.R., A.I. DuPont Inst., Wilmington, DE

X-ray absorption spectroscopy of the copper and iron atoms of cytochrome oxidase have identified forms of the oxidized enzyme in which the sulfur atom bridging the iron-copper components of the active site is present as in the "resting" and absent as in the "pulsed" forms of the oxidase. These states are also characterized by red shifts of the visible absorption bands and altered reactivity towards ligands, particularly cyanide. The question arises as to whether different cytochrome oxidase preparations differ in their physical and chemical properties, content of the non-bridged form, or in other structural features of the copper and iron atoms. This has been determined by X-ray absorption spectroscopy. Our results on Yonetani [1] and Hartzell/Beinert (HB) [2] preparations show distinct differences. The fourier transform of the EXAFS data show a highly significant split in the first shell Cu EXAFS in the latter preparation and none in the former; further differences are found in higher shells. These structural differences are correlated with biochemical reactivity differences as described by Brudvig, et al [3]. The differences of these cytochrome oxidase preparations now have a structural basis in terms of an altered environment of the Cu_{a3} atom and chemical/kinetic differences are reported elsewhere (Kumar, et al,this volume). Structurally responsive methods are essential for the detection of cytochrome oxidase conformation. Supported by NIH GM 28308 & SSRL Project 623B(DOE,BES,NSF,DMR&NIH,BRP,DDR). [1] Yonetani, T.(1961) J.Biol.Chem. 236:1680; [2] Hartzell, C.R. & Beinert, H (1974) Biochem.Biophys.Acta 368:318; [3] Brudvig, G.W., Stevens, T.H., Morse, R.H. & Chan, S.I. (1981) Biochem. 20:3912-3921.

T-PM-Pos29 CONTROL OF MITOCHONDRIAL METABOLISM BY ADP AS IDENTIFIED FROM ^{31}P NMR STUDIES OF PFK DEFICIENT HUMAN. Chance, B., Johnson Res.Fdn.,Univ.of Penna., Phila., PA; Eleff, S., Dept. of Anesthesia, Hosp. of Univ. of Penna., Phila., PA; Bank, W.W., Dept. of Neurology, Hosp.of Univ. of Penna.; Leigh, Jr., J.S., John.Res.Fdn.,Univ.of Penan, Phila.,PA; Warnell, R., Dept.of Surgery, Hosp.of Univ. of Penna., Phila., PA

Metabolic control of mitochondrial respiratory activity by inorganic phosphate, P_i, and adenosine diphosphate (ADP) has been a controversial topic and one which is difficult to approach by analytical biochemistry due to the artifactual increase of P_i during extraction. Recent ^{31}P NMR studies of the exercising arm and leg in an PFK deficient human has shown trapping of inorganic phosphate in sugar phosphates (mainly glucose-6 phosphate) to the extent that inorganic phosphate is maintained at a constant level during an activity/recovery (state 3→4) transition under conditions of constant ATP and rapidly increasing PCr; PCr increasing from half its maximal value to the maximum state 4 level (∿30 mM/kg). The constancy of inorganic phosphate is inconsistent with its role in the control of mitochondrial activity in this transition, leaving ADP as the key metabolic control element, further extending the original observations of Chance and Williams [1] and supporting the recent data of Jacobus, et al [2].

[1] Chance, B. & Williams, J.R. (1955) J. Biol. Chem. 217:383-393.
[2] Jacobus, W.E., Moreadity, R.W. & Vandegaer, K.M. (1982) Biophys. J. 37:407a.

T-PM-Pos30 GLUCAGON EFFECTS ON MITOCHONDRIAL $\Delta\psi$ AND Ca^{2+} INFLUX. D.E. Wingrove, T.E. Gunter and J.M. Amatruda. Dept. of Rad. Biol. and Biophys., Univ. of Rochester, Rochester, NY 14642

Numerous reports agree that in vivo administration of glucagon to rats stimulates Ca^{2+} influx in isolated hepatic mitochondria. To investigate the mechanism of this effect, Ca^{2+} influx and membrane potential are measured simultaneously. Rats are injected intraperitoneally with 0.3-0.6 mg/kg body wt. glucagon while controls are injected with saline; mitochondria are prepared in an identical manner from each. Mitochondria at 1 mg/ml are placed in a standard 0.3 OsM. 3:1 mannitol sucrose media containing 3 mM succinate, 100 μM antipyrlazo III and 20 μM TPP. The extramitochondrial calcium concentration is measured using the calcium indicator dye antipyrylazo (absorbance @ 720 - 790 nm) and initial rates of uptake calculated by computer. The tetraphenyl phosphonium electrode used to follow membrane potential with a time response of less than 8 sec., is inserted into the cuvette during absorbance measurements. Intramitochondrial volumes are calculated using $^{3}H_2O$ and ^{14}C-sucrose exclusion.

In addition to increasing the resting membrane potential (Taylor et al., 1980), glucagon treatment results in mitochondria maintaining a higher $\Delta\psi$ during influx of Ca^{2+}-typically 6-8 mV higher for moderate loads. An increase in Ca^{2+} uptake rate is accompanied by a larger $\Delta\psi$ than seen in controls, in all experiments thus far. Malonate + rotenone inhibition is used to decrease the membrane potential and study the effects of Ca^{2+} influx. This data is compared to the predictions of a current theory on carrier mediated electrolyte transport. Preliminary results suggest that most of the glucagon stimulation of Ca^{2+} influx can be explained by $\Delta\psi$ effects.

Partially supported by NIH Grant #T32 GM07356.

T-PM-Pos31 STRUCTURE OF THE H^+-ATPASE OF LIVER MITOCHONDRIA: INTERACTION OF THE γ SUBUNIT WITH BOTH THE α AND β SUBUNITS. Noreen Williams and Peter L. Pedersen, Department of Physiological Chemistry, The Johns Hopkins University School of Medicine, Baltimore, MD 21205.

The soluble F_1-ATPase of rat liver mitochondria has been shown by this laboratory (JBC 246:4987) to be composed of five distinct subunits ($\alpha,\beta,\gamma,\delta$ and ε). These subunits are in the apparent stoichiometric ratio of $\alpha_3\beta_3\gamma\delta\varepsilon$ (JBC 248:7247). The structure of the enzyme has recently been elucidated to 9 Å resolution (PNAS 79:5852). The rat liver F_1-ATPase possesses a two-fold axis of symmetry with each half of the dimer containing three equivalent masses. This implies that one of the α,β pairs (or other major subunit combination) must reside in a unique environment. Since it appears that γ,δ and ε exist in single copies one may infer that these small subunits interact with a single α,β pair in the intact F_1-ATPase complex. In order to test this hypothesis we have initiated the studies described below.

We report here that the rat liver F_1-ATPase upon cold treatment and subsequent warming shows a loss of activity and dissociates into two major discrete, reproducible complexes. The first complex forms a precipitate when warming occurs which appears to contain both α and γ subunits. The second major complex is separated from the remaining soluble fraction by chromatography on Sepharose CL6B. This major peak contains predominantly the β subunit with some γ subunit. These results indicate an association of the γ subunit with both the α and β subunits. The $\alpha\gamma$ interaction would seem to be stronger under the conditions of these experiments. These results appear to be consistent with the model developed on the basis of the crystallographic data in which one $\alpha\beta$ pair was assumed to be associated with the three smaller subunits. [Supported by NIH grant CA 10951.]

T-PM-Pos32 THE BINDING OF DICYCLOHEXYLCARBODIIMIDE TO CYTOCHROME b OF COMPLEX III AND ITS INHIBITION OF PROTON EJECTION by L. Clejan and D. S. Beattie, Mount Sinai School of Medicine, New York, N.Y. 10029

A purified $b\text{-}c_1$ complex (complex III) isolated from yeast mitochondria and incorporated into proteoliosomes is capable of energy conservation. In the reconstituted $b\text{-}c_1$ complex, dicyclophexylcarbodiimide (DCCD) blocked the function of the electrogenic proton translocating device in the forward direction of proton ejection as well as in the backwards direction, measured as reversed electron flow from cytochrome b to coenzyme Q_2 driven by a K^+-diffusion potential (negative inside). The primary effect of DCCD is localized on the proton ejection process, as the low proton conductance of the proteoliposome membrane was totally preservd after DCCD treatment. Subsequently, the maximum binding of the [^{14}C]DCCD to the complex was determined under identical incubation conditions. Maximum binding of approximately 2.0 nmoles of DCCD per nmol of cytochrome b was observed. The [^{14}C]DCCD ws not removed by extraction with chloroform-methanol, suggesting that DCCD is covalently bound. SDS-gel electrophoresis of the [^{14}C]DCCD treated complex indicated that DCCD bound selectively to cytochrome b with only slight labeling of subunits V and VI. These results, plus the DCCD inhibition of electrogenic proton ejection in the $b\text{-}c_1$ complex reconstituted into liposomes, suggest a major role for cytochrome b in proton translocation at site 2 in the respiratory chain. (Supported by NIH Grant HD-04007 and Fogarty International Fellowship TW-00616)

T-PM-Pos33 A NEW PHTOAFFINITY LABEL FOR ENERGIZED BEEF HEART SUBMITOCHONDRIAL MEMBRANES. Stephan J. Kopacz*, Alice T. L. Lo*, David M. Mueller and C. P. Lee, Department of Biochemistry, School of Medicine, Wayne State University, Detroit, Michigan 48201.

Similar to quinacrine (QA), 9-amino-3-chloro-7-methoxyacridine (9ACMA) exhibits an energy-linked fluorescence decrease when associated with beef heart submitochondrial membranes. The pH dependence of the fluorescence intensities of QA and 9ACMA associated with energized membranes indicates that a mechanism(s) other than protonation of the dye molecules, as is the case with QA, is responsible for the energy-linked fluorescence decrease of 9ACMA. Systematic analyses of the biochemical and biophysical parameters of QA and 9ACMA alone, and associated with membranes, indicate that the 9ACMA molecules bound to the energized membranes are in a non-fluorescent form (Huang, Kopacz and Lee, Biochim. Biophys. Acta, In press). A photoaffinity analogue of 9ACMA, 9AAMA, which differs from 9ACMA only in the substitution of the chloride group with the azide was made by amination of 3-azido-9-chloroacridine (Mueller, Hudson and Lee, Biochemistry 21, 1445-1453, 1982) with ammonium carbonate in a phenolic solution. Similar to 9ACMA, the absorption spectrum of 9AAMA in aqueous solution, in the visible region, changes with the pH of the medium in the range from 6.0 to 11.0, with an isosbestic point at 373 nm and a pK_a value of 9.3. When associated with submitochondrial membranes, 9AAMA exhibits an energy-linked fluorescence decrease which can be restored to its original level upon subsequent addition of uncoupler. 9AAMA exhibits first order kinetics of photodecomposition with $t_{\frac{1}{2}}$ = 3 - 5 seconds. Upon photolysis, the photolyzed products of 9AAMA bind covalently to the membrane. 9AAMA can, therefore, serve as a photoaffinity label for the binding site(s) of 9ACMA with energized submitochondrial membranes. Supported by grants from NIH and NSF.

WITHDRAWN

T-PM-Pos35 COMPARISON OF QUANTUM-MECHANICAL MATRIX ELEMENTS FOR ELECTRON TRANSFER. Don DeVault and Akinori Sarai, Univ. of Illinois, Dept. of Physiology and Biophysics, Urbana, IL 61801.

Quantum-mechanical Hamiltonian matrix elements used for electron transfer between electronic states, such as tunneling between sites, have usually been either an exchange interaction between diabatic states in which the electronic wave function is assumed independent of nuclear motion or as arising from the effect of nuclear motion on adiabatic states (i.e., the non-adiabaticity operator) in which all exchange interactions have already manifested before considering the nuclear motion. Professor Sigeo Yamosa (Nagoya University, personal communication) has suggested that electron transfer should be treated as between diabatic states whenever the transfer by exchange interactions is slower than the nuclear motion but that the non-adiabaticity operator matrix element should be the means of transfer.

We have set up a simple model system incorporating two electron sites with the possibility of slow (tunneling) exchange between the sites in which diabatic electronic wave functions for each site can be formulated so that their form depends on interaction with a nearby electrically charged oscillator which provides the nuclear motion to be used by a non-adiabaticity operator. (See figure.) The purpose is to compare both types of matrix elements in the same model. The rings imitate a porphyrin ring structure around which the electron moves freely. The bridge provides a tunneling path (V > E) for electron exchange. Preliminary calculations on this model with realistic parameters indicate the rate from exchange interaction may be a thousand times larger than that from the non-adiabaticity operator.

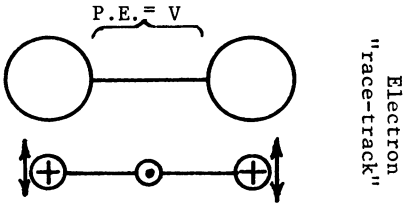

T-PM-Pos36 ACTION OF TINOPAL AN, A COMPLEX I INHIBITOR, ON SUBMITOCHONDRIAL PARTICLES. John J. Maguire, Grant A. Hartzog and Lester Packer. Membrane Bioenergetics Group, Lawrence Berkeley Laboratory, University of California, Berkeley, CA 94720.

Tinopal AN is an inhibitor of P. Denitrificans in growth phases that are both sensitive or insensitive to rotenone (Phillips and Kell, FEBS Letts, 104-248, 1982). Studies were made with rat liver submitochondrial particles to learn the location of inhibition within complex I. Enzyme analysis shows that NADH oxidase is approximately 50% inhibited with 30-40μM Tinopal (0.022mg/ml). NADH dehydogenase, measured by $K_3Fe(CN)_6$ reduction is not affected by Tinopal AN, but rotenone also has no effect on this enzyme. A difference in NADH-TEMPONE (4-oxo-2,2,6,6-tetramethylpiperidinooxy) reduction, followed by ESR, shows rotenone to partially inhibit the reaction but Tinopal AN has no effect.

Reduction of Fe-S clusters in the presence and absence of Tinopal AN using NADH as a reductant indicated that the block occurs after cluster N-2. Fe-S clusters reduced by ATP driven reversed electron flow also suggest the block is below center N-2, as no complex I clusters are reduced in the presense of Tinopal AN. It appears rotenone and Tinopal AN block electron flow at the same level of redox components, but bind at different sites.

(Supported by the Division of Biological Energy Research, Department of Energy)

T-PM-Pos37 UV AND HIGH-RESOLUTION PROTON NMR SPECTROSCOPIC STUDIES OF UBIQUINONE-LIPID STRUCTURE AND INTERACTIONS IN SYNTHETIC MEMBRANE VESICLES. E. L. Ulrich, M. E. Girvin, W. A. Cramer, and J. L. Markley, Depts. of Chemistry and Biological Sciences, Purdue University, W. Lafayette, IN 47907.

Ubiquinones with 2, 3, or 10 isoprenoid groups were incorporated into small sonicated vesicles made of DMPC or DPPC lipid. UV spectroscopy was used to monitor the oxidation state of the quinone. Oxidized UQ_2 in DMPC or DPPC vesicles was completely accessible to the reductant $NaBH_4$, whereas UQ_{10} was virtually inaccessible to $NaBH_4$ in DPPC and approximately 30% accessible to $NaBH_4$ in DMPC vesicles. 25-30% of the UQ_3 was reducible in vesicles prepared from either lipid. It was inferred that the ring of UQ_{10} must be confined to a position near the center of the DPPC bilayer, whereas the ring of UQ_2 must approach the lipid-aqueous interface. 470 MHz ^1H NMR studies showed that UQ_{10} perturbs the melting temperature of DPPC vesicles to a much smaller extent than do UQ_2 or UQ_3. The results are consistent with positioning UQ_{10} in the middle of the bilayer, where the fatty acyl chains are more disordered, and positioning UQ_2 or UQ_3 nearer the membrane surface, where their presence disrupts the packing and lowers the melting temperature. DMPC vesicles exhibit two resonances each for the acyl chain methylene and tail methyl groups. The effect of UQ_2 or UQ_{10} is to increase the intensity of the lower-field component at the expense of that at higher field. Both UQ_2 and UQ_{10}, therefore, affect the properties of fatty acyl chains at the center of the bilayer. The combined UV and NMR data imply that UQ_{10} is fixed close to the center of the bilayer but that UQ_2 either lies nearer the surface or undergoes "flip-flop" motions that bring it nearer the surface. It has been documented that physiological activities often require long-chain quinones as opposed to short-chain quinones, and we suggest that it is the unique positioning of these quinones in the hydrophobic core of the lipid bilayer, rather than a transmembrane "flip-flop" motion, that is essential for translocation of electrons and protons. [Supported by NIH RR 01077, NSF PCM-8022807, and USDA/SEA-9-8482-CRCR-1-1045.]

T-PM-Pos38 EFFECTS OF AMINE-FLUORESCAMINE COMPOUNDS ON MITOCHONDRIAL ENERGY-LINKED FUNCTIONS, F. Ramirez[a], S-I Tu[b], P. R. Chatterji[a], B. McKeever[a] and J. F. Marecek[a], Dept. of Chem., SUNY at Stony Brook, N.Y. 11794 and [b]U.S. Dept. of Agriculture, E.R.R.C., Wyndmoor, PA 19118

Studies of the noncovalent interactions that take place between components of the inner membrane of rat liver mitochondria and the fluorescent compounds ("the modifiers") made from the reaction of primary amines with fluorescamine (FL) have led to the following hypothesis. 1) Proton movement and its associated energy-yielding step, i.e., the redox events and the hydrolysis of MgATP, are only indirectly linked in oxidative phosphorylation. 2) The respiration-linked and ATPase-linked proton pumps interact directly with each other, and this step establishes the mutual regulation between ATPase and respiratory activities. 3) This pump-pump interaction is also responsible for the condensation of the tightly bound ADP with P_i in the synthesis of ATP. The $\Delta\mu H^+$ is an indispensible component of the energy transduction in the transport of metabolites. 4) The modifiers inhibit the activation of H^+ pumps as a result of implantation by H-bonding at the corresponding pump proteins. Initial rate of ATP synthesis associated with oxidation of succinate was followed by monitoring fluorometrically the ATP-linked NADPH production in the presence of hexokinase and glucose-6-phosphate dehydrogenase, with and without modifiers present, and with inhibition of adenylate kinase by AP_5A. Modifiers examined were made from the reaction of FL with amphotericin B, benzylamine, o,p-dimethylbenzylamine, β-phenylethylamine, p-aminobenzoic acid and ammonia. The modifiers were effective in inhibiting oxidative phosphorylation, but the P/O ratio remained constant (ca. 1.5). The inhibition of ATP-linked and succinate-linked H^+ extrusion rates was closely dependent on modifier structure and was least apparent in modifiers made from ammonia and p-aminobenzoic acid.

T-PM-Pos39 REDUCTION OF BACTERIAL $[4Fe\text{-}4S]^{3+}$ FERREDOXINS BY PHOTOREDUCED FREE FLAVINS. C. T. Przysiecki, G. Tollin, T. E. Meyer and M. A. Cusanovich (Dept. of Biochemistry, U of Arizona, Tucson, AZ 85721)

Laser flash photolysis has been utilized to study the reduction kinetics of C. vinosum high potential iron-sulfur protein (HiPIP) and other members of the $[4Fe\text{-}4S]^{3+,2+}$ ferredoxin (Fd) class by a variety of free flavin analogs. Both the semiquinone ($FH^{\cdot}$) and fully reduced (FH^{-}) flavin forms can reduce C. vinosum HiPIP; however, under the conditions studied the $FH^{\cdot}$ reaction accounts for >90% of HiPIP reduction and is the only reaction to be extensively studied for this protein. For all flavin analogs examined with C. vinosum HiPIP, no kinetic complexities due to heterogeneity or changes in the rate-determining step are observed. Removal of the methyl groups of the dimethylbenzene ring of the flavin moiety (10-methylisoalloxazine vs. lumiflavin) results in over a two fold increase in the apparent second order rate constant. Placement of a ribityl side chain in the N-10 position (riboflavin vs. lumiflavin) does not produce an appreciable change in rate. Addition of a negatively charged phosphate group to ribityl (FMN vs. riboflavin) decreases the rate over three-fold and produces a large ionic strength effect. Studies with Rp gelatinosa $[4Fe\text{-}4S]^{3+}$Fd give similar rate constants for all analogs except FMN where the rate constant is about twice that found for C. vinosum HiPIP and shows no ionic strength effects. A survey of the reaction rate of lumiflavin with additional members of the $[4Fe\text{-}4S]^{3+,2+}$Fd class possessing a wide range of $E_{M,7}$ values demonstrates a strong correlation between redox potential and reaction rate. The results have been interpreted utilizing available structural information and in terms of possible election tunneling or outer sphere mechanisms (NIH grant GM21277 to MAC).

T-PM-Pos40 INTERACTING SITES IN CYTOCHROME c OXIDASE: EVIDENCE FOR A MAGNETIC INTERACTION BETWEEN CYTOCHROME a_3 LIGATED WITH NITRIC OXIDE AND CYTOCHROME a. Charles P. Scholes, Rita Mascarenhas, Yau-Huei Wei, and Tsoo E. King, Department of Physics and Center for Biological Macromolecules and the Department of Chemistry and Laboratory of Bioenergetics, SUNY at Albany, Albany, NY 12222.

EPR spectra of nitric oxide complexes of cytochrome c oxidase were studied as a function of temperature in the fully reduced ($a^{2+} \cdot Cu_a^{1+} \cdot a_3^{2+}$ NO·Cu_{a3}^{1+}) form and a mixed valence ($a^{3+} \cdot Cu_a^{2+} \cdot a_3^{2+}$ NO·Cu_{a3}^{1+}) form. Temperature in a range of 12 to 77 K changed the EPR spectral lineshape of the mixed valence form but not the fully reduced. We interpret these changes as resulting from a magnetic interaction between cytochrome a_3-NO and a paramagnetic metal center in cytochrome a. The spectral changes are not due to a thermal equilibrium between two spectroscopically different forms of NO-ligated cytochrome a_3. The temperature-dependent spin-lattice relaxation of the center in cytochrome a modulates the magnetic interaction, and the effect of temperature is much better correlated with the spin relaxation behavior of the low spin ferric heme a in cytochrome a. The interaction is highly anisotropic and appears to be dipolar. From its strength we estimate a maximum distance between the heme iron centers of cytochrome a_3 and a to be 18 Å. From the average dipolar interaction a smaller distance of 15 Å was obtained.

This work was supported by NIH grants GM 16767, HLB 12576, AM 17884.

T-PM-Pos41 UNIDIRECTIONAL PHOSPHATE TRANSPORT CATALYZED BY IMPROVED MITOCHONDRIAL PHOSPHATE TRANSPORT PROTEIN/LIPOSOMES. Hartmut Wohlrab, Ann Collins, and Diane Costello. Boston Biomedical Research Institute and Harvard Medical School. The purified beef heart mitochondrial phosphate transport protein (PTP), copurified with several minor proteins and the adenine nucleotide translocase (ADT) (Wohlrab (1980) Ann. N. Y. Acad. Sci.. 358, 364)(the active PTP from flight muscle copurifies with almost no ADT) was incorporated into lipid vesicles by freezing the mixture in liquid nitrogen while agitating the sample and briefly vortexing it thereafter. A computer simulation of phosphate uptake (zero-trans) with pHi (intravesicular)=8.0, (Pi)i=0mM; pHe (extravesicular)=6.2, (Pi)e=0.35mM (Km=2mM), matches the equation $Pit=Pi_{\infty}(1-\alpha e^{-kt})$ with Pi =2.149, α =0.973, k=0.0185, and a standard deviation of 0.079, suggesting a homogeneous vesicle population. The Vmax (22°C) (zero-trans) is 260μmol phosphate/min mg PTP (pHi=8.0, pHe=6.8). At a low lipid/protein ratio zero-trans efflux shows similar initial rates and Δ pH dependence as uptake. The proteoliposomes, like mitochondria, are more sensitive to mersalyl than N-ethylmaleimide. Kinetic analyses with these proteoliposomes suggest that the monobasic phosphate is transported and that the transport protein has a proton binding site separate from the phosphate binding site; and also that the SH's that react with the lowest concentration of N-ethylmaleimide are not essential for phosphate transport since the Km for phosphate uptake increases before the Vmax decreases to a low value. Supported by NIH and NSF.

T-PM-Pos42 SUBUNIT INTERACTIONS DURING ATP HYDROLYSIS BY F_1 ATPase AT LOW AND HIGH ATP CONCENTRATIONS
O'Neal, C.C. and Boyer, P.D., Mol. Biol. Inst., Univ. of California, Los Angeles, Calif. 90024

Intermediate $P_i \rightleftharpoons HOH$ exchange catalyzed by F_1-ATPase from beef heart mitochondria has been studied as a function of ATP concentration, and the limiting values of the exchange parameters at high and low ATP concentrations have been determined. The number of water oxygens incorporated into the P_i produced during hydrolysis of ^{18}O-ATP increases from 1.02 ± 0.01 at high ATP to 3.96 ± 0.01 at low ATP. The number of reversals of the exchange step prior to P_i release increases from 0.02 ± 0.01 at high ATP to 400 ± 100 at low ATP. From 0.04 μM to about 10 μM, the total exchange rate of about 11 μmol/min/mg does not vary significantly suggesting that the rate of the exchange step is independent of ATP concentration. These findings mean that the rate of the P_i release is accelerated about 20,000 fold going from low to high ATP levels which corresponds to a free energy change of 6 kcal/mol. The distribution of ^{18}O in the product P_i was homogeneous at all ATP concentrations indicating that all catalytic sites participate in the reaction sequence in an equivalent manner. In our experiments, as in those of Gresser et al.[JBC (1982) 257, 12030] pyruvate kinase and phosphoenolpyruvate were used to regenerate ATP from ADP. To gain understanding of some apparent differences in rate and nucleotide binding behavior observed by Grubmeyer et al.[JBC(1982) 257, 12092], we have measured the rate of $^{32}P_i$ production and the amount of bound ^{32}P using their conditions and with excess F_1 as isolated and also with an ATP regeneration system present or using a glycerol-treated enzyme which has lost most of its bound nucleotides. With the latter two systems we observe a much faster rate of $^{32}P_i$ production and less bound ^{32}P, suggesting that a tightly bound inhibitory ADP may contribute to the reported differences in the behavior.

T-PM-Pos43 TOPOGRAPHICAL LOCATION OF THE RIESKE Fe-S CENTER IN MITOCHONDRIA.
V. G. Struble and H. J. Harmon (Intr. by H. L. Scott), Departments of Zoology and Physics, Oklahoma State University, Stillwater, OK 74078.

2-OH-3-undecyl-1,4-naphthoquinone (HUNQ) is a quinone analog that inhibits mitochondrial respiration in the cytochrome b-c_1 region with an apparent K_i of 2.5 X 10^{-7} M. It prevents the reduction of cytochrome c_1 but not its oxidation by oxygen and prevents oxidation of cytochrome b by succinate but not its reduction. It inhibits oxidant-induced reduction of cytochrome b in the presence of antimycin. Inhibition of succinate oxidase activity by HUNQ is pH-independent in electron transport particles. In intact mitochondria, inhibition of succinate oxidase activity decreases above pH 8. The apparent pK of the 2-OH group of the oxidized quinone is 6.6. This indicates that the pH dependency of the inhibition is not due to the pH-dependent changes of the quinone but is due to the pH dependency of the Rieske center (pK=8). This suggests that the Rieske center is located on the cytoplasmic side of the inner membrane where it is sensitive to the pH of the medium.

This research was supported by a Grant-in-Aid from the American Heart Association with funds contributed in part by the Oklahoma Affiliate.

T-PM-Pos44 Ca^{2+} TRANSPORT REVERSIBILITY AND STEADY STATE ACROSS THE INNER MITOCHONDRIAL MEMBRANE.
K.K. Gunter & T.E. Gunter, Dept. of Rad. Biol. & Biophys., Univ. of Rochester, Rochester, NY.

Liver mitochondrial Ca^{2+} transport is mediated by at least two separate mechanisms, which under steady state conditions oppose one another setting up zero net flux. Two conceptionally different types of phenomena, isotope exchange by a single mechanism and steady state isotope exchange through cycling, can be exploited to provide information about both the uniport and the Na^+-independent efflux mechanism. Rapid isotope exchange (usually indicating a passive mechanism) has been demonstrated earlier and can be shown to be mediated by the uniport. Such exchange, indicated by release of internal label upon uptake of large amounts of cold Ca^{2+}, Sr^{2+}, or Mn^{2+} by the uniport, can be shown to occur during the period of low membrane potential induced by rapid Ca^{2+} uptake. Rapid K^+ uptake via valinomycin causes a similar decrease in membrane potential and elicits a similar release of internal Ca^{2+} unless ruthenium red, an inhibitor of the uniport, is present. This clearly shows the reversibility of the uniport. Rapid isotope exchange cannot be induced via the ruthenium red-insensitive efflux mechanism, suggesting that it may not be a passive mechanism.

Following the earlier observation that the interplay between the uniport and Na^+-independent efflux mechanism can establish a true steady state, which likely plays a prominent role in regulation of cytosolic Ca^{2+} in vivo, an experiment may be set up in which very small amounts of labelled Ca^{2+} are added to a mitochondrial suspension, maintaining steady state distribution of Ca^{2+}. Measurement of influx of the added label provides an alternative means of measuring efflux (rate) permitting a demonstration that the usual EGTA procedure is free from artifact.

T-PM-Pos45 PURIFICATION AND CHARACTERIZATION OF AN ADENOSINE-5-TRIPHOSPHATASE FROM RICE (ORYZA SATIVA L.) SEEDLING MITOCHONDRIA. Amitabha Basu and Subhendu Mukherji. Plant Physiology Laboratory, Dept. of Botany, University of Calcutta, Calcutta 700019, India.

An adenosine-5triphosphatase (ATPase) was isolated from rice seedling mitochondria which has a relatively high molecular weight, multisubunit structure, oligomycin and azide sensitivity in membrane bound condition, oligomycin insensitivity and cold lability on solubilization. This finding is in contrast to the older hypothesis regarding the absence of the conventional F_1-ATPase like particles in the mitochondria of monocotyledonous species (Sperk and Tuppy, Plant Physiol. 59, 155, 1977). The purification of the enzyme was achieved through preparation of the submitochondrial vesicles by ultrasonication, washing of the vesicles and solubilization of the enzyme with different concentrations of Triton X-100, heat fractionation in the presence of ATP, and finally a gradient separation on 4-12% discontinuous glycerol gradient at 2,48,000 g for 3 h. The enzyme shows three major subunits of 55,000, 49,000 and 36,000 respectively on a typical SDS polyacrylamide (10%) gel electrophoresis. It also shows bicarbonate activation, a characteristic of F_1-ATPase in purified condition. The purified enzyme has an activity of 50 µmol of P_i/min/mg of protein in a reaction mixture consisting of 25 mM Tris-HCl, 10 mM $MgCl_2$ and ATP without any ATP recovery system.

T-PM-Pos46 "EPR analysis of iron-sulfur clusters in NADH-UQ oxidoreductase using resolved systems" T. Ohnishi (Dept. Biochem. & Biophys.), C.I. Ragan (Dept. Biochem., Univ. of Southampton, Southampton, U.K.), and Y. Hatefi (Dept. Biochem., Scripps Clinic and Res. Fdn., La Jolla, CA 92037).

Iron-sulfur clusters in the NADH-UQ oxidoreductase (18-22 Fe/flavin) have been studied by EPR analysis of the resolved subunit fractions, each containing equivalent concentrations of non-heme iron and acid labile sulfur (Ragan et al., ('82) Biochem. 21:590). FP fraction elicits EPR signals from two different species, Fe_2S_2 and Fe_4S_4 (or Fe_3S_3) type, each titrated as a n=1 redox component with distinct Em values. The former cluster seems to be in subunit II, and the latter in subunit I. IP fraction was resolved into IP-I and IP-II+III subfractions. IP-I exhibits only Fe_2S_2 type signals, while IP-II+III both Fe_2S_2 and Fe_4S_4 type. The cluster type was assigned based on such EPR parameters as spin relaxation and lineshape under relaxed protein constraints. In the hydrophobic P fraction, both Fe_2S_2 and Fe_4S_4 type signals were found and titrated with different thermodynamic parameters.

These data indicate the presence of at least five Fe_2S_2 and three Fe_4S_4 clusters in the NADH-UQ oxidoreductase. Correlation of the above described clusters with those identified in the NADH-UQ oxidoreductase and their spatial distribution in the mitochondrial inner membrane will be discussed along with subunit topography (Ragan ('80) Subcellular Biochem. 7:267) and spin-spin interactions detected in the NADH-UQ oxidoreductase (Ohnishi & Salerno ('82) Iron-Sulfur Proteins 4:286).

This work was supported by NSF Grant PCM 81-17284 and NIH Grant AM-08126.

T-PM-Pos47 Optical Spectrum, Decay Time, Temporal Distribution and Correlation With Peroxide of Human Breath Spontaneous Chemiluminescence. Britton Chance and Martin D. Williams. Johnson Foundation, University of Pennsylvania, Philadelphia, Pennsylvania 19104

Human breath spontaneously emits photons at a rate of approximately 7,000 per liter second. The emission has a peak in the red part of the spectrum and an ultraviolet contribution. The emission count rate correlates with peroxide concentration in a saturating manner with overall bimolecular stoichiometry under normal breathing conditions. When trapped in a balloon the breath luminescence count rate has a half decay time of approximately 20 minutes and exhibits more than one mode of decay. The photomultiplier pulses generated by breath luminescence arrive in bursts. Breathing through gauze intensifies the count rate but blowing air through gauze produces no signal. The signal from gauze after a breathing experiment is very weak. There are several chemiluminescent species always present in the atmosphere which might account for these observations. These include $^1\Delta_g$ O_2 which emits at 6324 A, oxygen atom ions-6300 A, hydroxyl radical-6329 A, and the water cation H_2O+ -6190 A. The intensification by gauze may be indicative of either free radical processes or singlet oxygen involvement since both are quenched by water which is partially removed by the gauze. The arrival of photomultiplier pulses in bursts is also consistent with the participation of free radicals, because of their common association with chain reactions, and with the participation of singlet oxygen since it is known to have an extremely long lifetime (approximately .5 seconds at atmospheric conditions) and therefore has a high probability of overlapping emission events. The long decay time also is indicative of singlet O_2 and/or radical chain rx'ns.

T-PM-Pos48 BEHAVIOR OF THE POTENTIAL-SENSITIVE MOLECULAR PROBE M540 IN SUBMITOCHONDRIAL PARTICLES

J. C. Smith, J. M. Graves, and M. Williamson, Dept. Chem. and LMBS, Georgia State Univ., Atlanta, GA - The addition of ATP to a M540-SMP suspension produces oligomycin-sensitive spectral changes with absolute maxima near 490, 530, and 565 nm; a 1-2 nm red shift of the dye absorption spectrum is also evident in the longer wavelength region of the spectrum. The ATP-induced optical signal was increased by the addition of NH_4Cl and could be subsequently restored to the control level by the permeant SCN anion. M540 may thus be specifically sensitive to the membrane potential portion of the electrochemical gradient. Binding analyses based on the Langmuir adsorption isotherm and the direct linear method indicate that the M540 dissociation constant is decreased by the presence of ATP with little or no change in the maximum number of binding sites. The M540 dissociation constant was markedly reduced when 0.1 M NaCl was present in the medium suggesting that the association of this probe with the membrane is subject to considerable surface charge repulsion. The binding analysis results indicate that the origin of the energy-dependent spectral changes may be an enhanced association of M540 with the SMP membrane resulting from the transfer of dye from the aqueous phase to membrane binding sites. The time course of the ATP-induced signal developed on a time scale of tens of seconds and follows a second order rate law suggesting that the rate limiting step in the development of the ATP-induced M540 signal may be the transfer of dye from the aqueous phase to membrane binding sites. In the 1 - 4μM range, the presence of M540 in SMP preparations did not alter either the rate or amplitude of the ATP-induced cytochrome c oxidase soret band shift signal suggesting that this dye does not permeate the SMP membrane, at least on the time scale of these experiments, approximately 5 seconds.
Support: NSF equipment award CDP-7924717, Public Health Service awards RR09201 and GM 30552